



# Designing a resonant panel based on Helmholtz resonators with reduced geometrical complexity

Master thesis by Jordy van Eijk

Master Thesis:

Designing a resonant panel based on Helmholtz resonators with reduced geometrical complexity

Mentors:

Michela Turrin

Martin Tenpierik

Written by:

Jordy van Eijk

Delft University of Technology:

Faculty of architecture and the build environment

Building technology



# Table of Contents

Abstract .....	6
Acknowledgements .....	7
List of symbols .....	8
0. Introduction.....	12
0.2 Problem statement.....	12
0.3 Objective.....	13
0.4 Case study.....	13
0.5 Research questions: .....	13
0.6 Approach and methodology.....	14
0.7 Relevance .....	14
1 Literature review .....	18
1.1 Acoustic principles.....	18
1.1.1 Sound Pressure.....	18
1.1.2 Frequency .....	18
1.1.3 Reverberation time and sound absorption .....	19
1.1.4 Sound absorption and viscous flow.....	20
1.1.5 Acoustic Impedance .....	21
1.1.6 Acoustic coupling.....	21
1.2 Measuring sound.....	22
1.2.1 Reverberation room .....	22
1.2.2 Impedance tube .....	23
1.2.3 In situ measurements.....	24
1.3 Passive sound absorbers .....	25
1.3.1 Porous absorbers.....	25
1.3.2 Resonant absorbers.....	26
1.3.4 Conclusion on resonant absorbers.....	31
1.4 Acoustics by additive manufacturing, previous work .....	33
1.4.1 Oliver Godbold, 2008 .....	33
1.4.2 Xiaobing Cai et al., 2014 .....	33
1.4.3 Junfei li et al., 2016.....	34
1.4.4 Zhiwen Ren et al., 2022 .....	35
1.4.5 Previous student work.....	35
1.5 Production techniques .....	39
1.5.1 CNC .....	40
1.5.2 Additive manufacturing.....	43

1.5.3 Conclusion on the presented production techniques .....	47
1.6 Computational Design .....	48
1.6.1 Form generation .....	48
1.6.2 Performance assessment .....	49
1.6.3 Optimalization .....	49
1.6.4 Materialization .....	51
1.6.5 Conclusion .....	52
2. Experimentation .....	54
2.1 Equipment and reference.....	54
2.2 Experiment 1: Neck position .....	57
2.2.1 Results Experiment 1.....	58
2.2.2 Conclusion experiment 1.....	58
2.3 Experiment 2: Crosstalk.....	59
2.3.1 Results experiment 2.....	60
2.3.2 Conclusions Experiment 2 .....	60
2.4 Experiment 3: cavity separations .....	61
2.4.1 Results Experiment 3.....	62
2.4.2 Conclusion experiment 3.....	62
2.5 Experiment 4 width of the absorption curve .....	63
2.5.1 Results experiment 4.....	64
2.5.2 Conclusion experiment 4.....	65
2.6 Experiment 5: L-shaped cavities.....	65
2.6.1 Results experiment 5.....	67
2.6.2 Conclusion experiment 5.....	70
2.7 Limitations regarding the experiments .....	70
2.8 Overall conclusions.....	70
3 Digital workflow .....	73
3.1 The user inputs .....	75
3.2 The acoustic optimizer .....	75
3.2.1 Resonator types.....	76
3.2.2 The calculations.....	77
3.2.3 Verification of the resonators .....	78
3.3 The resonator placement .....	79
3.4 Preparation for production .....	81
3.4.1 Intersections.....	82
3.4.2 Packing the panels onto the sheet material.....	83

3.5 Overview of the tool.....	83
4. Case study.....	86
4.1 Problem statement and method.....	87
4.2 The panels.....	88
4.3 Improvement of the room acoustics.....	89
5 Conclusions and recommendations.....	94
5.1 Conclusions.....	94
5.2 Recommendations.....	95
References.....	96
List of figures.....	99
List of tables.....	102
Annex 1: Measurement setup and sample measurements.....	104
Measurements of the samples after printing.....	104
Impedance tube measurement setup.....	105
.....	105
Annex 2: Results from the experiments.....	106
Additional graphs experiment 4.....	106
Original results experiment 5.....	107
Annex 3: Alternative resonator placement method.....	109
Annex 4: Python code.....	112
Acoustic optimizer.....	112
Resonator placement.....	117
Preparation for production.....	119

## Abstract

Acoustics combined with digital fabrication has been investigated for multiple years. Most research in this area has focused on the combination of acoustics and additive manufacturing. This is mainly due to the ability of this technique to create any geometry, which allows for very high absorption. However, it has the downside that additive manufacturing is quite expensive and the production process is time-consuming. Therefore, this study has chosen to put the geometry first and the performance of the resonators second.

To be able to produce a resonant panel based on Helmholtz resonators some additional knowledge was needed. Therefore, five experiments were performed to gain the knowledge needed to design the panel. The samples were printed using a fused filament printer and tested within an impedance tube located at the Faculty of Architecture in Delft. The experiments were concerned with:

- The position of the neck compared to the cavity: According to the results of the experiments the position of the neck has a minimal to no effect on the performance of the resonator.
- The crosstalk effect: According to the results of the experiments the effect of the crosstalk effect is minimal within the scope of this project. A small change in absorption was noticeable but so small as to be irrelevant.
- The effect of the cavity separation between two resonators: According to the results of the experiments the cavity separation can be removed without a large effect on the absorption of the resonators.
- The effect of the neck length on the width of the absorption curve: According to the results of the experiments a longer neck causes the width of the absorption curve to decrease.
- The impedance of resonators with L-shaped cavities: According to the results of the experiments an L-shaped cavity can be approximated by replacing the L-shaped cavity by a cavity with an identical horizontal section right below the orifice but altering the height, so the cavity has the same volume as the original L-shaped cavity.

After the experiments were done, a computational workflow was designed that is able to produce resonant panels based on the targeted frequency range and the possible size of the panel. The tool was theoretically verified using a case study. For the case study two panels were designed to improve the reverberation time for a room in the Faculty of Architecture. Using the Arau-Puchades method of calculating the reverberation time the panels showed to be effective at absorbing sound at low frequencies.

## Acknowledgements

Ever since I started the Bachelor at the faculty of architecture, acoustics has been a topic within the the Built Environment that has interested me. During my studies I found an interest for computational design and specifically parametric design. Being able to combine the two fields in this project has been very interesting and kept me motivated to continue.

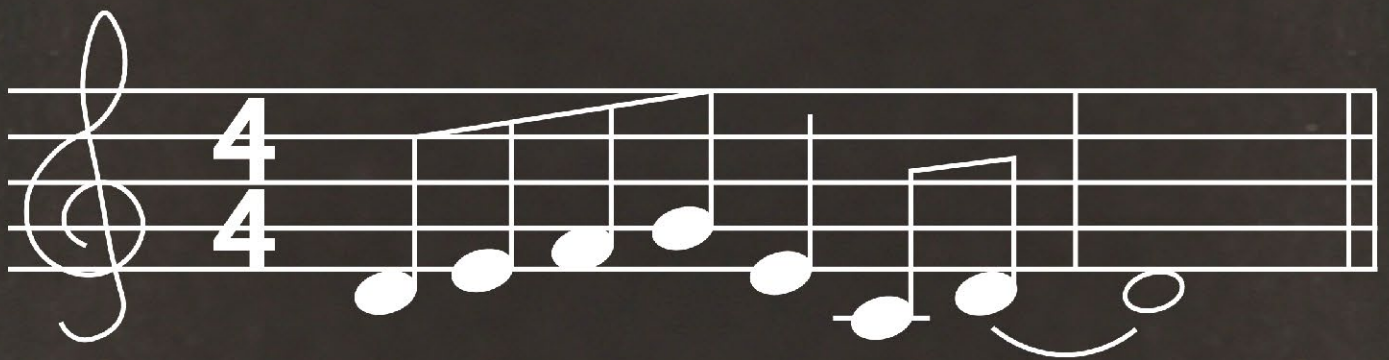
This project would not have been possible without the aid of my mentors Michela Turrin and Martin Tenpierik. Firstly, I would like to thank Martin Tenpierik for his near instant feedback on all questions and all previous iterations of the report. I would like to thank Michela Turrin for always considering the end goal of the project. Besides my tutors I would like to thank Sanne Maring for proof-reading every part of the report and taking the pictures for the report.

## List of symbols

L	dB	Sound pressure level
p	pa	Sound pressure
$\lambda$	m	Wavelength
c	$m*s^{(-1)}$	speed of sound
f	Hz	frequency
T	s	reverberation time
V	$m^3$	Volume of the room
Aeq	$m^2$	Total equivalent sound absorption area
S	$m^2$	Surface area of the room
Si	$m^2$	Surface of wall i
$\alpha_i$	-	absorption coefficient of wall i
$\alpha_e$	-	random-incidence energy absorption coefficient
$\alpha$	-	sound absorption coefficient
R	-	reflection coefficient
z	$Pa*s*m^{-2}$	acoustic impedance
$\rho$	kg/m <sup>3</sup>	density of air
$\psi$	rad	incidence angle
m	-	air absorption Constant
Ss	$m^2$	Surface are of the sample
p <sub>max</sub>	Pa	maximum pressure
p <sub>min</sub>	Pa	minimum pressure
H	-	transfer function
j	-	$\sqrt{-1}$
k	$m^{(-1)}$	wavenumber
s	-	standing wave ratio
z <sub>1</sub>	m	position of microphone 1
z <sub>2</sub>	m	position of microphone 2

$I$	$W \cdot m^{-2}$	Sound intensity
$\omega$	rad/s	angular frequency
$\sigma$	$(MPa \cdot s) / m^3$	flow resistivity of fibrous material
$d$	m	material thickness
$l$	m	neck length
$l\Delta$	m	end correction
$R$	m	diameter of the neck
$Z_r$	$kg / (m^2 \cdot s^2)$	total impedance of a Helmholtz resonator
$Z_v$	$kg / (m^2 \cdot s^2)$	cavity impedance of a Helmholtz resonator
$Z_m$	$kg / (m^2 \cdot s^2)$	impedance around the resonator mouth
$t$	m	cavity depth
$S_a$	$m^2$	orifice area
$S_b$	$m^2$	cover plate area
$a$	m	radius of the orifice
$\nu$	$m^2 / s$	kinematic viscosity of air
$\Omega$	-	porosity
$\eta$	$Pa \cdot s$	dynamic viscosity of air
$N$	-	number of identical tubes
$A_{tube}$	$m^2$	cross-sectional area of the tube
$A_{wall}$	$m^2$	area of the wall
$\Gamma$	-	propagation constant
$n_i$	-	polytropic coefficient
$J_0$	-	Bessel function of the first kind of order 0
$J_2$	-	Bessel function of the first kind of order 2
$s$	-	shear wave number
$\gamma$	-	ratio of specific heats
$\sigma$	-	square root of the Prandtl number
$\mu$	$Pa \cdot s$	dynamic viscosity

$C_p$	$J \cdot kg^{-1} \cdot K^{-1}$	specific heat
$\lambda$	$W \cdot m^{-1} \cdot K^{-1}$	thermal conductivity
$R$	m	radius of the tube
$f_{range}$	Hz	frequency range
$\bar{a}_x$	-	average absorption in the x direction
$S_x$	m <sup>2</sup>	surface area perpendicular to the x axis



0

Introduction

## 0. Introduction

In the last couple of years most people experienced the importance of acoustics. From microphones transmitting more noise than speech, to coworkers video calling for hours on end at the desk right next to yours. Being able to hear and be heard is essential in our day-to-day life. Sadly, acoustics is often overlooked by architects when designing a building (Nijs, 2007). Acoustics then becomes something that needs to be taken care of after the building has already been put into use.

Sound can cause problems both within a room or between rooms. The Dutch building regulations identify five relevant topics concerned with sound (Dessing, 2005).

1. Reduction of noise from outside
2. Reduction of noise from climate systems
3. Reduction of noise between room with the same function
4. Reducing reverberations
5. Reduction of noise between rooms with different functions

This thesis will concern itself with point four: Reducing reverberations. The other topics are concerned with sound transmission between rooms while reverberations occur within a room. According to Dessing (2005), Reverberations create difficulties when trying to understand each other and can increase the overall sound level. Sound absorbing materials can aid in the reduction of reverberations. The time it takes for sound to reduce in sound pressure level by 60 dB is called the reverberation time (Cox, D'Antonio, 2009). Sound absorbing materials lower the reverberation time within a room (Dessing, 2005), and thus improve the acoustic performance.

Sound absorption is not equal over the whole frequency band. Each frequency reacts differently to a sound absorbing material (Dessing, 2005). To achieve maximum absorption,  $\frac{1}{4}$  of the wavelength needs to be inside of the material (van der Linden, 2011). Low frequencies have a large wavelength. For example a frequency of 100 Hz is 3,43 meters long. Which means that porous material would take up a lot of space to absorb these frequencies, which is not always available. Resonant absorbers are very efficient at the absorption of low frequencies in a panel with a small depth but have the downside that they only target a specific frequency (Godbold, 2008). Combining multiple resonators can result in broadband absorption for low frequencies.

### 0.2 Problem statement

Due to the rise of 3D-printing, or additive manufacturing as it is known in the academic world, the production of complex geometries has become more available. In room acoustics this has resulted in the research of resonant absorption through additive manufacturing. The research focuses mainly on the performance of the Resonant absorbers and disregards the traditional geometrical concerns because of the ability to generate most shapes using a 3D printer.

This increase in complexity ties efficient resonant absorption to additive manufacturing, because most other manufacturing techniques are not able to produce this type of geometry while also meeting the other requirements set by the resonator. The increased complexity of the elements and the associated production techniques make resonant absorbers more of a niche product and not widely available. Additive manufacturing is rapidly increasing its suitability for large scale production, but at this moment in time it has the downside that it does not scale very well to larger scale production. If a product would be mass produced, additive manufacturing does not increase in speed. Other production methods do benefit from mass production resulting in the decrease of cost for the absorbers and therefore a wider availability. To summarize: Due to the high geometrical complexity the manufacturing of resonant panels can be very expensive, making it a niche product.

### 0.3 Objective

The aim of this thesis is to generate a resonant panel based on Helmholtz resonators focusing on the geometry first and the performance second. This will be done to see if there is a possibility to reduce the geometrical complexity of a panel based on Helmholtz resonators providing broadband absorption for low frequencies. Production of large panels by the use of additive manufacturing allows for a lot of freedom in geometry but increases the price and reduces the availability. If the complexity of the geometry is reduced, more production techniques become available. Therefore, research needs to be done to see which techniques become available and if they can outperform additive manufacturing. In order to be able to design this absorber a good understanding of the possible absorbers is needed.

The end goal of this thesis is to produce a workflow for the design of an acoustic absorber with reduced geometrical complexity compared to current examples. The inputs will be the targeted frequency or frequency band. The output is the geometry that can serve as the input for the chosen production technique.

### 0.4 Case study

The case study for this thesis will be a small meeting room in the faculty of architecture at the TU Delft, 1.060 West. This case study is mainly chosen for convenience. The location is easily accessible, and the small size of the room makes it so that only a small area of the resonant absorbing panel is needed if there is time to perform in situ tests.

### 0.5 Research questions:

The main research question of this thesis will be:

How can an acoustic panel based on Helmholtz resonators be designed with reduced geometrical complexity while retaining a broadband high absorption coefficient for low frequencies?

Sub questions regarding background knowledge:

- Which room acoustic variables can be used to decide upon the acoustic quality of an office?
- What are the main types of acoustic absorbers available for single material broadband acoustic absorption?
- What type of production techniques are available and practical to use when manufacturing resonant absorbers?
- In recent years, what research has already been done into resonant absorbers for room acoustics aimed at high absorption over multiple octave bands?
- What computer-controlled manufacturing techniques are suitable for the production of resonant absorbers?
- What processes are needed to be included in a digital design workflow for the design of resonant absorbers?

Sub questions regarding the development of the design:

- Where can the complexity of the geometry be reduced and where is the complexity a necessity for the functioning of the resonator?
- How can the location of the resonator orifices be optimized?
- What kind of effect do the resonators have on each other?
- How do the internal boundaries of the cavities affect the performance of the resonators?
- Has the reduction in geometrical complexity resulted in availability of additional production techniques?

## 0.6 Approach and methodology

The first part of this thesis will consist of a literature review. In this part the main principles of room acoustics will be discussed to gain a solid theoretical background for the rest of the project. The second part of the literature review looks at the possible resonators that can be used in a panel for acoustic absorption. Sound measuring techniques are discussed in the third part of the first chapter. The fourth part of the literature review consist of work from other authors already done regarding resonant absorption made by using additive manufacturing. The fifth part of this report is concerned with an overview of manufacturing techniques able to make the resonator panels. The last part of the literature review consists of an overview of the processes within the computational workflow produced in the second part of this thesis.

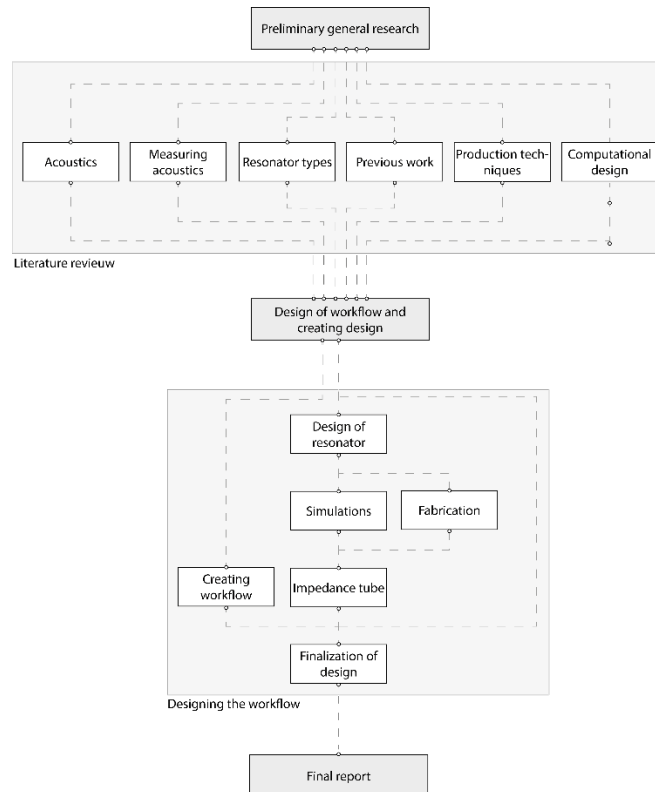


Figure 2: Workflow through the project

With the knowledge from the literature review sets of experiments will be designed to fill the gaps in knowledge needed to produce the resonant panel. The samples will be generated within Grasshopper to then be produced with a 3D printer to be tested. The tested samples will be compared with existing theory to confirm the results.

With the knowledge from the literature review and the experiments a workflow for the resonant panel will be developed. This will fully be done within Grasshopper within Rhino. An attempt will be made to make the workflow without the use of external plugin to make the script more usable and more available.

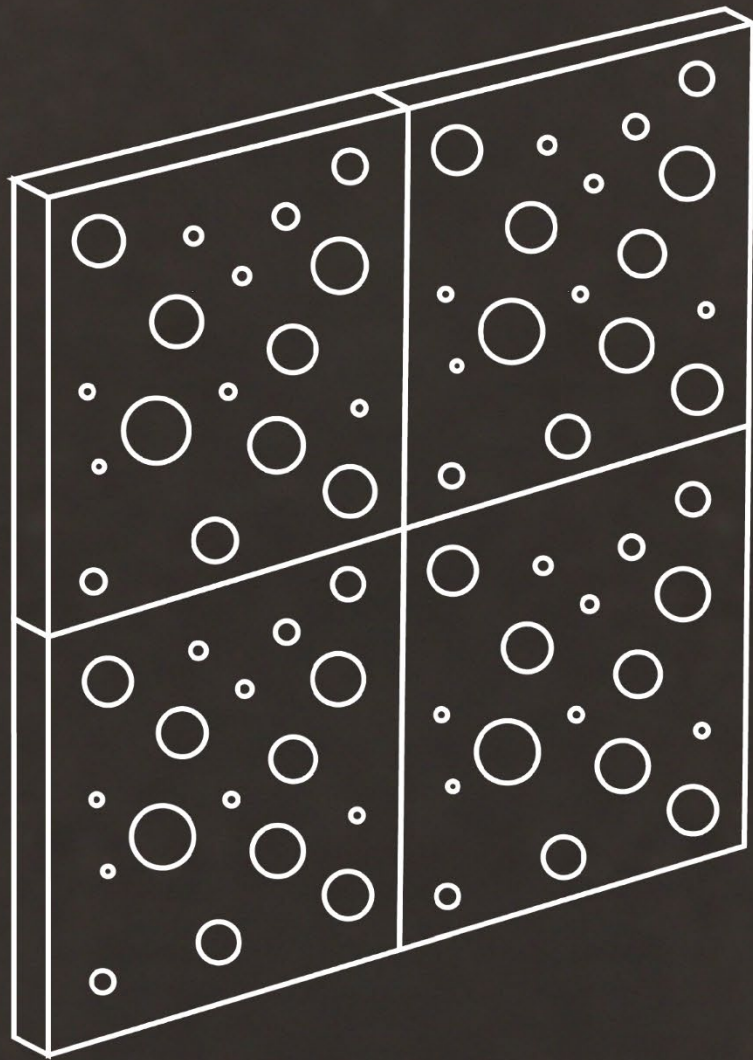
## 0.7 Relevance

The societal and professional relevance of this thesis can be seen in the workflow produced. This workflow can make resonant panel absorbers more accessible for a wider audience. The reduction of the geometrical complexity makes way for a wider variety of production methods. This includes production methods that could produce the product faster and cheaper.

The scientific relevance of this thesis can be seen in the reduction of geometrical complexity. A lot of research has been done investigating how to increase the performance of existing resonators (Godbold, 2008)( Gommer, 2016). This generally leads to an increase in complexity of the resonator geometry. The reduction of the panel thickness is also a large topic within the field of acoustic by additive manufacturing (Cai, 2014)(Setaki, 2014). Again, the complexity is increased. Increasing the complexity binds the product to a specific production method. By looking into the reduction of the geometrical complexity a wider array of production techniques become available.

A second scientifically relevant part this Thesis is the aims to investigate is the influence of the partition walls that separate the cavities of two Helmholtz resonators on the performance of those resonators. If the partitions between the cavities of the resonators are deemed unnecessary the geometrical complexity of the panels could be reduced significantly.





**1**

**Literature review**

# 1 Literature review

This chapter will provide a theoretical background to the research presented in later chapters. First, the general acoustic principles regarding room acoustics will be discussed. Then, an overview of the different ways of measuring acoustical properties of materials or resonators will be presented. Possibilities for absorbing sound will be discussed in the third part of this chapter. The fourth part is concerned with the current state of progress within the field of acoustics by additive manufacturing. The fifth part will deal with possible manufacturing techniques that can be used within the scope of this project. The final part of this chapter will be concerned with the possibilities for the computational workflow.

## 1.1 Acoustic principles

Although not visible, sound plays a big role in our everyday lives. These pressure waves enter our ears which, through a series of components, end up in the brain. These simple changes in the atmospheric pressure can be the sound of a bird whistling, a band playing or a human talking.

More generally, acoustics is the science of generation, transmission and reception of energy as vibrations in a medium (Kinsler et al, 2000). With acoustics being such a broad field, this thesis will only focus on some fundamentals of acoustics and room acoustics.

### 1.1.1 Sound Pressure

When we speak, we create sound. This sound causes molecules to vibrate. Because of the movement of the molecules very minute changes in the atmospheric pressure start to occur. The louder we speak, the bigger the vibration of the molecules becomes and the bigger the pressure differences become. Sound pressure is measured in Pascal (Pa). Because this results in a massive range of small numbers, the more common way of describing the sound pressure is in Decibels (dB). Decibels are a normalized and compressed description that is easier to grasp than the tiny numbers that Pa would provide (Ermann, 2015).

$$1. \quad Lp = 10 \log \left( \frac{p_{eff}^2}{p_0^2} \right)$$

Formula for converting sound pressure (Pa) to sound pressure level in dB, with  $p_{eff}$  being the sound pressure in Pa and  $p_0$  being the reference pressure being 20 micro Pascal.

This logarithmic scale makes it so that two values cannot simply be added up. Two identical sound sources producing 60 dB do not add up to 120 dB but to 63 dB. When two identical sound sources are combined the sound becomes three decibels louder (van der Linden, 2016).

### 1.1.2 Frequency

Every voice sounds different. Some are higher pitched some are lower pitched. The pitch of sound can be defined as the number of vibrations per second and is expressed in Hertz (Hz). A higher pitch sound causes the molecules of the medium to vibrate more frequently than a low sound. The higher the pitch of the sound the more Hertz. For a young person the hearing range is from approximately 20 to 20.000 Hz (Kinsler et al. 2000). Everything below 20Hz is heard as a beat instead of a tonal sound.

$$2. \quad \lambda = \frac{c}{f}$$

Formula for calculating the wavelength from the speed of sound and the frequency, with  $c$  being the speed of sound in m/s and  $f$  being the frequency in Hz

Because the speed of sound is constant for all frequencies, assuming the temperature humidity and air pressure are constant, and frequency is the number of vibrations per second, we can calculate the length of the wave. The length of the wave is the distance between two equal pressures (van den Linden, 2016). Knowing the length of the soundwave is useful when working with resonators.

A single constant frequency is called a pure tone. This means that all the energy of the sound is focused on a singular frequency. Examples of sounds that are pure tones or come very close are a pitchfork, tone generators and the back-up beeper of a car. Most sounds we hear are composed of multiple frequencies. These are called complex sounds (Ermann, 2015). With complex sounds the energy of the sound is divided over multiple frequencies. If two different instruments would play the same note, the two would still sound different. This has to do with the timbre of the instruments. The timbre is the division of energy over the frequencies which are not the fundamental frequency, the so-called harmonics.

### 1.1.3 Reverberation time and sound absorption

Within room acoustics one of the main concerns is the reverberation time. This is defined as the time it takes for a sound to lower in sound pressure level by 60 dB (Cox, D'Antonio, 2009). Different types of rooms require different reverberation times. For example, a concert hall can benefit from a longer reverberation time, while an office building preferably has a shorter reverberation time.

$$3. \quad T = 0.161 \frac{V}{A_{eq}}$$

Sabine's formula for the reverberation time with V being the volume of the room in m<sup>3</sup> and A<sub>eq</sub> being the total equivalent sound absorption area in m<sup>2</sup>.

When a sound hits a wall, not all of the acoustic energy is reflected back. Besides the part that is reflected, part of the sound is transmitted through the material and another part is absorbed by the material. The fraction of the sound that is not reflected back into the room is called the absorption coefficient (van der Linden et al., 2011).

$$4. \quad A_{eq} = \sum_i^1 S_i \alpha_i$$

Formula for the Total equivalent sound absorption area, with S<sub>i</sub> being the surface area of wall I in m<sup>2</sup> and α<sub>i</sub> being the sound absorption coefficient of wall i.

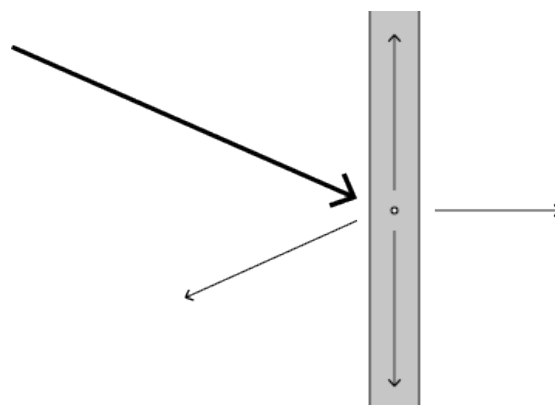


Figure 4: absorption, reflection, transmission

To calculate the reverberation time the Total equivalent sound absorption area is needed. This is the area-weighted average of all the Sabine absorptivity present in the room. The formula works on the basis of some assumptions. Sabine assumed that the total sound absorption would be the weighted

sum of the individual sound absorptions not taking the geometry of the room into account. Besides that, the loss of acoustic energy in the air is also neglected (Kinsler et al, 2000).

Besides Sabine, Eyring and Norris amongst others also developed a formula for the calculation of the reverberation time in a room. For small absorption coefficients both formula's give approximately the same result but when the  $\alpha$  becomes bigger, Sabine's formula predicts longer reverberation times. The formula made by Eyring and Norris is based on the mean free path between reflections. For rectangular rooms the mean free path can be calculated with  $L_m = 4V/S$ . The number of reflections will become  $N = cS/4V$  (Kinsler et al, 2000).

$$5. \quad T = \frac{0.161V}{-S \ln(1-\alpha e)}$$

Eyring and Norris formula for reverberation time, with  $S$  being the total surface area of the room in  $m^2$ .

$$6. \quad \alpha e = \frac{1}{S} \sum_i S_i \alpha_i$$

Formula for the random-incidence energy absorption coefficient.

There is no agreement on what method to use. But amongst researchers the Sabine formula is the most commonly used together with the experimental determination of the absorption coefficient (Kinsler et al, 2000).

The absorption coefficient can be calculated from the pressure reflection coefficient  $R$  which is often determined when doing physical tests for example the ones described in section 1.2. Theoretical models often give the acoustical impedance. With the impedance, the reflection coefficient can be calculated, with which the absorption coefficient can be calculated.

$$7. \quad \alpha = 1 - |R|^2$$

Formula for the calculation of the absorption coefficient from the pressure reflection coefficient.

$$8. \quad R = \frac{\frac{z_1}{\rho c} \cos(\psi) - 1}{\frac{z_1}{\rho c} \cos(\psi) + 1}$$

Formula for the pressure reflection coefficient from the acoustic impedance, with  $z_1$  being the acoustic impedance of layer 1 in  $Pa \cdot s \cdot m^{-2}$ ,  $\rho$  being the density of air in  $kg/m^3$  and  $\psi$  being the incidence angle of the soundwave in rad.

This coefficient depends upon the frequency of the sound hitting the wall. To test a material for all the frequencies individually would be very hard and overly detailed. Therefore, octave bands were introduced. When a frequency doubles it is called an octave. Within music it represents the same note, but a higher version. Within architectural acoustics the most common octave bands are: 125Hz, 250Hz, 500Hz, 1000Hz, 2000Hz and 4000Hz. Sometimes the range is expanded with 63Hz or 8000 Hz.

#### 1.1.4 Sound absorption and viscous flow

As a soundwave travels through a medium, particles of the medium start to vibrate in the direction of the wave. This causes changes in density and pressure (Rossing, 2007). The relative motion between molecules due to the changes in density and pressure causes friction between the molecules, which converts the acoustic energy into heat. This causes all sound to eventually be converted into heat (Godbold, 2008). This conversion of acoustic energy into heat is called sound absorption.

When a sound flows over a surface a viscous flow occurs. The particles that lay on the surface do not move while the soundwave that travels over it is indeed in motion. The distance between the surface and the molecules that move freely through the air is called the viscous boundary layer (Godbold, 2008). Because of the relatively high speed difference between the molecules the friction that occurs here is a lot bigger than the friction that occurs in unobstructed air. Therefore this concept can be used to create a sound absorber. This type of absorption is called visco-thermal damping.

#### 1.1.5 Acoustic Impedance

An important concept when dealing with resonators and acoustic absorption is the acoustic impedance. It can be seen as the resistance an object exerts on a soundwave traveling through a medium. Or more formally: "The acoustic impedance exhibited by a surface of area  $S$  is the complex quotient of the acoustic pressure at the surface divided by the volume velocity at the surface." (Kinsler et al., 2000).

Lumped acoustic elements describes the way that elements which are considerably smaller than the wavelength they produce can be described. It can then be assumed that the pressure inside the element is constant (Kinsler et al., 2000). Resonators can often be described as lumped acoustic elements. The acoustic impedance for the entire element can then be calculated.

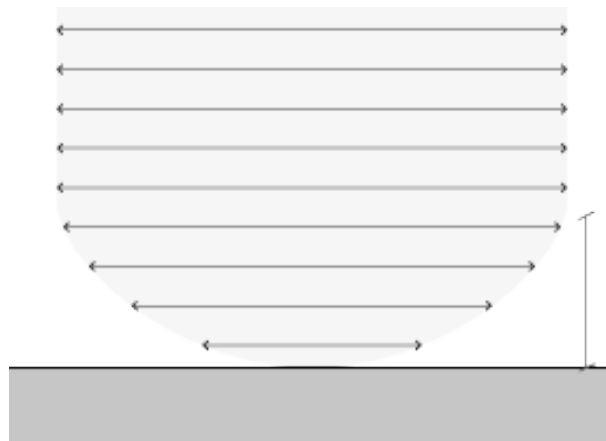


Figure 5: viscous boundary layer

The specific acoustic impedance is defined as the pressure over the particle speed. It is a characteristic of the medium and the wave in which it propagates (Kinsler et al., 2000). The specific acoustic impedance is useful for calculations involving the transmission of acoustic waves from one medium to the next. And when describing sound confined within a space.

#### 1.1.6 Acoustic coupling

Acoustic coupling is the transmission of acoustic waves from one resonator to another resonator. Often acoustic coupling is undesirable, because the sound travels out of its regular bounds. For example, if two resonators are side by side there is the risk that sound from one resonator is transmitted to the second resonator. This can cause many undesired effects in the second resonator like reducing the absorbent qualities, because the frequencies may passively constructively interfere. Acoustic coupling can also be used to enhance the performance of resonators (Li et al., 2016). This can be done if the phase angle between the resonators is exactly 180 degrees.

## 1.2 Measuring sound

Validating the theoretical results with practical results will be a critical part of this project. Therefore, an overview of the most common ways of testing a material or product for its acoustical properties are presented in this part of the report.

### 1.2.1 Reverberation room

In a reverberation room a sample can be tested for its effect on the reverberation time. From this test, the random incidence absorption coefficient can be determined. The random incidence absorption coefficient is the most used value to specify the absorption coefficient of a material (Cox, D'Antonio, 2009). First the reverberation time of the test room is tested. Secondly the reverberation time with the sample in the test room is tested. By calculating the difference in absorption, the absorption and absorption coefficient of the sample can be determined.

$$9. T_0 = \frac{55.3V}{c \alpha_0 S + 4Vm_1}$$

Formula for the reverberation time before the sample is placed, with  $\alpha_0$  being the sound absorption coefficient of the empty reverberation room and  $m_1$  being the air absorption constant.

$$10. T_1 = \frac{55.3V}{c(\alpha_0[S - S_s] + \alpha_s S_s + 4Vm_1)}$$

Formula for the reverberation time after the sample is placed, with  $S_s$  being the surface area of the sample in  $m^2$  and  $\alpha_s$  being the absorption coefficient of the sample.

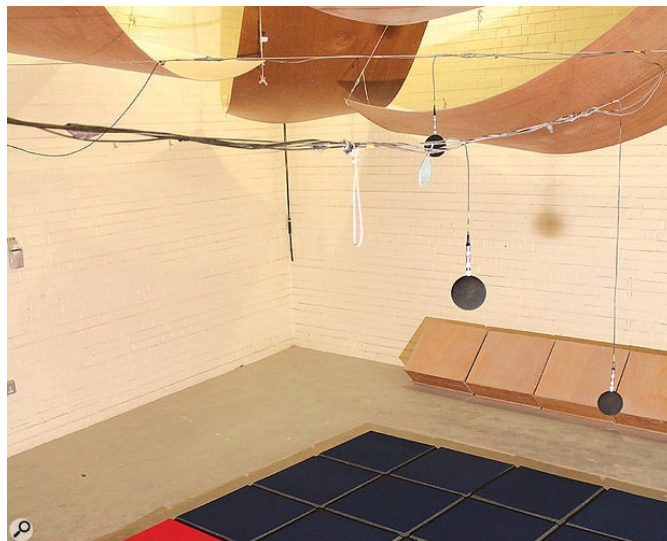


Figure 6: reverberation room

To be able to compare the test of different samples, the standard ISO 354:2003 gives guidelines on the room and the size of the sample that is being tested. Although the values gained from the reverberation room test are among the most used, they are not always as useful. Calculating the random incidence sound absorption coefficient is quite difficult and is therefore not frequently used to validate the results of theoretical models (Cox, D'Antonio, 2009). For the reverberation room test, a special room of around 200  $m^3$  is needed to perform the tests in. Besides that, a large sample of 10-12  $m^2$  is needed to place inside the room.

### 1.2.2 Impedance tube

The impedance tube is a very common way of testing a material for its normal incidence absorption coefficient and the surface impedance (Cox, D'Antonio, 2009). The test can be used to validate theoretical results. The main advantage is that the impedance tube only needs a small sample of the material that will be tested. Besides that, the impedance tube creates a controlled environment without the need for a large room. The disadvantage is that the small samples are not always representative for the bigger scale samples. This is mainly the case with resonators. Because resonators are dependent on their geometry, they can influence each other. Porous material does not have this problem and can produce very good results within an impedance tube (Cox, D'Antonio, 2009).

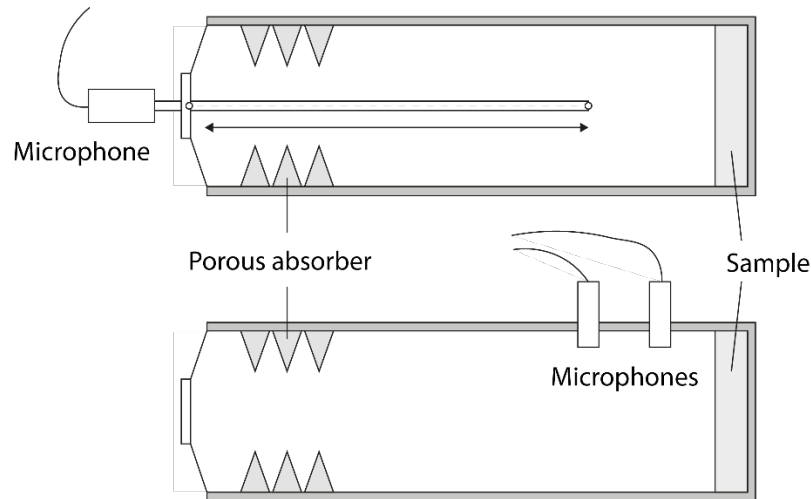


Figure 7: Impedance tube

Within an impedance tube two types of tests can be performed. The first one is the standing wave method. This method measures the maximum and the minimum pressure within the tube to determine the standing wave ratio which can determine the reflection coefficient.

$$11. s = \frac{p_{max}}{p_{min}}$$

Formula for the standing wave ratio, with  $p_{max}$  being the maximum pressure in Pa and  $p_{min}$  being the minimum pressure in Pa.

To determine the reflection coefficient a moving microphone is needed to find the maximum and minimum pressures. When the distance between the first minimum and the sample is known it is also possible to calculate the impedance of the sample (Cox, D'Antonio, 2009). The disadvantage of the standing wave method is that it only measures one frequency at a time. The advantage on the other hand is that the method is quite foolproof.

The second way an impedance tube can be used is the transfer function method, otherwise known as two microphone method. The pressure is measured at two points inside of the tube. It is then possible to set up an equation for the reflection coefficient. From there it is possible to calculate the impedance and the absorption coefficient.

$$12. |R| = \frac{s-1}{s+1}$$

Formula for the reflection coefficient.

$$13. R = \frac{He^{jkz_1} - e^{jkz_2}}{e^{-jkz_2} - He^{-jkz_1}}$$

Formula for the reflection coefficient for the transfer function method, with H being the transfer function, k being the wavenumber in  $m^{-1}$ ,  $z_1$  being the position of the first microphone in m and  $z_2$  being the position of the second microphone in m.

The main advantage of the standing wave method is the ability to calculate the absorption and impedance for all required frequencies with a couple tests (Cox, D'Antonio, 2009). The transfer function H can be calculated by dividing the pressure at position 2 by the pressure at position 1.

### 1.2.3 In situ measurements

Another way of measuring the absorption coefficient and surface impedance of an absorber is on the site it is designed for. A possibility is the two-microphone free field method. It resembles the transfer function method, explained in section 1.2.2, but placed inside of a room instead of an impedance tube. Again, two microphones are placed at different distances from the sample. A soundwave is transmitted towards the sample at a predetermined angle. In this way the incidence angle of the sound can be determined to see how the sample reacts to the sound at specific angles (Cox, D'Antonio, 2009).

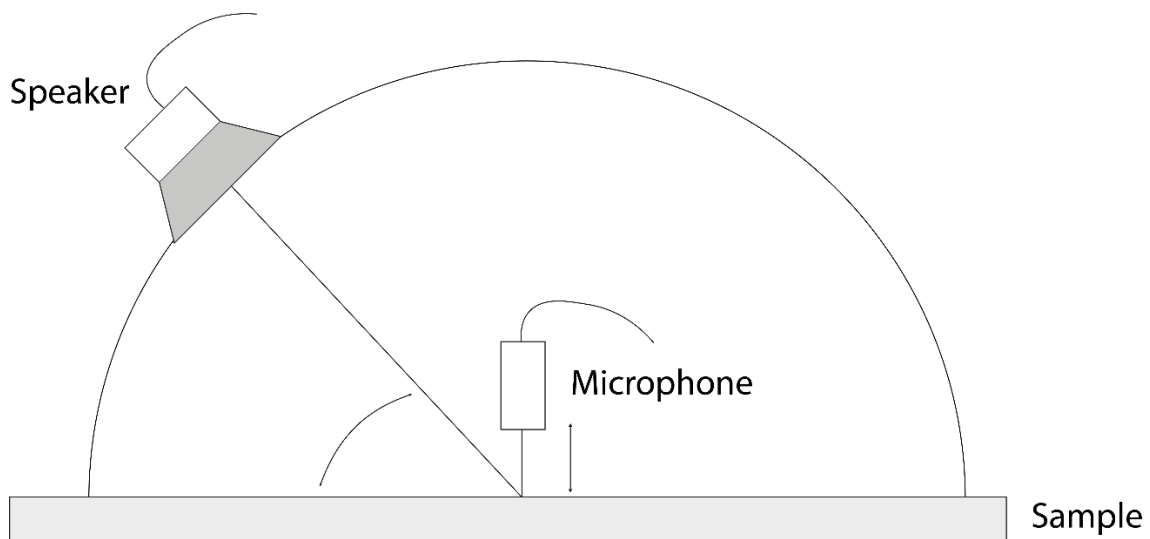


Figure 8: two microphone free field method

Like with the reverberation room a large sample is needed to test the material. Doing tests inside a room not designed for that purpose can cause difficulties. To obtain accurate results any unwanted reflections need to be removed from the measurement. Besides that, non-planar wave reflections need to be prevented as much as possible, because they can cause inaccuracies in the measurements. When this is done, accurate results can be achieved (Cox, D'Antonio, 2009).

$$14. R = \frac{H_{12} e^{jkz_1 \cos(\psi)} - e^{jkz_2 \cos(\psi)}}{e^{-jkz_2 \cos(\psi)} - H_{12} e^{-jkz_1 \cos(\psi)}}$$

Reflection coefficient R in a two microphones free field method.

### 1.3 Passive sound absorbers

To absorb sound the energy of the soundwave needs to be converted into heat. This happens automatically while the sound travels through the air but can also occur through interactions with other media (Godbold, 2008). Sound absorption can be stimulated in two ways:

- Increasing the surface area that the air oscillates over. This can be seen in porous materials
- Increasing the magnitude of the air oscillations over the surface. This can be seen in resonant absorbers.

#### 1.3.1 Porous absorbers

Materials like foam (figure 9) can be used as porous absorbers. When sound hits a porous absorber, the soundwave starts to seek a way through the material. Because of the many small airways in the material, viscous frictional energy conversion starts to occur. This effect causes the acoustic energy to dissipate as heat (Godbold, 2008). Another effect that helps in the absorption of the sound energy is the constant change in flow direction and the irregularity of the cross section of the pore the sound travels through (Ermann, 2015).



Figure 9: Porous material

Porous absorbers are most effective at high frequencies because the maximum velocity of the air particles needs to be inside of the material to achieve maximum sound absorption. If sound would hit a wall, the maximum particle velocity will occur at  $\frac{1}{4}$  of the length of the wave from the wall. If the porous material would be thinner than  $\frac{1}{4}$  of the wavelength the maximum velocity would not occur within the material and the sound absorption would be low(er) (van der Linden, 2016).

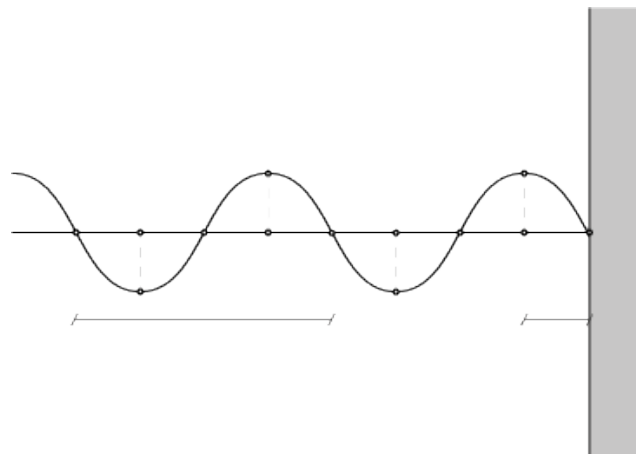


Figure 10: Particle velocity

The prediction of the sound absorption for porous absorbers is difficult. The actual thickness and porosity of the material can vary a lot, influencing the sound absorbing properties of the material (van den Eerden, 2000).

An attempt has been made to find a mathematical model. This resulted in semi-mathematical, semi-empirical models which are hard to use and cannot give all the required parameters for some materials (Cox, D'Antonio, 2009). Delany and Bazley (1969) developed a completely empirical model for the impedance and wavenumber of porous materials. They tested a large number of samples in two impedance tubes to then fit a curve through the data.

$$15. z_c = \rho_0 c_0 (1 + 0.0571X^{-0.754} - j 0.087X^{-0.732})$$

Formula for the characteristic impedance of a porous material.

$$16. k = \frac{\omega}{c_0} (1 + 0.0978X^{-0.7} - j0.189X^{-0.595})$$

Formula for the wavenumber of a porous material, with  $\omega$  being the angular frequency in rad/s.

$$17. X = \frac{\rho_0 f}{\sigma}$$

Formula for the value X when working with porous materials, with  $\sigma$  being the flow resistivity of fibrous material in (Mpa\*s)/m<sup>3</sup>.

$$18. z_{s1} = -j z_c \cot(k d)$$

Formula for the impedance at the surface of layer s when dealing with one layer, with d being the material thickness in m.

The flow resistivity ( $\sigma$ ) is a value that says something about how easily air can enter and flow through a porous absorber. The values for flow resistivity are found using empirically found formulas that depend on the orientation of the sound to the fibers and the type of material (Cox, D'Antonio, 2009).

### 1.3.2 Resonant absorbers

Resonant absorbers attempt to increase the magnitude with which the soundwave oscillates over a surface. Resonant absorbers are especially useful for mid to low frequencies. Broadband sound absorption with resonators is difficult to achieve because resonators are tuned to singular frequencies (Cox, D'Antonio, 2009).

Porous absorbers absorb sound equally over the entire surface. Resonant absorbers have a absorption cross section. This is the area of influence of the resonator on the wall.

$$19. A_{max} = \frac{\lambda^2}{4\pi}$$

Formula for the absorption cross section (Beranek and Ver, 1992)

Beranek and Ver formulated the absorption cross section as can be seen in formula X. When the absorption cross section is considered to be a circle the area can be substituted for the area of a circle. Then the radius that the resonator covers can be calculated. From this radius the maximum distance between resonators of the same frequency can be calculated. Costa (2016) described that this distance is too large for the circles would only touch on their edges, and an area between the circles would be left. The maximum distance that would still fully cover the wall can be derived from formula X.

$$20. d_{max} = 2h = \frac{\sqrt{3}}{\pi} \lambda$$

Formula for the distance between resonators by Costa(2016)

### 1.3.2.1 Helmholtz Resonator

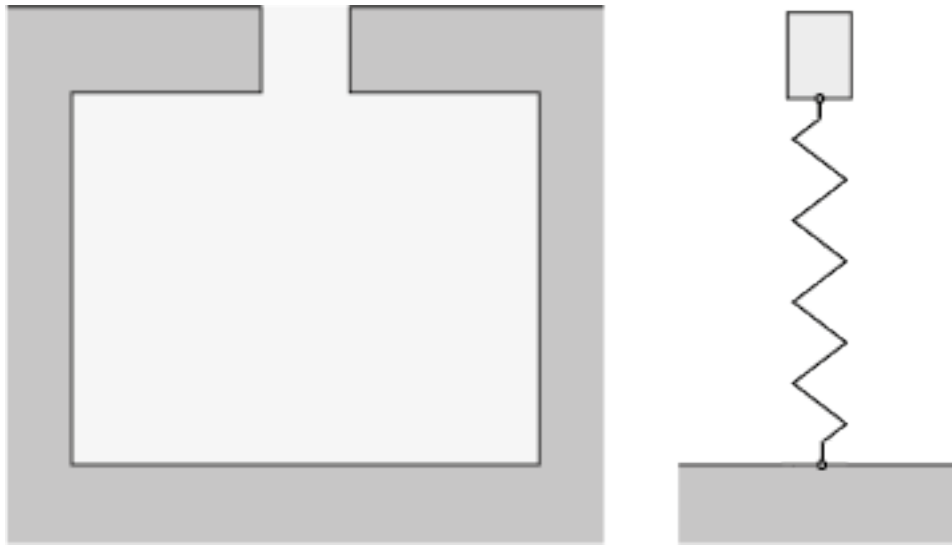


Figure 11: Helmholtz resonator

A commonly used resonant absorber is the Helmholtz resonator. Named after the German physicist Hermann von Helmholtz who developed them to single out pure tones from complex sounds. The resonator consists of a cavity and a neck. The volume of air in the neck acts as a mass and the bigger volume behind it acts as a spring (Kinsler et al., 2000,). The mass of the volume of air in the neck is dependent on the length and the opening area. The stiffness of the “spring” is dependent on the volume of the cavity. The resonant frequency of a Helmholtz resonator can be calculated with formula 19 (Godbold, 2008). As can be seen from formula 19 the shape of the volume has no effect on the frequency of the resonator. If the value resulting from  $S/(L+l\Delta)V$  is the same the resonator can be seen as essentially identical (Kinsler, 2000).

$$21. f = \left(\frac{c}{2\pi}\right) \sqrt{\frac{S}{V(l+l\Delta)}}$$

Formula for the calculation of the resonant frequency of a Helmholtz resonator, with  $S$  being the orifice area of the neck in  $m^2$ ,  $V$  being the volume of the resonator in  $m^3$  and  $l$  being the length of the neck of the resonator in  $m$ .

$$22. l\Delta = \frac{8R}{3\pi}$$

Formula for the end correction of the neck, with  $R$  being the diameter of the neck in  $m$ .

Because the end of the resonator emits a pressure wave into its surroundings the effective length of a pipe is longer than the actual length of the pipe. This end correction is not dependent on the frequency but only on the geometry of the pipe (Kinsler et al., 2000). Not including the end correction would result in the incorrect frequency.

The conversion of acoustic energy into heat occurs in the neck of the resonator. Here, the air in the neck and the neck itself generate thermos-viscous losses of acoustic energy (Kinsler et at, 2000). Besides the resistance in the neck there is also a resistance around the orifice of the neck. This resistance occurs because the resonator emits sounds with a frequency equal to the resonant frequency of the resonator. This gives a radiation resistance and a radiation mass.

The impedance of a Helmholtz resonator can be calculated using formula's found in Beranek and Ver (1992). The impedance consists of a four parts. A real and an imaginary part for the cavity impedance  $Z_v$ . And a real and an imaginary part for the impedance in and around the resonator mouth  $Z_m$ .

$$23. Z_r = Z_v + Z_m = (Z'_v + jZ''_v) + (Z'_m + jZ''_m)$$

Formula for the total impedance of a Helmholtz resonator

The real part of the cavity impedance is often disregarded for its minimal impact on the total impedance. This results in three parts making up the total impedance.

$$24. Z_v = -j\rho c \cot(kt) \frac{S_a}{S_b}$$

Formula for the cavity impedance: with  $t$  being the cavity depth,  $S_a$  being the orifice area of the resonator and  $S_b$  being the cover plate area of the resonator

$$25. Z'_m = \rho \left[ \sqrt{8\nu\omega} \left( 1 + \frac{l}{2a} \right) + \frac{(2\omega a)^2}{16c} \right] + Z_s$$

Formula for the real part of the orifice impedance: with  $\nu$  being the kinematic viscosity of air

$$26. Z''_m = \omega\rho \left[ l + \left( \frac{8}{3\pi} \right) 2a \right] + \left( l + \frac{l}{2a} \right) \sqrt{8\nu\omega}$$

Formula for the imaginary part of the orifice impedance

The impedance of the cavity is determined using the depth and the horizontal section of the resonator. This formulation therefor only applies on cavity shapes with a constant section. In order to calculate the impedance for resonators with different cavity shapes another formula was developed.

$$27. Z_v = -j \frac{\rho c^2}{\omega} \frac{S_a}{V}$$

Formula for the cavity impedance using the volume

This formula takes the volume of the cavity instead of the individual dimensions. This formula only applies when the wavenumber times the cavity depth is smaller than 1. Making it so that the formula can not just be applied in all circumstances.

In the paper Absorption of sound by resonant panels (Sacerdote et al., 1951) it is implied that for perforated panel absorbers the cavity is equally divided between the orifices of the perforations. Eliminating the need for cavity separations. Making it essentially an array of Helmholtz resonators. The formula was tested against impedance tube tests confirming the implication made earlier in the paper.

### 1.3.2.2 ¼ wavelength tubes

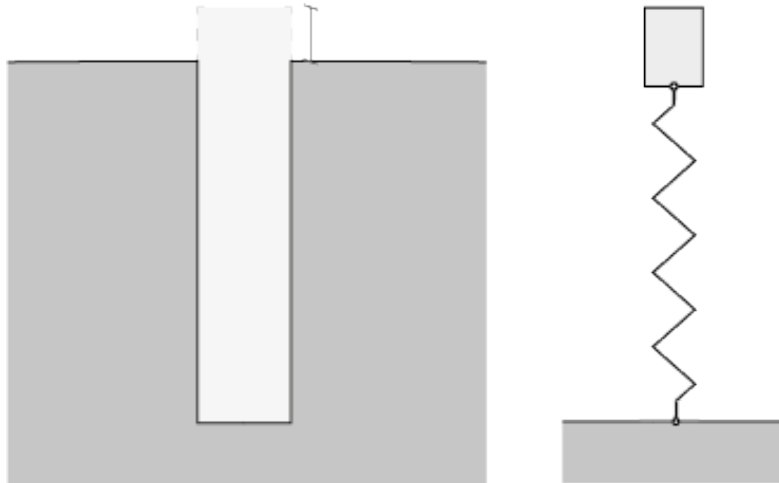


Figure 12: Quarter wavelength tube

¼ wavelength tubes are another type of acoustic resonator. The tube resonates when ¼ of the wavelength fits inside of the tube. As with the Helmholtz resonator the tube can be described as a mass spring system where the functionality is continuously distributed in the tube (van den Eerden, 2000). As with the Helmholtz resonators the tube has an end correction due to the inlet effects. The Acoustic impedance of ¼ wavelength tubes is only dependent on the radius and the length of the tube.

$$28. f = \frac{c}{4(L+\Delta L)}$$

Formula for the resonant frequency of a ¼ wavelength tube. Can be multiplied with (2n-1) to get the harmonics.

Besides the visco-thermal damping the tube reflects the incoming frequency back into the room. The reflection is out of phase with the original wave. At points where the original wave had low pressure the reflected wave has high pressure therefore the pressure equalizes. This is called passive destructive interference (van den Eerden, 2000).

$$29. Zw = \frac{1}{\sum \frac{\Omega_i}{Z_i}}$$

Formula for the acoustic impedance of a wall with multiple different ¼ wavelength tubes, with Zi being the acoustical impedance of the resonators i and Ω being the porosity relating to resonators i.

$$30. \Omega = \frac{N \cdot A_{tube}}{A_{wall}}$$

Formula for the porosity of a wall, with N being the number of identical tubes, Atube being the cross-sectional area of the tube and A wall being the area of the wall.

$$31. Z_i = \rho c \frac{\Gamma_i n_i}{j\gamma} \coth(\Gamma_i k L_i)$$

Formula for the acoustic impedance of a ¼ wavelength tube, with Γi being the propagation constant of tube i, ni being a polytropic coefficient which relates the pressure and density (van den Eerden 2000).

$$32. \Gamma = \sqrt{\frac{J_0(j\sqrt{j}s)\gamma}{J_2(j\sqrt{j}s)n}}$$

Formula for the wave propagation coefficient, with  $J_0$  and  $J_2$  being the Bessel functions of the first kind of order 0 and 2,  $s$  being the shear wave number and  $\gamma$  being the ratio of specific heats.

$$33. n = \left(1 + \frac{\gamma-1}{\gamma} \frac{J_2(j\sqrt{j}s\sigma)}{J_0(j\sqrt{j}s\sigma)}\right)^{-1}$$

Formula for the polytropic coefficient, with  $\sigma$  being the square root of the Prandtl number.

$$34. \sigma = \sqrt{\frac{\mu C_p}{\lambda}}$$

Formula for the square root of the Prandtl number, with  $\mu$  being the dynamic viscosity in Pa\*s,  $C_p$  being the specific heat in J/kg\*K and  $\lambda$  being the thermal conductivity in W/m\*K

$$35. s = R \sqrt{\frac{\rho \omega}{\mu}}$$

Formula for the shear wave number, with  $R$  being the radius of the tube.

The absorption coefficient for the quarter wavelength tubes can be calculated with the low reduced frequency model. Which was developed by Zwicker and Kosten in 1949. This solution has proven to be the most suitable for practical applications (Tijdeman, 1975) and is therefore the one presented in this report.

#### 1.3.2.2 Panel absorbers



Figure 13: Panel absorber

Panel absorbers are a commonly used absorbers for low frequencies. A sheet material is placed in front of a cavity. When the panel is hit with its resonant frequency the panel starts to vibrate. As with the other resonant absorbers the system can be described as a mass spring system. The panel being the mass and air in the cavity being the spring. The mounting points of the panel convert the acoustic energy into heat. A panel absorber is often combined with porous material. The addition of the porous material reduces the absorption coefficient significantly but widens the range of absorbed frequencies (van der Linden, 2016).

The performance of panel absorbers is hard to predict. This is because the edges of the panel need to be airtight attached to a frame. This causes a part of the panel to be constrained from movement and thus not resonate. This decreases the effective mass of the absorber. The panel can be attached to a non-rigid material so the entire mass can vibrate freely. Ensuring the cavity is airtight can prove to be problematic (Cox, D'Antonio, 2009).

### 1.3.2.3 Micro perforated panel absorbers



14: Micro perforated panel

Micro perforated panels are panels with holes in them often measuring less than one millimeter. The holes function as the neck of a Helmholtz resonator but are only slightly larger than the boundary layer created by the soundwave. This causes very high viscous losses (Cox, D'Antonio, 2009). The high viscous losses eliminate the need for fibrous material in the cavity to enhance the performance. Altering the performance of the panel can be done by curving, tilting or shaping it to redirect or diffuse the sound.

D.Y. Maa (1998) showed that for high absorption coefficients the sheet thickness and the hole diameter need to be approximately the same (Cox, D'Antonio, 2009). When absorption for higher frequencies is required the panel and the holes need to become very thin (0.1 mm). The thin material, small holes and high precision required can cause problems when manufacturing.

An advantage of the micro perforated panel is that it can be a rather strong panel. The sheets with the perforations can be made from any material and can be attached to for example a honeycomb structure to increase the strength of the panel. Another advantage is that the panel does not get clogged up with dust. Due to the vibrating air in the neck of the resonator the dust is blown out of the orifice (Cox, D'Antonio, 2009).

### 1.3.4 Conclusion on resonant absorbers

Due to the large amount of information available and the geometric freedom, the Helmholtz resonator is the chosen resonator type for this project. Because of the large amount of research done for Helmholtz resonators all of the values that will be measured in the end can be calculated beforehand to predict the outcome of the physical test. Besides the availability of information, the Helmholtz resonators allow for the combining of the cavities. This gives the opportunity to reduce the geometrical complexity and possibly material.

	Geometrical complexity, precision required	Predictability	Low frequency absorption	Broadband absorption
Porous absorber	● ● ● ● ○	● ● ○ ○ ○	● ○ ○ ○ ○	● ● ● ● ●
Helmholtz resonator	● ● ● ○ ○	● ● ● ● ●	● ● ● ● ●	● ● ○ ○ ○
1/4 wavelength tube	● ● ○ ○ ○	● ● ● ● ○	● ● ● ● ●	● ○ ○ ○ ○
Panel absorber	● ● ● ● ○	● ○ ○ ○ ○	● ● ● ● ○	● ● ○ ○ ○
Micro perforated panel	● ○ ○ ○ ○	● ● ● ○ ○	● ● ● ● ○	● ● ● ● ○

Figure 15: Conclusion table regarding resonators

#### 1.4 Acoustics by additive manufacturing, previous work

In recent years research was done regarding passive broadband absorption through resonant absorbers. To be able to build upon this research short summaries of previous work are presented in this part of the report. Both theoretical and practical progress will be reviewed so a good view on the current state of progress can be formed.

##### 1.4.1 Oliver Godbold, 2008

In 2008 Oliver Godbold wrote his doctoral thesis on the topic of broadband absorption by using rapid manufacturing. He found that single material broadband absorption was possible with Helmholtz resonators.

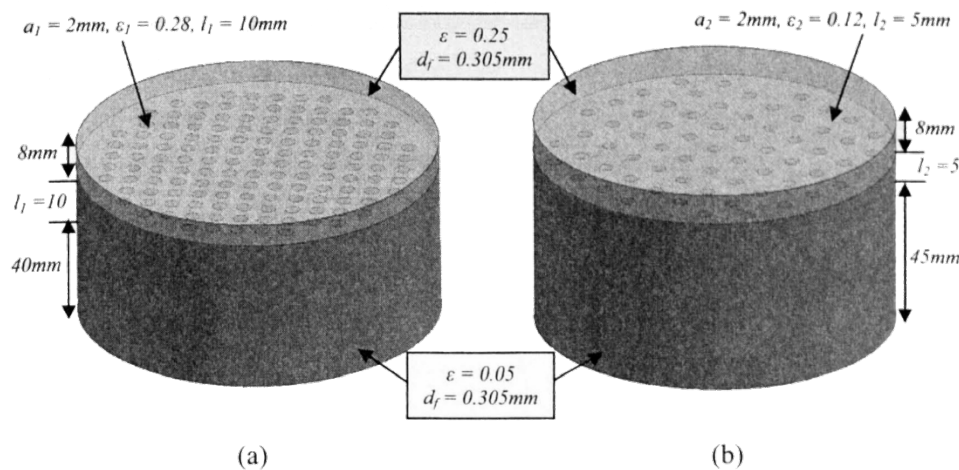


Figure 16: Godbold (2008)

Godbold attempted to increase the resistance of the cavity by adding resistive material. This was done by using additive manufacturing techniques. The main focus was to increase the bandwidth of the absorbers by altering the cavity geometry. The orifice size, orifice shape and cavity volume are kept constant. The addition of a perforated plate inside of the cavity showed promising results. The resistance provided by the perforated plate caused an absorption coefficient of 0.4 over three octaves. Using rapid manufacturing made it possible to add the material inside the cavity while ensuring airtightness.

The most successful of the experiments was the design of two perforated panels behind each other. The first one tuned to a lower frequency and the one further in the tube tuned to a higher frequency. Both the theoretical models and the physical models showed that a sound absorption of over three octave bands is possible.

All of the experiments done within this research were done inside an impedance tube. This is mainly because in 2008 the additive manufacturing techniques were not as far developed that  $10\text{m}^2$  of the resonant material could be produced.

##### 1.4.2 Xiaobing Cai et al., 2014

Cai et al. (2014) investigated the possibility of reducing the panel thickness of resonant absorbers. Experiments were done on  $\frac{1}{4}$  wavelength tubes and on Helmholtz resonators.

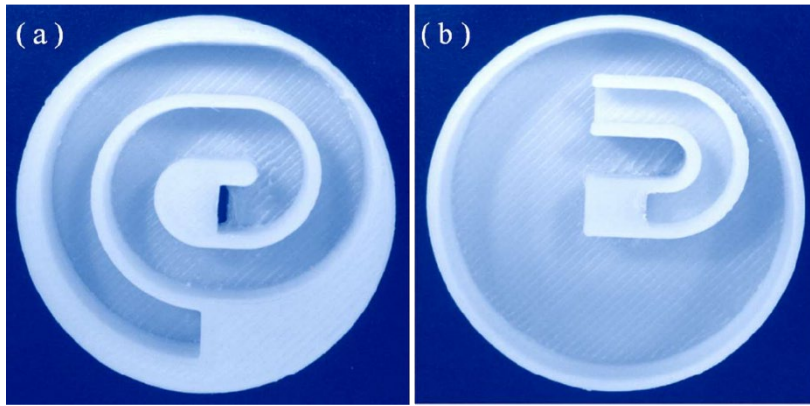


Figure 17: Cai et al. (2014)

The  $\frac{1}{4}$  wavelength tubes were coiled up behind the front face of the panel. Resulting in a panel that has a thickness of about two percent of the wavelength. Both the theoretical analysis and experimental measurements showed that the coiled tube performed as previous theory expected and showed good resonant qualities.

Besides the  $\frac{1}{4}$  wavelength tubes, Helmholtz resonators were also tested. As concluded in section 1.3.2.1. the shape of the resonator does not affect the resonant frequency at which the resonance occurs. Therefore, an attempt was made to reduce the thickness of the resonator to about one percent of the wavelength. As with the spiral tube both the theory and the experiments confirmed that it is possible to obtain resonance within an thin panel.

#### 1.4.3 Junfei li et al., 2016

In 2016 Junfei et al. designed and tested a metasurface based on coupled resonators. This resulted in near complete absorption of the targeted frequency, both theoretical and experimental. The project was not focused on broadband sound absorption but the acoustic coupling of the resonators and achieving perfect absorption. A second focus of the project was to create a durable and structurally stable module that would not have to rely on membrane type absorption.

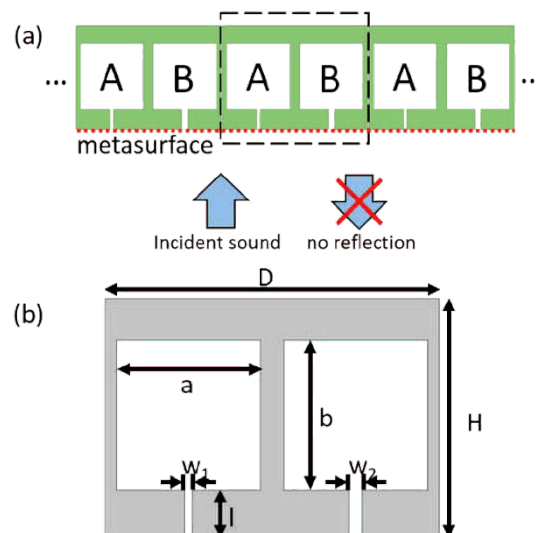


Figure 18: Li et al. (2016)

The two resonators are focused on two slightly different frequencies, so the total absorption was observed. The two resonators have a phase angle of 180 degrees between them so the oscillation of the air in the resonator is opposite. The impedance tube test showed an absorption of 98.4% and more

than 50% absorption over a bandwidth of 100Hz. The samples were made with fused filament fabrication and made of acrylonitrile butadiene styrene.

#### 1.4.4 Zhiwen Ren et al., 2022

Ren et al. (2022) designed and tested a low-frequency broadband sound absorber that would have enough strength so it could be used within another structure. The panel was made up of honeycomb shaped CRIET resonators (cavity resonators with internally extended tubes). Multiple resonators were designed to react to different frequencies. When all the resonators were designed, an optimization was performed to place the individual resonators in such a way that the coherent coupling effect would have the least amount of negative effect. The optimization resulted in a panel that could absorb sound between 600 and a 1000 Hz with an average absorption of 0.9. Afterwards these simulations were validated with an experiment.

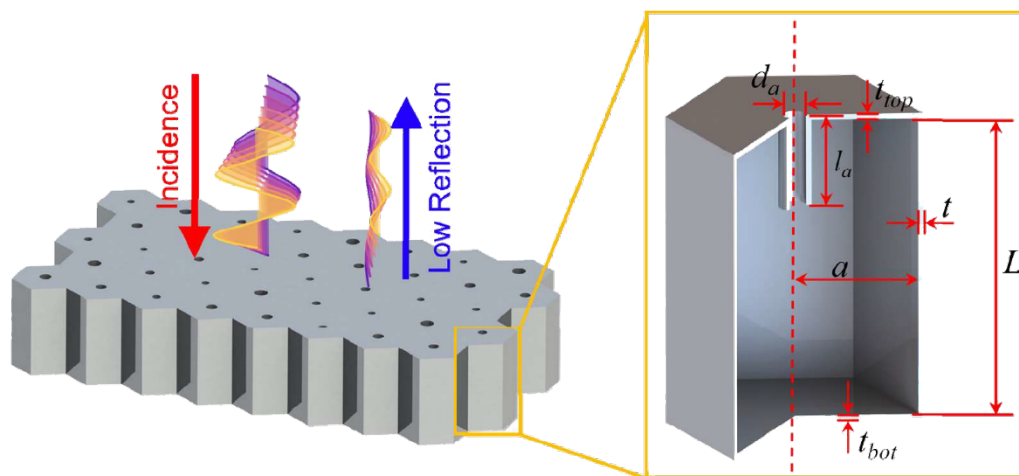


Figure 19: Ren et al. (2022)

Besides the acoustic properties the mechanical properties of the panel were also tested. The structure performed well in the compression experiments. It could therefore be applied within another structure to create a multifunctional structure.

#### 1.4.5 Previous student work

Within the master track Building Technology at the Delft University of Technology some research on the topic of resonant absorbers has already been done by previous students. Presented here is a short overview.

In 2012 Fonteini Setaki graduated of the topic of acoustics by additive manufacturing. The goal was to combine additive manufacturing with room acoustics. This was done by designing a sound absorber that was completely reliant on its geometry. Passively destructively interfering tubes where the chosen sound “absorber”.

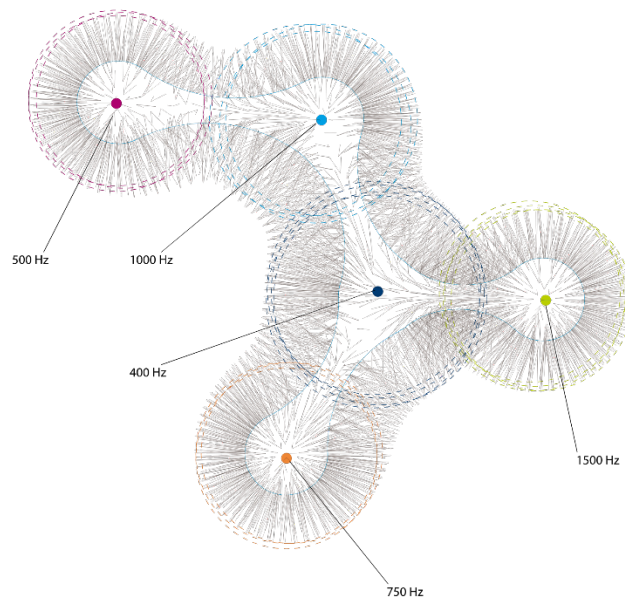


Figure 20: Setaki (2012)

The result was an organic looking structure that could be hung from a ceiling. This research was done in an early stage of acoustics by additive manufacturing. The aim therefore was to see how the integration between the two fields was possible and how the advantages of additive manufacturing could aid in the performance of acoustic absorption.

In 2016 Bettine Gommer graduated on the topic of adding resistance to Helmholtz resonators. This was done by adding geometry in the neck of the resonator to increase the impedance. The idea being that sudden changes in geometry can change the pressure and speed. Which in turn could increase the impedance.



Figure 21: Gommer (2016)

An increase in resistance was obtained by adding surface area in the direction of the flow and altering the orifice shape. The latter showed potential because both the absorption and the bandwidth increased but the resonant frequency remained the same.

Sebastian Costa graduated in 2016 on the topic of thin resonant acoustic panels for the absorption of low frequency sound. He attempted to coil up the quarter wavelength tubes behind a panel to create super thin resonant panel.

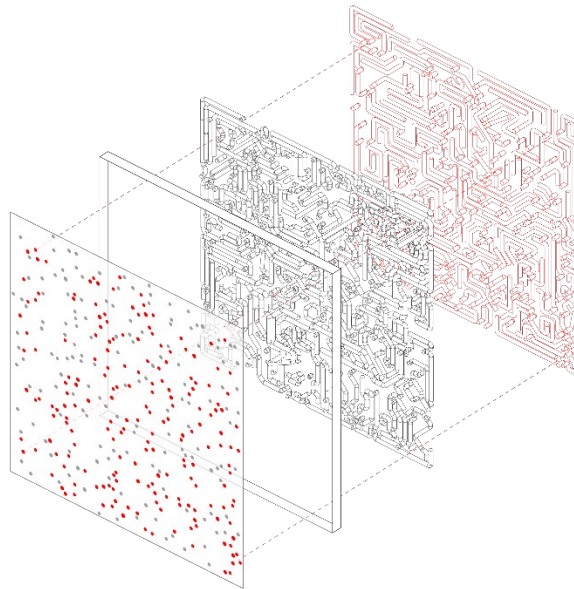


Figure 22: Costa (2016)

Within his thesis he focused on testing small scale samples to see if there was a conformation between the calculated and the measured results. Most experiments agreed with the theoretical results. The design of the full panel was only theorized due to the high cost of printing the sample.

Ioanna Christia graduated with her project STRAW in 2017. The main objective of this thesis was to decrease the cost of production for resonant acoustic absorbers. This was done by looking at the influence of geometry on the manufacturing process. A requirement for the panel was to make it thin, a thickness of approximately  $1/10$  of the wavelength.



Figure 23: Christia (2017)

The result was a 1:1 panel made of ordinary drinking straws. The panel was tested at the faculty of architecture. It showed indications of lowering the reverberation time, but the sample seemed too small to have the desired result. The prototype was harder to make than expected and less stable due to its very low weight.

In 2018 Tom Scholten wrote his graduation thesis on achieving broadband absorption using coupled quarter wavelength tubes. The aim was to further investigate the possibilities of coupling multiple resonators to achieve broadband absorption. The goal was to provide a design tool which could be applied to multiple cases.

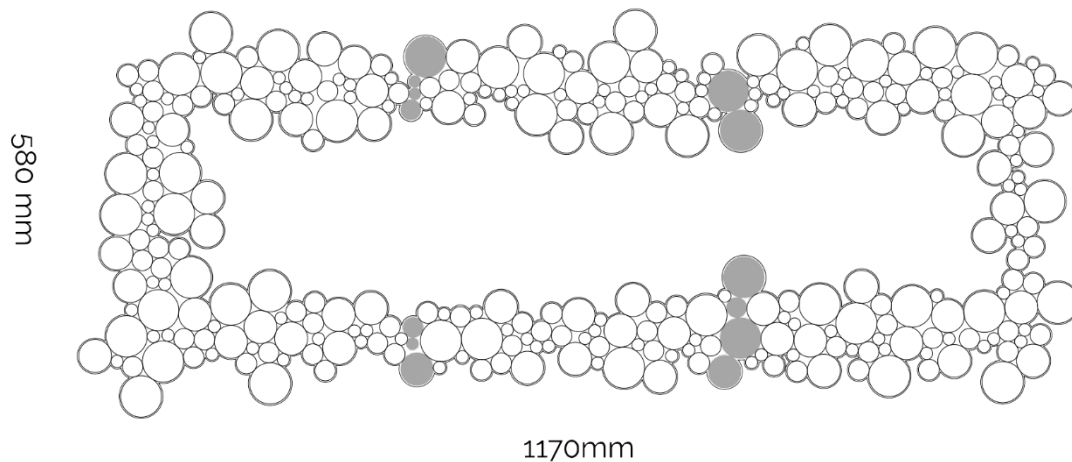


Figure 24: Scholten (2018)

He found that at the time of writing the report there was no possibility to create a broadband absorbing device based on coupled quarter wavelength tubes. The effect the tubes have on each other is rather large and not always easy to predict. With an increase in the number of tubes the complexity of the behavior of the  $\frac{1}{4}$  wavelength tubes increases exponentially (Scholten, 2018). He was able to create resonators with two coupled tubes but due to the limitations in additive manufacturing more tubes where not possible.

## 1.5 Production techniques

In this part of the literature review possible production techniques will be presented. Quite some research has focused on additive manufacturing techniques when designing resonant absorbers (Cai, 2014)(Godbold, 2008)(Li, 2016)(Ren, 2022)(Setaki, 2014). Because of the high geometrical complexity of the resonant absorbers, additive manufacturing was the most apparent choice. Since the focus of this research is to reduce the geometrical complexity of the resonant absorbers, other techniques besides additive manufacturing will also be discussed, for their ability to produce some types of geometry is more efficient.

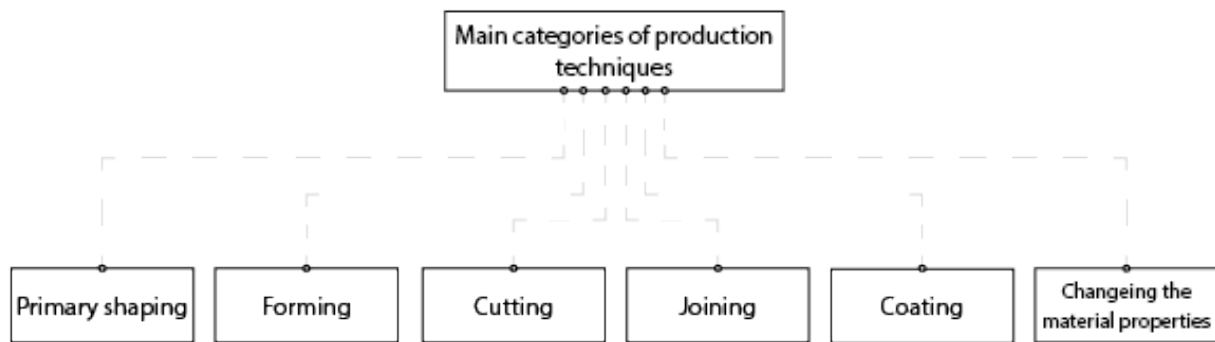


Figure 25: Primary groups of production techniques

According to the standard DIN 8580 there are six main categories of production techniques. The groups are made on the criteria of what the process does to the material cohesion. The six groups of production techniques are: Primary shaping, forming, cutting, joining, coating and changing of material properties. Every production technique falls within at least one category, although sometimes multiple groups are applicable to a technique (Kals et al., 2007).

1. Primary shaping is shaping a material from something without a shape to the desired shape (Kals et al., 2007). This is often accomplished by changing the phase of the material. Examples of primary shaping are casting or additive manufacturing. Primary shaping is a category that has great potential when making complex shapes. By altering the phase of a material, it can be shaped into any other shape. This allows for complex geometry.
2. Forming is the shaping of a material without changing the phase of the material (Kals et al., 2007). Often large forces are applied to the material causing permanent deformations without altering the mass or the volume of the material. An example of forming is rolling. Forming has the advantage over primary shaping that no heat is required. The disadvantage is that the force required is a lot bigger.
3. Cutting removes a part of the material that is not desired (Kals et al., 2007). Cutting leaves leftover material which can possibly be used in another production process. Some cutting techniques destroy the undesired material leaving it useless. An example of cutting is milling. An advantage over the previously mentioned categories is that no heat and no large forces are required. The downside compared to the previously mentioned categories is the waste material that is generated by using cutting.

The last three groups of processes do not have the ability to alter the geometry of a material. For the completion of the overview, they are presented below but the groups will not be considered further in the report.

4. Joining adds parts of material together (Kals et al., 2007). This can be done either permanently or detachable. Joining can be done with only the materials that need to be joined but can also use other materials to join the two. Examples of joining are bolting or welding.

5. Coating adds material to the surface of another material (Kals et al., 2007). This can for example be done to protect the underlying material or to alter the aesthetics. Examples of coating are painting or chroming.
6. Changing the material properties often refers to the thermal processing of metal (Kals et al., 2007). Changing the material properties can for example be done to make a material stronger or less prone to wear. Examples of changing the material properties are tempering or polishing.

The main focus will be on a production method that allows for fast production and relatively cheap materials. The accuracy of the production technique needs to be above a certain threshold for the resonators to consistently resonate at the frequency they were designed to. The accuracy of the process is dependent on a lot of factors and differs between machines and different brands.

From the groups presented above primary shaping and cutting seem the most appropriate for this thesis. Forming has the ability to produce complex geometry but lacks the consumer availability that the other groups do have. Besides the availability most forming techniques lack the ability to change the output geometry quickly based on the inputs that the digital model provides. Often a mold is required or the alteration to the geometry is very limited.

The presented techniques have been selected for their compatibility with CAD software and their availability for consumers. Either as a service or being a process available for home use. Cutting methods presented in this chapter will focus on machining sheet material. Using sheet material would result in a reduction of the geometrical complexity as compared to additive manufacturing techniques due to reduction of one dimension. The primary shaping techniques presented in this chapter are focused on additive manufacturing and thus three dimensional.

#### 1.5.1 CNC

CNC stands for computer numerical control. This means that a machine is controlled with number inputs given by a computer (Kief et al, 2013). The idea behind numerical control is to be able to change the task a machine is performing as fast as possible, without error and without manual interference. This is done by taking the dimensions of a drawing and converting those into relative positions of the machine. By measuring the current position of the head, the distance that each axis would need to move could be communicated to the servos. The servos can then move the head to the desired position. The inputs for the machine would consist only of numbers, hence the name numerical control (Kief et al., 2013).



Figure 26: 3 Axes CNC machine

For the movement of CNC machine, the cartesian coordinate system is used. Every movement the head of the CNC machine has to make can be described in a combination of numbers relating to the three axis and the three rotations around these axes (Kief et al., 2013). In some applications the head makes

the movements to reach the part. In other applications the part moves so it reaches the head. Not all CNC controlled machines can move in all directions or have the ability to rotate in any or all directions.



Figure 27: 6 Axes CNC machine

There are many types of numerical control systems with different applications. Here, only the systems from the group cutting that are able to machine sheet material are presented. For these are the most applicable to this thesis. The way the system operates remains very similar between the different options only the tool on the head differs. For this reason, only the characteristics of the head will be discussed.

*1.5.1.1 CNC milling*

The NC mill was the first NC type machine. Between 1949 and 1952 the Parsons Corporation and MIT developed the first control system for machining tools. For this research the first three axis continuous path milling machine was build (Kief et al., 2013). The machine was built for the US air force to create parts that where difficult for a human to produce.

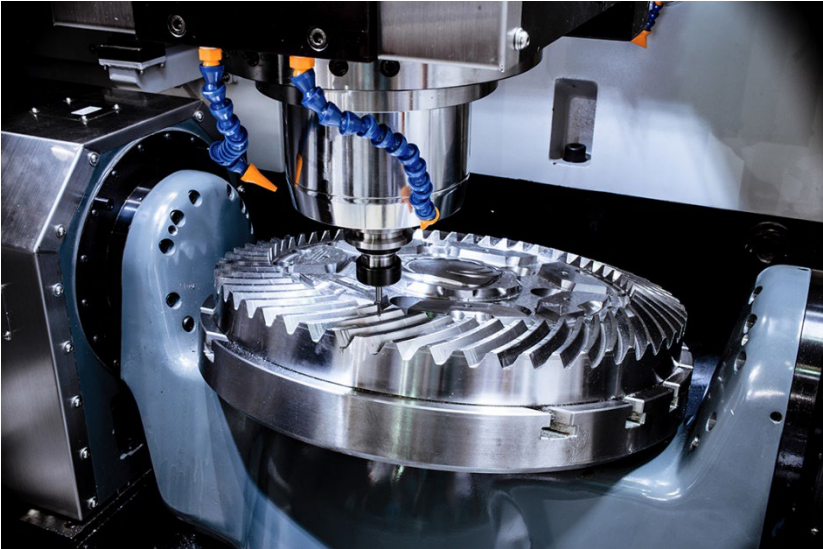


Figure 28: CNC milling machine

A CNC milling machine is essentially a computer operated router. A block or sheet of material is placed on the working bed of the machine. The head with the router bit moves around to take away material

from the sheet or block. The router bit rotates at a very high speed, moving perpendicular to the face of the material that is being milled (Groover, 2010).

The materials that can be used with CNC milling depend largely on the tool attached to the head (Zhang, 2021). Both metals and wood are common materials to mill. Milling is less suitable when working with brittle or soft materials like ceramics or textiles respectively.

#### *1.5.1.2 Laser cutting*

In 1967 Peter Holdcroft used a CO<sub>2</sub> focused laser beam to cut through a sheet of metal. This laser cutter was developed because the automotive industry was unsatisfied with the speed and precision of the, at the time, current thermal cutting processes (Hilton, 2007).



Figure 29: Laser cutter

Laser machining systems use lasers to cut through a material. A Laser is a beam of light that theoretically consist of one wavelength and all the light beams are almost parallel (Groover, 2010). This results in a high-power density on a small area. The laser vaporizes, melts or burns the material.

A laser does not only have the ability to cut a material but also to engrave with a very high precision. Holes down to 0.025 mm are possible due to the small area where the light beams are focused. The surface finish or cutting edges are smooth because of the high precision and often do not require further post processing (Groover, 2010).

Virtually any material can be machined with a laser cutter. Because a laser is able to melt, burn or vaporize material, any material can be machined from fabric to high strength metals. Most commonly though a laser is used to machine hard sheet material.

#### *1.5.1.3 Water jet cutting*

Cutting sheet metal with high pressure water was patented by Norman Franz in 1968. The machine was used by a furniture manufacturing company to cut wood (Birtu et al., 2012).



Figure 30: Water jet cutter

Water jet cutting uses a high-pressure stream of water to cut through a material. Water is pressurized up to 400MPa after which it is directed to the material that needs to be cut. The speed of the water can reach up to 900m/s (Groover, 2010). Due to the large pressure and the high speed, the nozzle of the water jet needs to be made of a gemstone to withstand the high forces. When the force of the water is not enough to cut through the material abrasive material can be added to the water stream to increase the cutting potential of the method (Kief et al., 2013).

The materials that can be cut by water jet cutting are mainly flat sheet materials like plastic, cardboard and leather. Brittle materials are not suitable for water jet cutting because these materials tend to crack under the high pressure of the jet. Most commonly soft materials like paper and cardboard are cut with a water jet cutter (Groover, 2010).

#### 1.5.2 Additive manufacturing

Another group of CNC methods are the additive manufacturing methods. These are part of the group primitive shaping because the material changes phase while the model is being build (Kals et al., 2007).

In the 1980's in different parts of the world patents were filed for the same kind of technology. (Gibson, 2021). A machine that could produce 3D models by building up layers of material. This was a completely new way of producing three dimensional models. Additive manufacturing differs from traditional manufacturing techniques in the fact that it adds material instead of taking it away (Zhang, 2021). This reduces the amount of waste material. Some types of additive manufacturing techniques do require some support material to be able to solidify without deforming. Therefore, the waste material is not completely eliminated.

Due to the expiring of the original patents the cost of a 3D printer has decreased significantly, making it more accessible (Bhatia, 2021). Besides the price reduction, the quality of the printers and the amount of print materials has increased (Gibson et al., 2021). The precision a printer has now is much better than only a couple of years ago. The increase in the use of rapid manufacturing is also due to the development of other technologies. Computer-aided design, computer-aided manufacturing and computer numerical control play an important role when working with additive manufacturing (Gibson et al., 2021). Without the development of these technologies the state of additive manufacturing would not be the way we see it today.

Additive manufacturing was originally used by designers to show the form of an object. Due to the technological advances and increased precision models can now also be used to test fit for the final element. Besides the printers the materials that can be used have also improved. Due to this

improvement parts made by additive manufacturing can also be used as the final product (Gibson, 2021).

The production of a part made by additive manufacturing always starts with a digital model made within a CAD software. Every part needs to be a solid, if the part would lack a thickness the element cannot be printed. When the CAD model is done, it can be converted into a STL file. An STL file is the most common way for a printer to receive a 3D model. When the machine has the STL model and has some information regarding the material, it can start making the part (Zhang, 2021). Presented in this part of the literature review are a couple of the most common additive manufacturing techniques.

#### 1.5.2.1 Stereolithography

In 1984 Charles Hull applied for a patent on the process of Stereolithography. Being one of the first to patent and manufacture an additive manufacturer (Cooper, 2001).

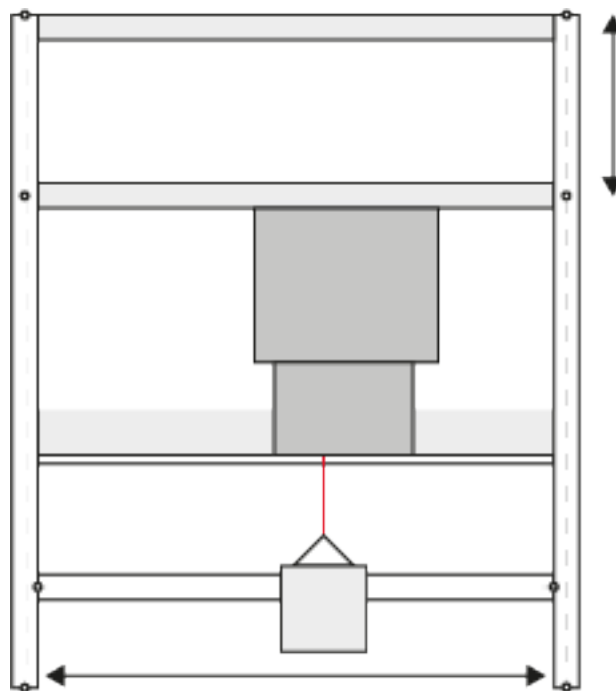


Figure 31: stereolithography

Stereolithography works by shooting ultraviolet light at a reservoir of resin. When the light hits the resin, it cures very locally, allowing for very precise models to be produced. The light can move in the x and y direction allowing it to cure the material in different places. When a layer of the model is complete, the bed on which the model rests, moves down. The movement of the bed allows the resin to flow over the solid layer, allowing the ultraviolet light to cure the next layer. This process continues until the entire model is complete (Davoudinejad, 2021).

A disadvantage of this type of additive manufacturing is that there is a need for support materials when overhangs are created. These need to be removed by hand after the model is complete. Besides the removal of the support materials the model also needs to be cleaned after the printing is completed. A special solvent needs to be used in order to remove all of the leftover resin on the model. A third disadvantage of stereolithography is the cost of the proses. The resin needed for the printing of the material is quite expensive.

A large advantage of stereolithography is the precision at which the models can be produced.

Stereolithography uses photopolymers. This is a specific type of material that changes its physical or chemical properties when it is exposed to light (Crivello, 2013). This specific requirement on the material greatly limits the applications for which stereolithography can be used.

#### 1.5.2.2 Selective laser sintering

Carl R. Deckard invented the selective laser sintering method. The method was patented in 1986.

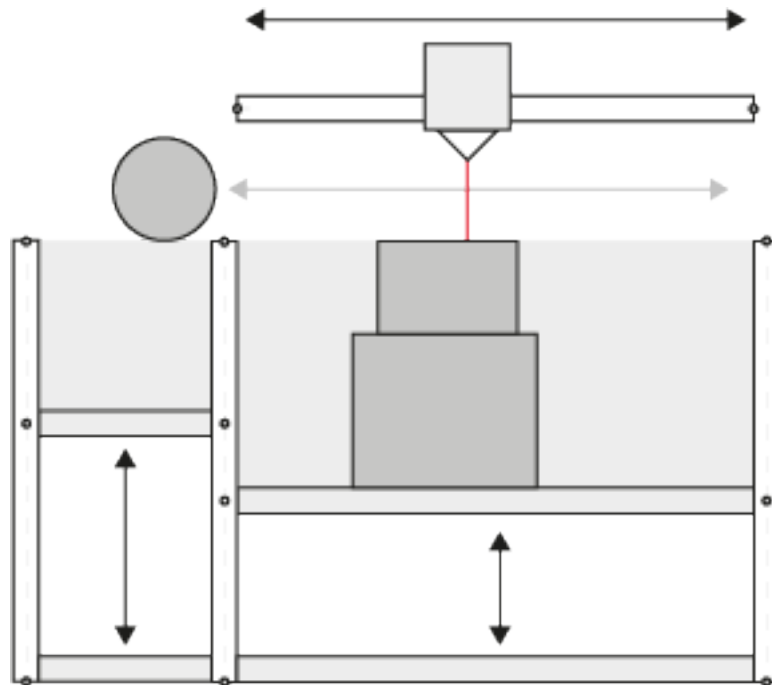


Figure 32: Selective laser sintering

Selective laser sintering uses a laser to produce three dimensional models. The laser is aimed at a container filled with powdered material. The laser causes the powder to partially melt locally and solidify. The laser can move over the x- and y-axis allowing the creation of two-dimensional layers. When the layer is finished the bottom of the container moves down. New material is placed on top of the finished layer and the material is compressed with a roller. The laser is now able to create the next layer of the model on top of the previous layer. When the model is done the container is removed and the model emerges from the excess powder (Yasa, 2021).

An advantage of selective laser sintering is the lack of need for support materials. When the model is made, the excess powder acts as a support for the model. When the printing is finished only the powder needs to be removed before the model can be used. The models made by SLS are often stronger than models produced by other manufacturing techniques (Zhang, 2021).

The surface finish of selective laser sintering is often inferior to the surface finish of liquid based additive manufacturing techniques. The time it takes to make a part with SLS is also often longer compared to other manufacturing techniques. This is due to the preheating and cooling of the model (Gibson, 2021).

Laser sintering, like most additive manufacturing techniques, mainly uses plastics. However, besides plastic SLS also has the ability to process metal or ceramics. To process metal a stronger laser is needed to melt the material (Yasa, 2021).

### 1.5.2.3 Fused filament printing

In 1988 Scott Crump developed the first Fused Deposition modeling printer (Siemiński, 2021). The printing technique was patented by the Stratasys Company until 2009. Since the patent expired, the production of this type of printer has increased a lot. Fused filament printing is currently the most popular type of 3D printing (Hubs, 2020).

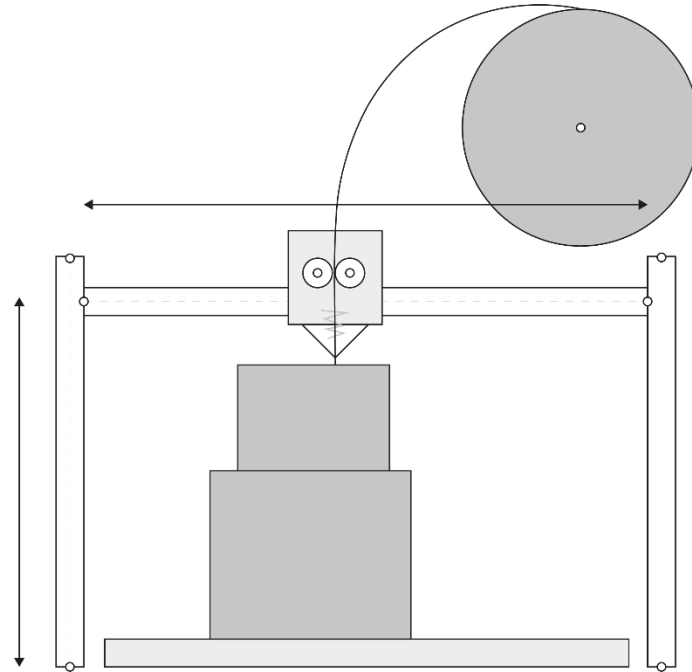


Figure 33: Fused filament printing

Fused filament printing uses a solid material. Often this is a coil of wirelike material. This material is fed into a head where it is heated to its melting point. The material is pressed out of a nozzle to form the desired shape. Most commonly the head can move in all three directions to create any shape. The head is unable to rotate, limiting the printer to work in flat layers in the x- and y-directions before starting the next layer on a higher z coordinate (Zhang, 2021).

The main advantage of fused filament printing is the low costs. Both the cost of the machine and the material are quite low, making it the most accessible additive manufacturing method. The process requires only the printer itself. No additional finishing is needed, and the printer can be placed in any room. A controlled environment is not necessary.

A disadvantage of fused filament printing is the need for supporting materials. The material does not cure instantly. When an overhang is created, the need for support material arises. When the model is fully cured the supports can be removed. This requires a small amount of post processing before the model is finished. A second downside to this production technique is the poor resolution and surface finish (Zhang, 2021). Compared to the techniques discussed in chapter 1.4.1.1 and 1.4.1.2 the accuracy is quite low possibly resulting in values that are slightly off from the calculated values when working with small resonators.

Most commonly, thermoplastics are used for fused filament printing. Thermoplastics are plastics that melt when heated and become solid when cooled down again (Siemiński, 2021). There are many different types of thermoplastics with different material properties.

### 1.5.3 Conclusion on the presented production techniques

This thesis aims to investigate the potential of cheaper techniques to increase the availability of resonant absorbing panels. Figure 34 is based upon findings from Groover (2010), Kals et al. (2007) and Kalpakjian and Schmid (2008). The scores are given in a way that more points means better score e.g. a cheap process will get more points than a expensive process. The author is aware that the sources used to make figure x are not very recent. It is assumed that the general proportions between the productions processes has remained the same.

	Price	Precision	Speed
CNC Milling	● ● ● ● ○	● ● ● ○ ○	● ● ● ○ ○
Laser cutting	● ● ● ● ●	● ● ● ● ●	● ● ● ● ○
Water Jet Cutting	● ● ○ ○ ○	● ● ● ● ○	● ● ● ● ●
Stereolithography	● ○ ○ ○ ○	● ● ● ● ●	● ○ ○ ○ ○
Selective laser sintering	● ● ● ○ ○	● ● ● ● ●	● ○ ○ ○ ○
Fused filament printing	● ● ● ● ○	● ● ○ ○ ○	● ● ● ○ ○

Figure 34: Concluding table regarding production techniques

As can be seen in figure 34 laser cutting scores high in all three categories. The main downside of laser cutting is the general inability to work on three dimensional objects. With the reduction of the geometrical complexity of the resonators this becomes less of an issue. Laser cutting will therefor be the starting point regarding production techniques within this Thesis.

From the additive manufacturing techniques fused filament printing has the lowest price. The precision of this technique is lower compared to the other techniques but the relative low price of the technique makes it interesting to investigate within the scope of this thesis. If the need for three dimensional geometry does arise, fused filament printing will be the selected production technique.

CNC milling is a third method with relative low costs. For machining flat sheets of material it is generally outperformed by laser cutting. But the ability to generate three dimensional geometry makes it an interesting production method. Although not the starting point regarding production techniques in both two and three dimensions, it will be considered as an option going forward.

## 1.6 Computational Design

The aim of this thesis is to provide a workflow that is able to generate design solutions to the problem frequencies. With one of the outputs being the drawings required to make a resonant absorber. The changing nature of the inputs does not allow for a single solution. Every input results in a different solution. For the automation of the design a computational workflow is needed.

The name computer-aided design originates from the Massachusetts Institute of Technology, where in 1959 D. Ross and his team of researchers developed the first design tool for a computer. In the paper “Computer-aided design related to the engineering design process” (Coons, Mann, 1960), the potential of using a computer to aid the designs in many fields of work is described.

CAD modeling can be done in either 2D or 3D. Dependent on the application of the model a different type of CAD will be used. When the end goal of the CAD model is to produce a laser cut template a 2D model is needed for most laser cutters can only work in two dimensions. A fused filament printer requires a 3D model to generate a three-dimensional model.

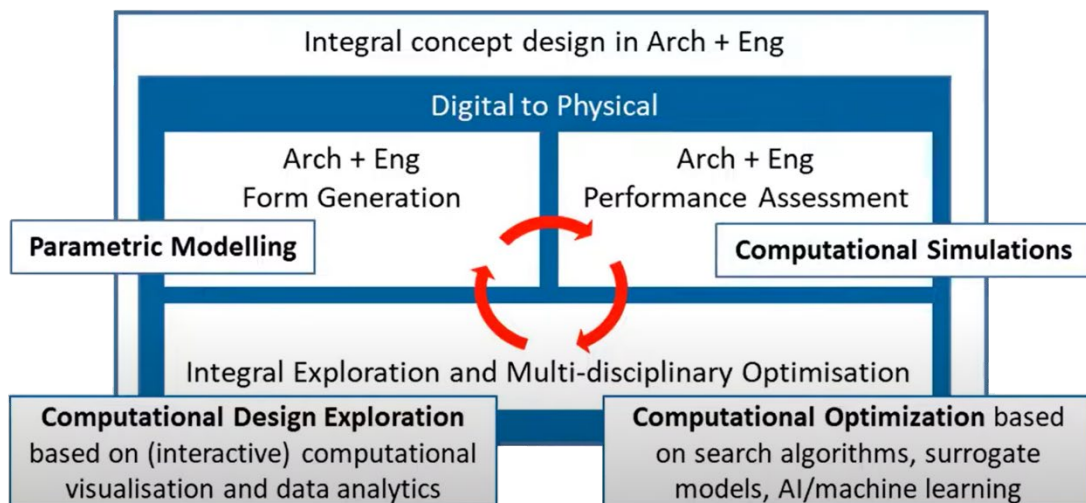


Figure 35: Performative computational architecture

The use of computer-aided design allows for the connection to other types of software which can enhance or verify the design, allowing the ability to create a workflow between the different software types according to the workflow presented in figure 35. The framework is called performative computational architecture, or PGA (Ekici et al., 2018). This chapter describes the elements that are needed to generate, evaluate and optimize a design based on certain criteria.

### 1.6.1 Form generation

When one is designing certain constraints are set. These constraints can involve physical boundaries due to the size of the building site, or financial constraints due to the budget of the client. Only the solutions that fall within those constraints are available as solutions (Hudson, 2010). Because there is no one solution in design, the designer needs to set some boundaries themselves, in addition to the bounds found within the brief. Experienced designers will create their own constraints quite quickly because they know from experience that certain decisions will lead to unfeasible solutions and others to more feasible ones (Wortmann, 2018).

#### 1.6.1.1 Parametric design

To make a problem a parametric problem the degrees of freedom within the design space need to be identified. The degrees of freedom are the values that can differ within the final design (Hudson, 2010).

A parametric model can be seen as a representation of the design space (Hudson, 2010). In order to create a parametric model, the problems within the design space need to be described, requiring understanding of the underlying concepts of the problem to be able to know what the variations of the problem can be (Aish, Woodbury, 2005). A parametric model allows for easier exploration of the design space which has been defined as a key task within architectural design (Hudson, 2010).

### 1.6.2 Performance assessment

The use of computer-aided design allowed for the coupling of the design software to analysis software to gain feedback on the design. Finite element modeling (FEM) is a method of subdividing a continuous model into discrete elements (Bhavikatti, 2004). This discretization allows for the calculation of all the parts of the model. The boundary conditions can then be introduced onto the generated reassembled model and the result of can then be analyzed after the calculation of the model (Bhavikatti, 2004). Common areas where FEM analyses are used are: structural design, heat propagation or the flow of fluids.

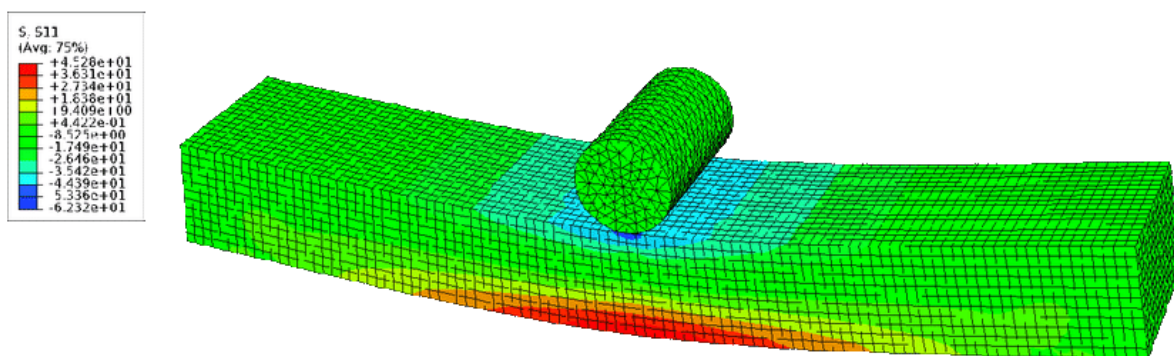


Figure 36: finite element modeling

To simulate the acoustic behavior of materials a Multiphysics software is needed. As mentioned before, in a resonator acoustic energy is converted into heat. This involves the propagation of the sound wave, the interaction between the soundwave and the solid and the conversion of sound into heat (Liu, 2018). The multi-faceted nature of this problem involves multiple physical fields requiring a Multiphysics software to simulate the problem.

### 1.6.3 Optimization

When a design space is defined and the range of the input values is determined, the optimal solution needs to be found. Within certain problems there is only one solution. In architecture the problem is often multi-faceted making the problem multi-dimensional (Hudson, 2010). The differentiation in focus of designers means that there is no one solution. Emphasizing a certain part of the design will most likely result in neglecting another part. Finding a good balance between all of the parts of a design can be a difficult task.

If all the parts of a design can be quantified, an optimization can be performed to get to the best solution. An optimization can either be a single or multi objective optimization. A single objective analysis looks to maximize or minimize one specific output value (Wortman, 2018). Because there is only one value that can be optimized, every outcome can objectively be compared to every other outcome. Dependent on the task either the highest or the lowest value will be the best one.

A multi-objective optimization attempts to optimize the value of multiple criteria at the same time (Wortman, 2018). These criteria can be complimentary, good results on one criteria will also be

beneficial for the other criteria. Or the criteria can be conflicting, meaning the optimization of one of the values will have a negative effect on the second value.

Pareto efficiency describes a situation within a nontrivial multi-objective optimization where none of the criteria can be improved without a negative effect on the other criteria. All the solution of a multi-criteria optimization that have this characteristic are called the Pareto front. The Pareto front is thus not a single point but a collection of points which all can be seen as the optimal solution (Burczyński, 2010). A good approximation is found when the Pareto front is as wide as possible. Meaning a diverse set of solutions that meet the criteria Pareto efficient. From the resulting set of optimizations a single one needs to be selected based on preferences or external criteria (Wortmann, 2018).

Black box optimizations are optimizations where the input and the output are known, but the process in between is unknown (Audet, 2017). Computer simulations are the most common form of black box optimizations. The relationship between the outputs, continuity or smoothness, of the optimization are generally unknown before the optimization is started.

The multi-physics simulations that will be performed in the second part of this thesis can be considered black-box problems. The problem can also be seen as a Pareto efficient problem. All of the problematic frequencies need to be absorbed therefore none can be neglected or considerably lower than the other frequencies. According to Wortmann (2018) there are three important algorithm categories able to solve black box problems. These are Heuristics, direct search and model-based algorithms. A short overview of the three types is presented below.

#### *1.6.3.1 Heuristics*

Heuristic optimization is an optimization where there is no guarantee for success of finding the exact optimum. Often Heuristic methods rely on randomness to generate new possible solutions which are tested simultaneously (Wortmann, 2018). There are many types of Heuristic algorithms, a common example is a genetic algorithm.

A genetic algorithm creates genes which start to search for the optimal solution. When the first generation is done searching the genes evolve by means of chromosome crossover and random mutation (Wortmann, 2018). The genes that performed well will be used to create the next generation of genes similarly to natural selection (Holland, 1992). The advantage of this kind of optimization is the simplicity of the and the ease of implementation (Wortman, 2018). The genetic algorithms tend to be very effective in finding the area where the optimized solution is but are less effective when the actual optimum is needed (Miles, 2010).

#### *1.6.3.2 Direct search*

Direct search optimization techniques are techniques that sequentially examine solutions and compare them to the best solution that has been obtained so far. Based on those results it will be determined where the next solution will be (Hooke, Jeeves, 1960). Direct search methods do not employ derivatives, randomizations, populations or mathematical models (Wortmann, 2018).

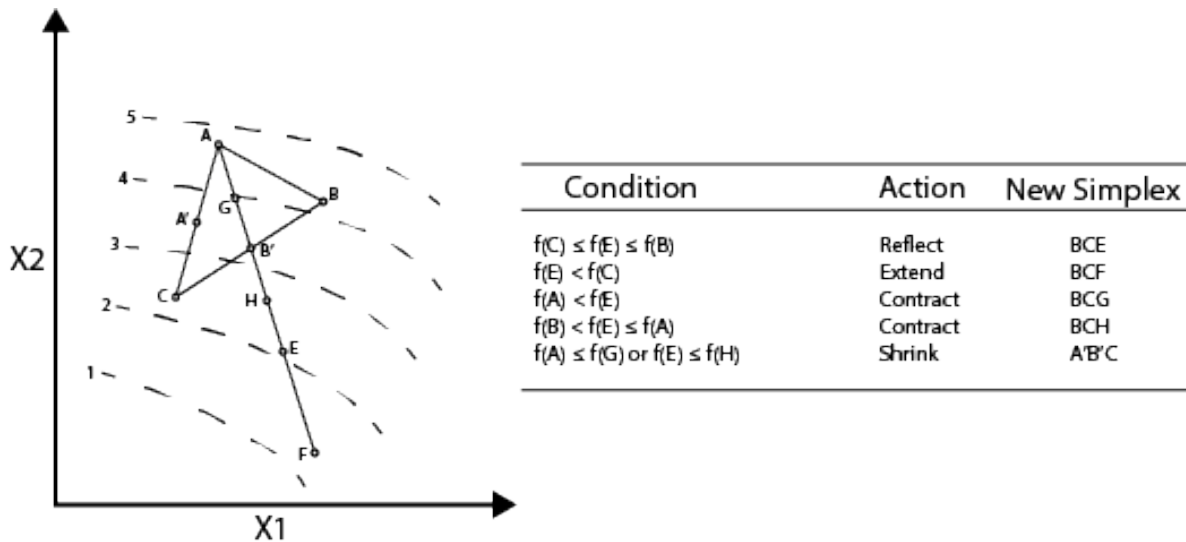


Figure 37: direct search optimization algorithm

A common example of a direct search algorithm is the Nelder-Mead method. The method starts by placing a simplex within the design space. The point of the simplex with the highest value will be moved to another location based on some conditions as seen in figure 37. These conditions are applied to the simplex until a stopping criterion is reached (Olsson, Nelson, 1975). Direct search algorithms are designed to be single objective optimization techniques but versions that can do multi-objective optimizations also exist (Wortmann, 2018)

#### 1.6.3.3 Model-based

In model-based optimizations a surrogate model for the black box function is generated. Surrogate models are a helpful tool for reducing the running time of an optimization (Wortmann, 2018). Instead of looking at all the possible solutions and seeing which one is the best surrogate models run simulations beforehand. The inputs are randomized and evenly distributed among the input parameters. When the simulations have finished the surrogate model interpolates the data found from the simulation to estimate where the optimal solution might be based on an approximation of the function within the black box (Wortmann, 2018).

If the surrogate model is accurate, it can reduce optimization times significantly. This way of performing an optimization requires a large amount of time and work beforehand. But the optimisation itself will be very quick, because the approximation of the function within the black box can replace the more time-consuming original simulation (Wortmann, 2018). The accuracy of the surrogate model is often a concern (Yang et al, 2016). The accuracy is dependent on the number of simulations that is used to generate the model (Yang et al, 2016).

#### 1.6.4 Materialization

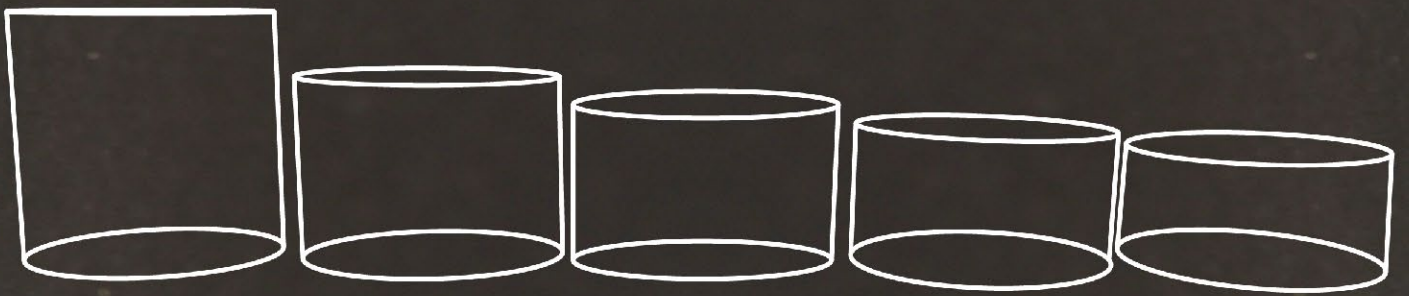
As discussed before CNC methods are computer-controlled production methods. CAD models are often the basis for CNC production techniques. CAD models are converted into G-code. G-code is the most common way of instructing a CNC machine (Kief et al., 2013). G-code contains information about the movement, speed and the information regarding the tool that is being used. In the case of fused filament printing, it can contain the temperature of the nozzle used to melt the material.

### 1.6.5 Conclusion

Presented in this chapter are the parts of the performative computational architecture framework as presented in Ekici et al. (2018). The workflow that will be developed in the second part of this thesis will consist of four parts:

1. Form generation: The shape of the resonator will be generated based upon the problem frequencies. Initial placement of the resonators within the panel will take place.
2. Performance evaluation: The performance of the resonator will be evaluated with the use of a simulation.
3. Optimization: The evaluated resonators will be compared to each other to find the optimal solution. The evaluation of the resonant panels will be based upon the numerical values resulting from the performance evaluation.
4. Materialization: When the optimum or close to the optimum has been found and the results of the performance evaluation are satisfactory. The step can be made towards the generation of the final design and a link can be made to computational aided manufacturing. A model can be generated as an input for the chosen manufacturing technique.

At time of writing this, a decision on the type of optimization algorithm has not yet been made due to the authors inexperience with two of the three categories mentioned in this chapter. When the framework will be implemented in the process of designing the resonant panels the optimization algorithms will be reassessed.



**2**

**Experiments**

## 2. Experimentation

This chapter provides an overview of the equipment that is used to execute the experiments, the methodology, and the results of the experiments. These experiments are performed to fill the gaps in knowledge needed to create a resonant panel.

The topics of the five experiments performed in this project are:

- The neck position of the resonator compared to the cavity. This experiment consists of three samples. One with a central orifice position, one with the orifice at the middle of the edge of the cavity and one with the orifice positioned in the corner of the cavity.
- The crosstalk effect of resonators with peak frequencies that are close together. This experiment consists of four samples with two resonators per sample. The first sample places the orifices in the center of the cavity's and across the samples the orifices move towards the cavity separation shared by the two cavity's.
- The effect of the cavity separation on resonators with different peak frequencies. This experiment consists of five samples with two resonators per sample. The first sample serves as a benchmark and places a cavity separation between the two resonators. In the rest of the samples the cavity separation is removed and the placement of the orifices is altered to see if the cavity has the ability to split itself to resonate at the correct frequencies.
- The effect of the dimensions of the resonator on the width of the absorption curve. This experiment consists of three samples. The resonators have an increasingly long neck but resonate at the same peak frequency.
- The effect of an L shaped resonator cavity. The final experiment in this project consists of five samples. The samples are designed to resonate spread across a frequency range of 100 to 750 Hz.

Some of the topics of the experiments are referenced by other authors, but the information is either incomplete for its use in this thesis or the implementation of the theory is not directly possible. The conclusions drawn by the other authors will be presented in the sub chapters regarding those experiments.

### 2.1 Equipment and reference

All experiments were performed in an impedance tube at the Faculty of Architecture in the Built Environment at the Delft University of Technology. The impedance tube used in this project is a B&K 4206. The tube has a diameter of 100 mm and uses the transfer function method to determine the absorption coefficient of the sample. The frequency range at which the samples are tested is 50-1600 Hz with a resolution of 1 Hz. Further information on the impedance tube and the conditions that the tests were performed in can be found in the annex 1 of this report.

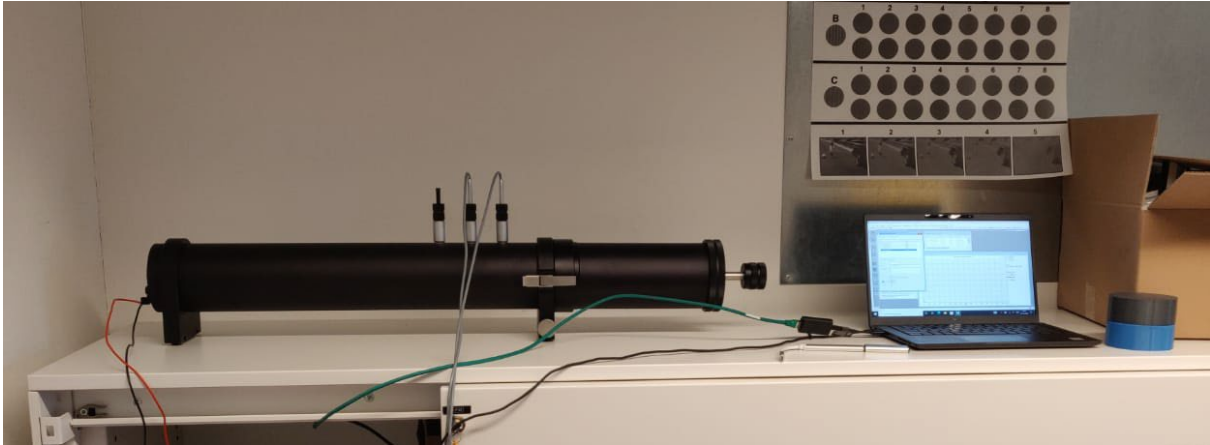


Figure 38: B&K 4206

The geometry of the samples was generated with a Grasshopper script and baked in Rhino 7. The geometry was saved as an STL file and exported to CreaLity slicer 4.8.2 to be processed.

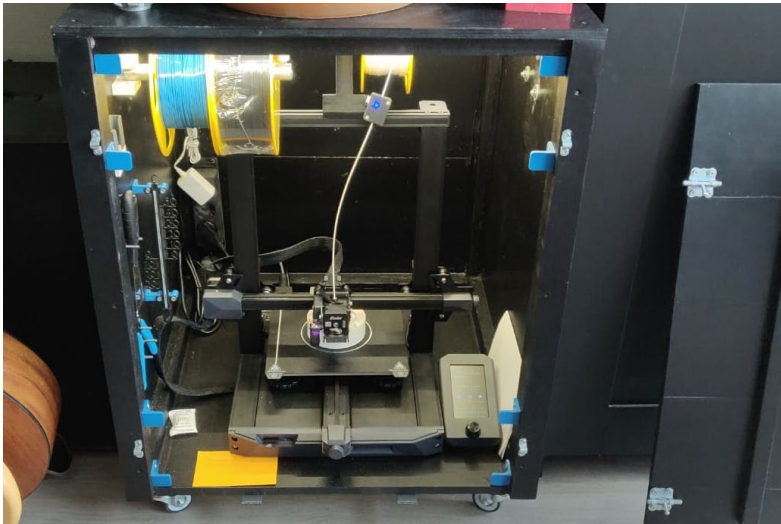


Figure 39: CreaLity Ender 3 S1 3d printer

The samples were printed using a CreaLity Ender 3 S1 printer. All samples were printed on the ultrafine setting, in order to print the samples as precise as possible. This made the layer height 0.12 mm and the line width of the printer 0.4 mm. The print speed was set to 500mm/s. The filament used is 123-3D filament 1,75 mm PLA from the Jupiter series in various colors. The nozzle temperature is 200 degrees Celsius, and the bed temperature is 60 degrees Celsius.

The samples showed small imperfections in the orifice of the resonator. An attempt was made to get rid of these imperfections by using a hand file. This might have led to a slight alteration of the resonator dimensions. The second set of samples of experiment 5 do not have these defects. This is due to a printer setting that was overlooked throughout most of the printing.

Throughout the generation of the different sets of samples, the percentage of infill material of the samples, which is used to provide stiffness to the samples, was altered to save printing time and materials. In the description of the experiments, the percentage of infill will be mentioned, as well as other notable differences between the experiments.

To compare the experimental results to, a spreadsheet was made to calculate the absorption coefficient based on the theory found in *Noise and Vibration Control Engineering Principles and Applications* by Beranek and Ver (1992). The formulas can also be found in the first chapter of this report.

When testing the samples, a significant shift from the theoretical results was noticed at first. After measuring the samples with a caliper, it was found that the 3D printed samples had slightly different dimensions than the designed digital samples. To correct for these imperfections the theoretical values were altered to the dimensions of the samples instead of the designed dimensions. All of the graphs in this chapter will therefore have a non-corrected line, representing the original designed dimensions, and a corrected line, representing measured dimensions of the printed samples.

## 2.2 Experiment 1: Neck position

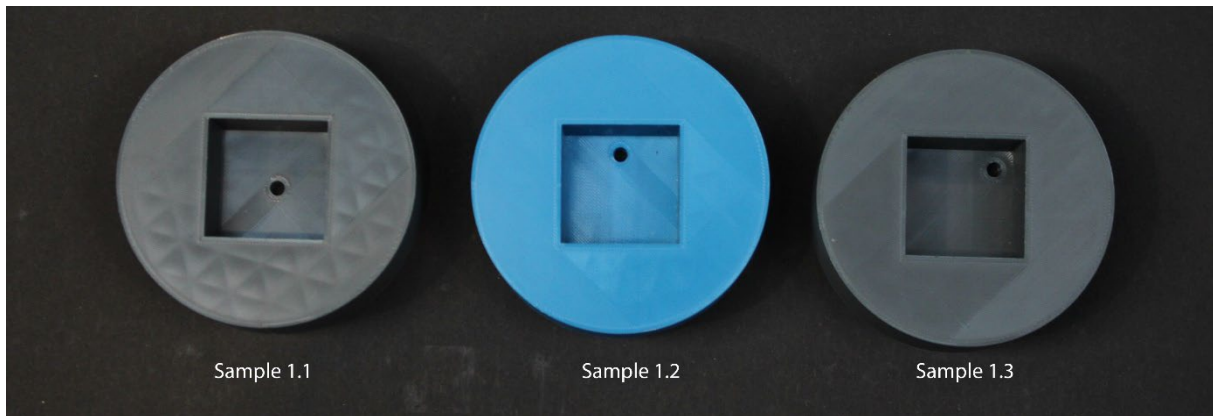


Figure 40: printed resonator with altering neck positions, sample 1.1 to 1.3

The first experiment concerns the position of the neck compared to the cavity. In previous research regarding Helmholtz resonators, the neck was mainly placed in the center of the cavity (Setaki (2012), Ren et al. (2022), Li (2016), Griffin (2001)). According to Chanaud (1994) there can be a significant reduction in the resonance frequency due to the orifice position. He claims the position of the orifice affects the interior end correction, and thereby the resonance frequency. To see this effect in practice and to see the extent of this effect three samples were generated.

The dimensions of all samples are identical except the position of the orifice. The first sample has the orifice in the center of the cavity. The second sample has the orifice in the middle of one of the cavity edges. The third sample has its orifice in the corner of the cavity. The dimensions of the samples are stated in the table below.

	Theoretical Peak frequency	Sample diameter	Neck radius	Neck length	Cavity width	Cavity length	Cavity depth	Infill percentage
Non-Corrected	312 Hz	100 mm	2.61 mm	8.0 mm	40.0 mm	40.0 mm	32.0 mm	10%
Corrected	297 Hz	100 mm	2.40 mm	8.00 mm	39.80 mm	39.80 mm	31.80 mm	10%

Table 1: Dimensions of the samples from the first experiment

### 2.2.1 Results Experiment 1

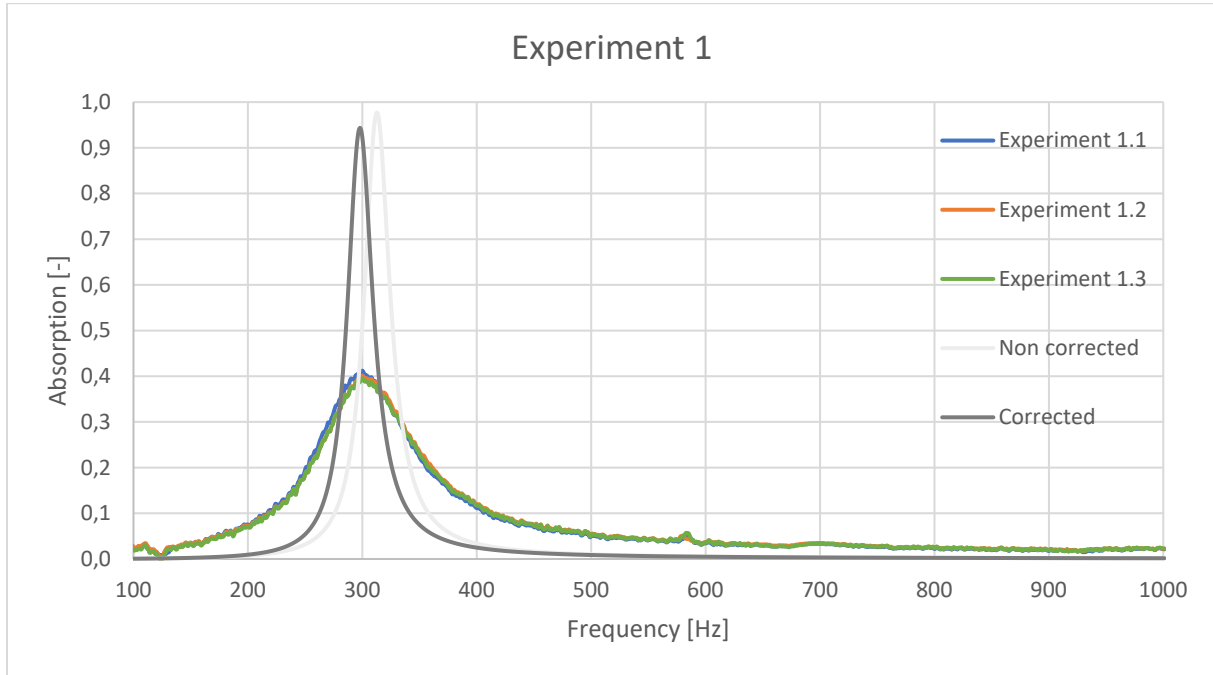


Figure 41: Graph containing the measured data from the samples in set 1, compared to the theoretical values

As can be seen from the data in the graph, the absorption of the three samples is very similar. Sample 1.1 has a slightly higher absorption compared to 1.2 which in turn has a slightly higher absorption than 1.3. However, these differences are within the margin of error of the measurement.

Comparing the samples to the theory, it stands out that the absorption of the measured samples is about half of the theoretical resonators. Besides this, the curves of the experimental samples are wider compared to the curves of the theoretical samples.

	Non corrected	Corrected	Experiment 1.1	Experiment 1.2	Experiment 1.3
Peak frequency	312 Hz	297 Hz	299 Hz	299 Hz	299 Hz
Absorption	0.977	0.943	0.412	0.401	0.395

Table 2: absorption and peak frequency from the samples of experiment one

### 2.2.2 Conclusion experiment 1

The position of the frequency peaks do align well between measurements and theory. The difference in absorption coefficient between the theoretical and experimental results is rather large. As of the moment of writing the report, an explanation has not yet been found. The difference in width of the peak is a more common occurrence when comparing theoretical results to tested samples.

Besides the difference between theory and experiments, the samples show that there is only a small difference in absorption between the samples. The location of the neck seems to only have a limited influence on the performance.

These findings lead to more options for the full panel. The relocation of a resonator neck can lead to an increase in the number of resonators that can be placed in the panel. This tighter packing should in turn lead to a higher overall absorption.

### 2.3 Experiment 2: Crosstalk

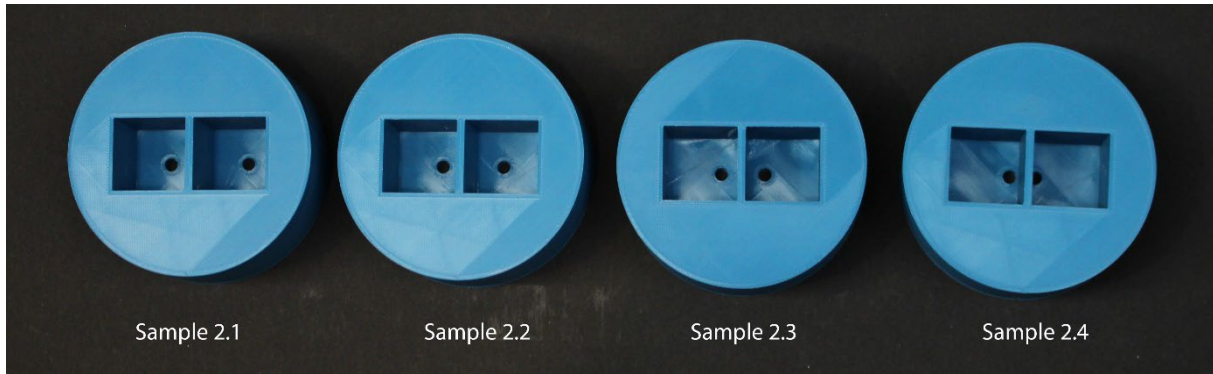


Figure 42: samples with altering neck positions, sample 2.1 to 2.4

The second experiment is concerned with the crosstalk effect. As described by M. Hannink (2007) the proximity of resonator necks can have a negative influence on the performance of the resonator. While the phenomenon is described by M. Hannink, there is no further information about distances when cross talk starts to occur or how far peak frequencies need to be apart to not suffer from any interaction, or at what distance the interaction becomes insignificant.

As with the first set of samples the only difference between the samples is the position of the neck. In the first sample, the necks of both resonators are placed in a central location to their respective cavities. The fourth sample has the orifices near the cavity separation. The neck locations of the other two samples are in between the other the first and the fourth.

	Theoretical Peak frequency	Sample diameter	Neck radius	Neck length	Cavity width	Cavity length	Cavity depth	Infill percentage
Non corrected 1	423	100 mm	2.786 mm	6 mm	30 mm	30 mm	40 mm	5 %
Non corrected 2	428	100 mm	2.834 mm	6 mm	30 mm	30 mm	40 mm	5%
Corrected 1	400	100 mm	2.50 mm	6.00 mm	29.75 mm	29.75 mm	39.50 mm	5%
Corrected 2	400	100 mm	2.50 mm	6.00 mm	29.75 mm	29.75 mm	39.50 mm	5%

Table 3: Dimensions of the individual resonators from the second experiment

### 2.3.1 Results experiment 2

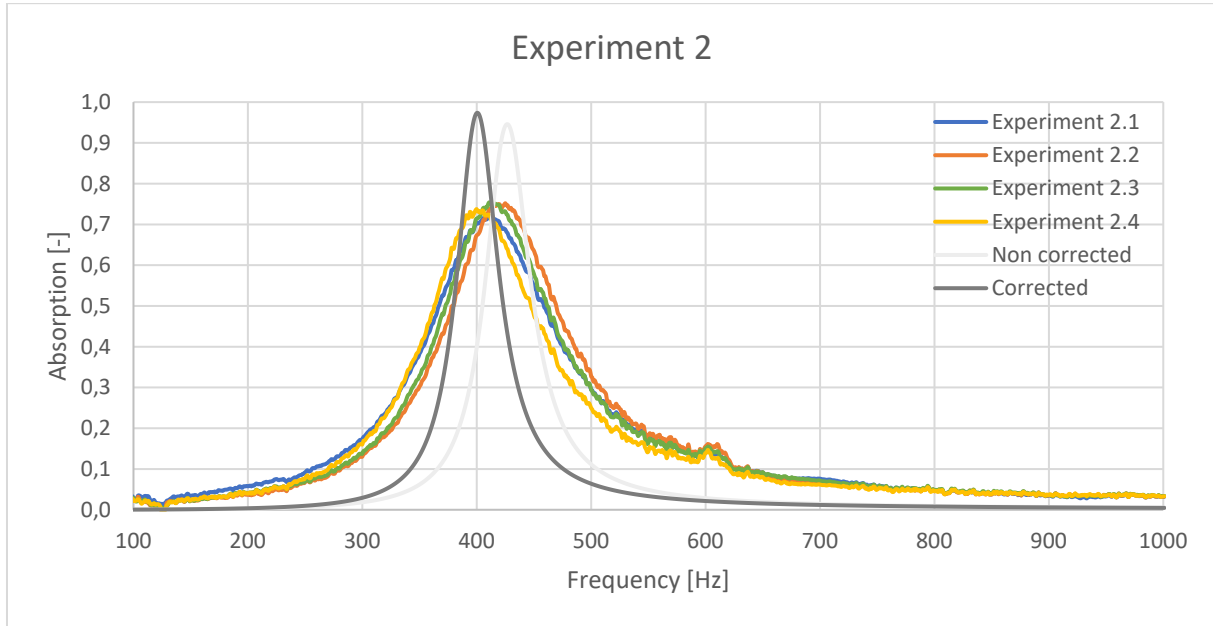


Figure 43: Graph containing the measured data from the samples in set 2 compared to the theoretical values

As also seen in experiment 1, the theoretical result differs from the experimental results. As in experiment one, the peak of the theoretical result is higher and less wide. The difference in the height of the peak is noticeably smaller compared to experiment 1. The peak frequency of sample 2.4 is close to the peak frequency of the theoretical results. It would be logical if sample 2.1 would comply with the theoretical results even more but as can be seen from figure x it does not.

When looking at the results of the experiment in comparison to each other, there is a small but noticeable difference between the samples. Samples 2.2, 2.3 and 2.4 show a trend in the way the absorption curve shifts. It seems that the closer the orifices come together, the lower the peak frequency becomes. The outlier in this set of experiments is 2.1. Following the trend seen between the other samples it would be expected that the curve would have a peak frequency that is slightly higher than 2.2. Another possible explanation could be that the imperfections in the necks of samples 2.1 caused this shift.

The peak absorption of sample 2.2 and 2.3 is very similar and only slightly apart. Sample 2.4 has a lower absorption which would be in correspondence with the statements by M. Hannink (2007) that resonators of similar frequencies have a negative effect on the absorption of the resonators. Sample 2.1 is an outlier and does not comply with the expectations for the peak absorption values.

	Non corrected	Corrected	Experiment 2.1	Experiment 2.2	Experiment 2.3	Experiment 2.4
Peak frequency	429 Hz	400 Hz	410 Hz	424 Hz	410 Hz	404 Hz
Absorption	0.945	0.973	0.72	0.752	0.754	0.735

Table 4: absorption and peak frequency from the samples of experiment two

### 2.3.2 Conclusions Experiment 2

If the assumption is made that the measurements from sample 2.1 are slightly incorrect, it can be concluded that the crosstalk effect does increase when the orifices of the resonators move closer.

Besides a lower absorption, the peak frequency also becomes lower when the orifices move closer together. Although the effect is noticeable, it is rather small. If the relocation of the resonator necks leads to an increase in the number of resonators that can be placed within the resonant panel this slight loss in absorption is acceptable.

As with the results from experiment one, it is generally beneficial to place the neck of the resonator as central to the cavity as possible. This is because both the absorption will be marginally higher, and the distance between equal resonators will always be as large as the material and half of the distance of the cavities.

2.4 Experiment 3: cavity separations

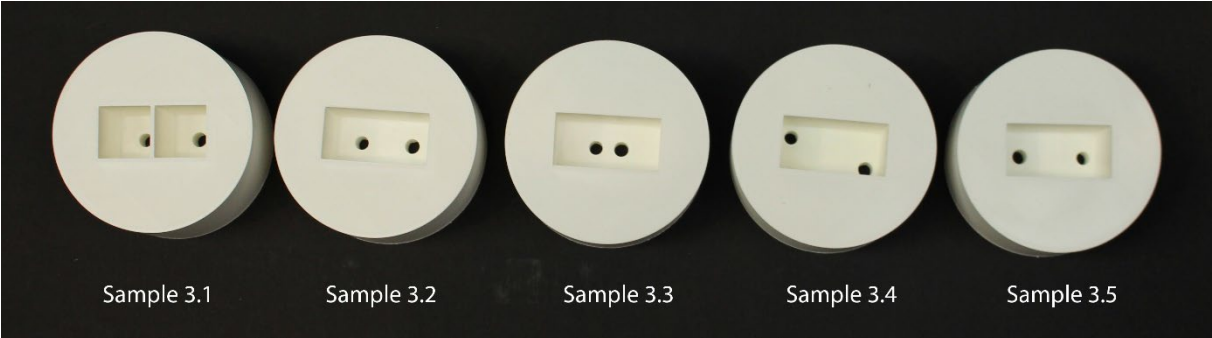


Figure 44: Samples with and without cavity separations, sample 3.1 to 3.5

The third experiment in this project is concerned with the separation of cavities from multiple resonators with different target frequencies. In the common perforated panel absorbers, the cavity behind the panel is not segmented into separate resonator volumes as can be seen in Beranek and Ver (1992). Because all resonators have the same dimensions, the cavity behaves as though it were individual volumes per orifice.

This experiment will attempt to find if there is a possibility to remove the cavity separations between two resonators when the target peak frequency of the resonators is different. Sample 3.1 will serve as a reference sample with a cavity separation. Samples 3.2 till 3.5 will lack a cavity separation and have different orifice positions to see in what way the cavity can divide itself. Samples 3.2 to 3.5 have the same dimension only the position of the orifice differs. The cavity volume of Sample 3.1 is identical to the volume of 3.2 till 3.5.

	Theoretical Peak frequency	Sample diameter	Neck radius	Neck length	Cavity width	Cavity length	Cavity depth	Infill percentage
Non corrected 1	470 Hz	100 mm	3.6 mm	12.6 mm	26 mm	26 mm	41 mm	2 %
Non corrected 2	500 Hz	100 mm	3.90 mm	12.60 mm	26.00 mm	26.00 mm	41.00 mm	2 %
Corrected 1	442 Hz	100 mm	3.25 mm	12.50 mm	25.80 mm	25.80 mm	40.80 mm	2%
Corrected 2	475 Hz	100 mm	3.55 mm	12.50 mm	25.80 mm	25.80 mm	40.80 mm	2%

Table 5: Dimensions of the individual resonators from the third experiment

### 2.4.1 Results Experiment 3

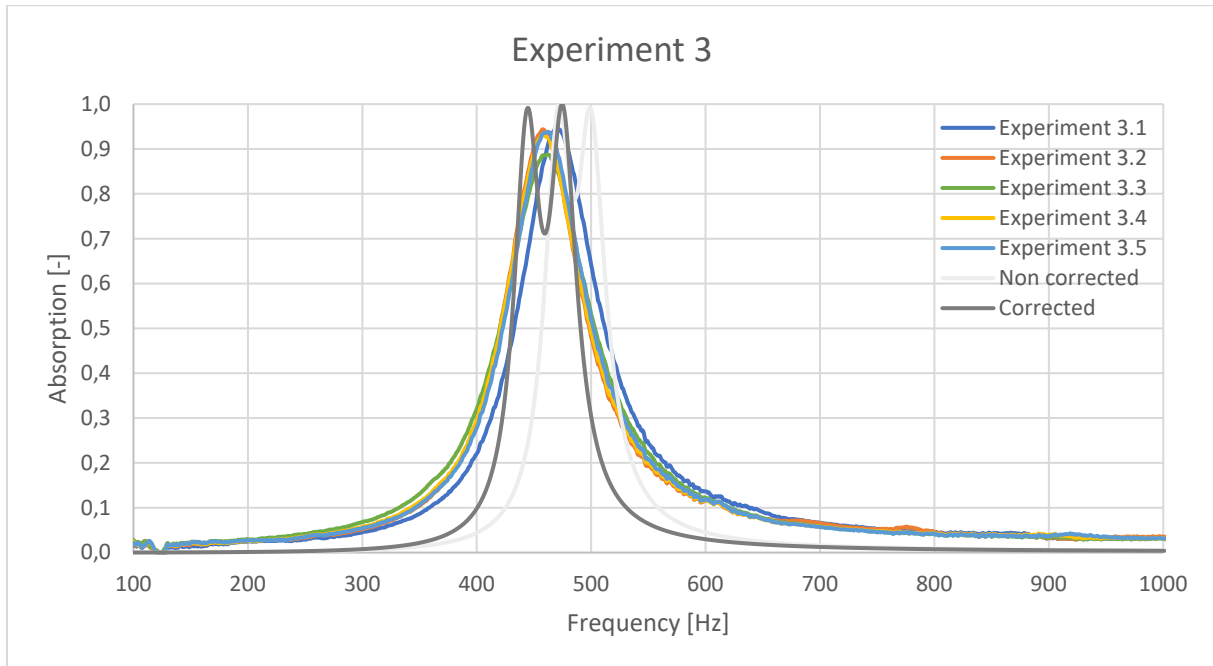


Figure 45: Graph containing the measured data from the samples in set 3 compared to the theoretical values

In contradiction to experiment 1 and 2, the theoretical results from experiment 3 seem to follow the measured results quite well. The main notable difference is the lack of two absorption peaks in the tested samples. Besides the single peak compared to two peaks, the height of the absorption is similar between the theoretical results and the measured results.

When comparing the measured results amongst each other it stands out that 3.2 3.4 and 3.5 have similar curves. The height, the width and the location are very much alike. Sample 3.3 differs only in the height of the absorption being slightly lower compared to the other samples. Sample 3.1 differs from the other samples in its peak frequency, being slightly higher. A possible explanation could be that the cavity separation of sample 3.1 caused the dimensional error from the printing being twice as large. The cavity width of sample 3.1 is twice 25.80 mm while the cavity width of the other samples within this experiment are 51.80 mm resulting in a 0.2 mm difference.

	Non corrected	Corrected	Experiment 3.1	Experiment 3.2	Experiment 3.3	Experiment 3.4	Experiment 3.5
Peak frequency	471 Hz 498 Hz	444 Hz 474 Hz	468 Hz	457 Hz	461 Hz	457 Hz	461 Hz
Absorption	0.999 0.992	0.991 0.999	0.947	0.944	0.888	0.933	0.938

Table 6: absorption and peak frequency from the samples of experiment three

### 2.4.2 Conclusion experiment 3

The biggest difference that can be noticed in experiment 3 is the shift from two peaks in the theory to one peak in the samples. This is likely due to the increased resistance in the system. This is also a possible explanation for the increased width of the absorption curve compared to the theoretical values.

When comparing the experimental samples, it stands out that the results are remarkably similar. The effect of the cavity separation is smaller than anticipated. Even the non-symmetrical placement of the

orifices as can be seen in sample 3.5 has a minimal effect on the performance of the resonators. Sample 3.3 show a lower absorption compared to the other samples. This might be due to the crosstalk effect, which seems to have more effect now that the cavity separations are removed. The give a definitive conclusion on this more experimentation needs to be done.

Removing the cavity separation in the resonant panel will lead to a decrease in the amount of material that is needed to construct the panel. This will increase the ease of assembly and lower the production time of the product. When removing the cavity separations, extra attention needs to be given to the location of the orifice, because the crosstalk effect seems to have more effect now that the separations are gone.

2.5 Experiment 4 width of the absorption curve

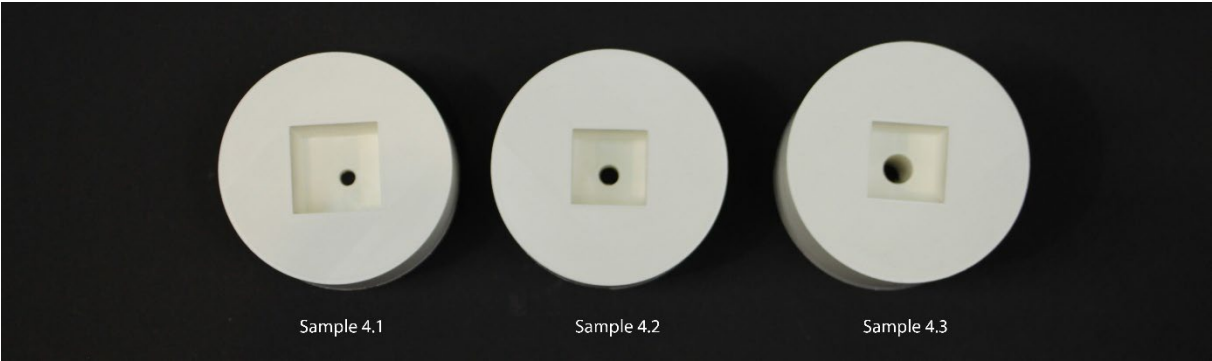


Figure 46: Samples with altering neck lengths, Sample 4.1 to 4.3

The fourth experiment is concerned with the effects of the size of a resonator on the width of the absorption curve. During the process of designing the resonators for the panel it stood out that larger resonators seem to have a thinner absorption curve than smaller resonators tuned to the same frequency. To investigate this further an experiment was designed. In contradiction to the other experiments the theory confirmed this suspicion. The three resonators have increasing neck lengths and orifice diameters and decreasing cavity volumes, so they are tuned to the same frequency. The decision to do this experiment in the impedance tube was made because the samples made for the previous experiments all had wider absorption curves than theoretically expected. To investigate this phenomenon further these samples where generated.

The design of three resonators with the same peak frequency and the same absorption capacity while having vastly different sizes proved quite challenging. Therefore, the resonators have slightly different absorptions at the peak frequency, which becomes more extreme in the corrected dimensions.

	Theoretical Peak frequency	Sample diameter	Neck radius	Neck length	Cavity width	Cavity length	Cavity depth	Infill percentage
Non corrected 1	400	100 mm	3.9 mm	6 mm	38 mm	38 mm	46 mm	5 %
Non corrected 2	400	100 mm	4.7 mm	16.2 mm	32 mm	32 mm	49 mm	5 %
Non corrected 3	400	100 mm	6.6 mm	53.4 mm	32 mm	32 mm	37 mm	5 %
Corrected 1	369	100 mm	3.55 mm	7.00 mm	37.50 mm	37.50 mm	46.00 mm	5%
Corrected 2	392	100 mm	4.45 mm	16.00 mm	31.80 mm	31.80 mm	48.80 mm	5%
Corrected 3	386	100 mm	6.20 mm	53.00 mm	31.80 mm	31.80 mm	37.00 mm	5%

Table 7: Dimensions of the samples from the fourth experiment

2.5.1 Results experiment 4

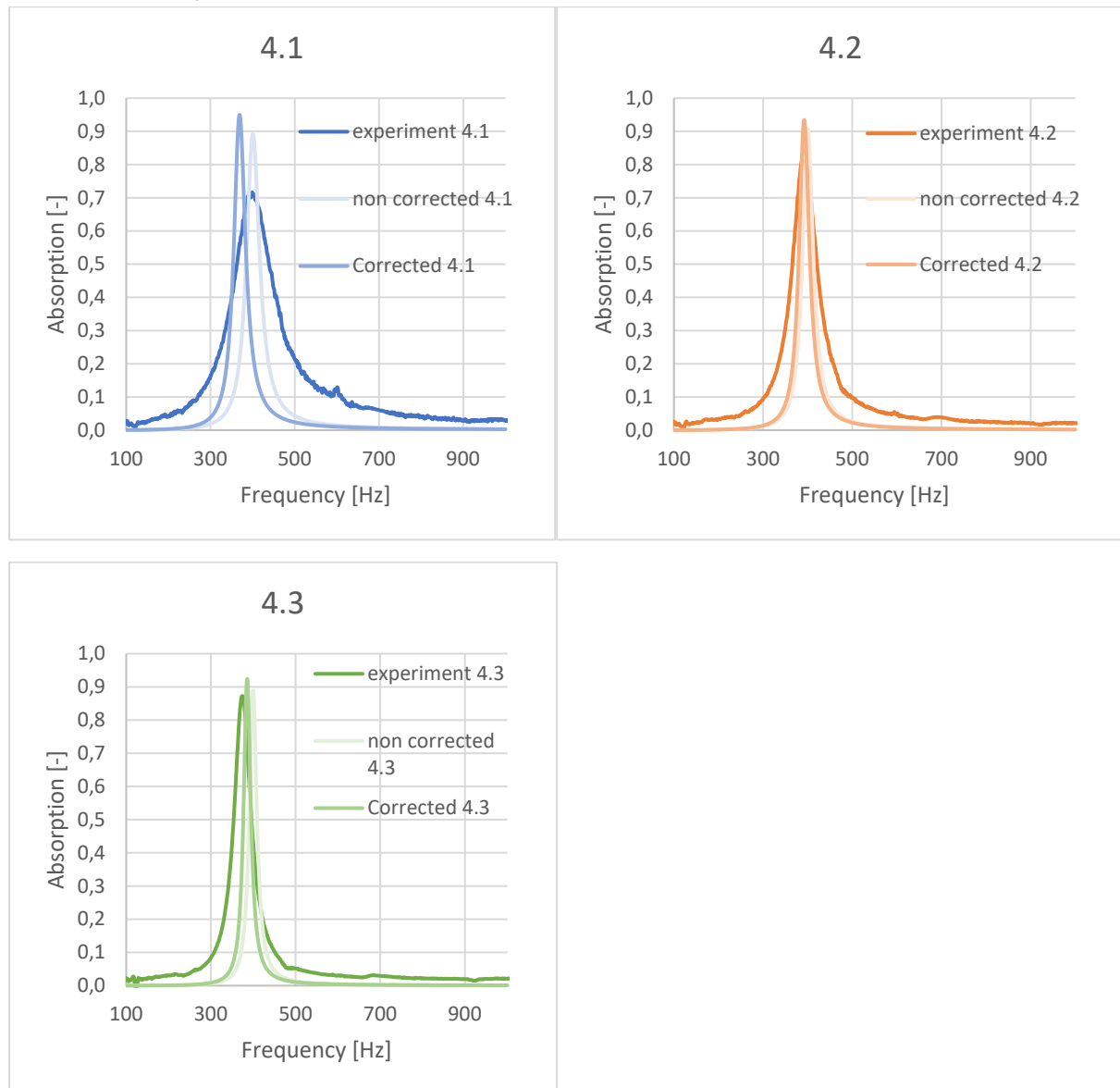


Figure 47: Graphs containing the measured data form the samples in set 4 compared to the theoretical values

When considering the resonators compared to their theoretical counterpart it is very clear that the bigger the dimensions are, the better the theory fits the experiment. This is because the dimensional defects made by the 3D printer are percentage wise smaller than with the smaller samples. Although that is not the focus of this experiment, this experiment shows it quite well.

Again, comparing the theoretical results to the results of the experiment, the width of the absorption curve is wider in the experimental results compared to the theoretical results. The height of the absorption is similar in the theoretical results across the samples. While in the results of the experiment the absorption peak is lower in sample 4.1 and increases in sample 4.2 and 4.3.

The graphs containing only the experiments, or the corrected lines can be found in annex 2 of this report as well as the graphs per resonator.

	Non corrected 4.1	Corrected 4.1	Experiment 4.1
Peak frequency	401 Hz	369 Hz	399 Hz
Absorption	0.891	0.950	0.717
Range at ½ absorption	37 Hz	35 Hz	117 Hz

	Non corrected 4.2	Corrected 4.2	Experiment 4.2
Peak frequency	400 Hz	392 Hz	390 Hz
Absorption	0.907	0.934	0.842
Range at ½ absorption	31 Hz	28 Hz	64 Hz

	Non corrected 4.3	Corrected 4.3	Experiment 4.3
Peak frequency	400 Hz	386 Hz	374 Hz
Absorption	0.889	0.923	0.873
Range at ½ absorption	21 Hz	21 Hz	50 Hz

Table 8: absorption, peak frequency, and the frequency range at ½ of the absorption from the samples of experiment four

### 2.5.2 Conclusion experiment 4

Comparing the width of the absorption curves across the non-corrected, corrected and results of the experiment shows that the length of the neck influences the width of the absorption curve. The longer the neck is, the thinner the absorption curve is.

The implication of these results is that the necks of the resonators in the panel need to be kept as short as possible to widen the absorption per resonator. If a single resonator can span a wider frequency range, then less resonators are required for broadband absorption. Therefore, the panel can either be smaller or more identical resonators can be placed to improve the absorption.

### 2.6 Experiment 5: L-shaped cavities

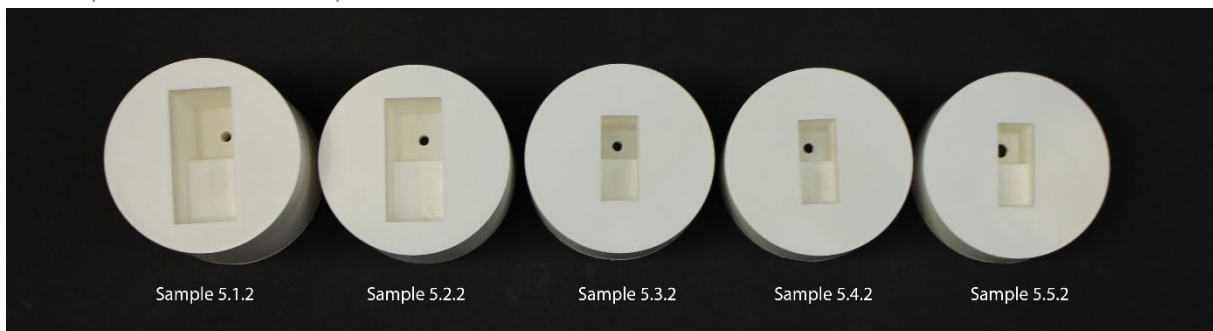


Figure 48: Samples with L shaped cavities, Sample 5.4.2 and 5.5.2

The fifth experiment is concerned with finding the correct way of determining the impedance of a resonator with an L-shaped cavity. Following up on the results of experiment four, it is beneficial to keep the neck of a resonator short. In order to still have a two layered resonant panel, a larger resonator needs to go under smaller resonators. To do this without the use of a long neck an L-shaped cavity is needed.

In the book *Noise and Vibration Control Engineering Principles and Applications* by Beranek and Ver (1992) it is mentioned that the shape of the cavity is irrelevant if the wavenumber multiplied by the cavity depth is smaller than one ( $k_0t \ll 1$ ). Then the impedance of the volume can be rewritten to only include the volume of the cavity instead of the length, width, and height. In this project  $k_0t \ll 1$  does

not apply. In the higher part of the frequency range the wavenumber times the cavity depth goes above one and the absorption is not comparable anymore.

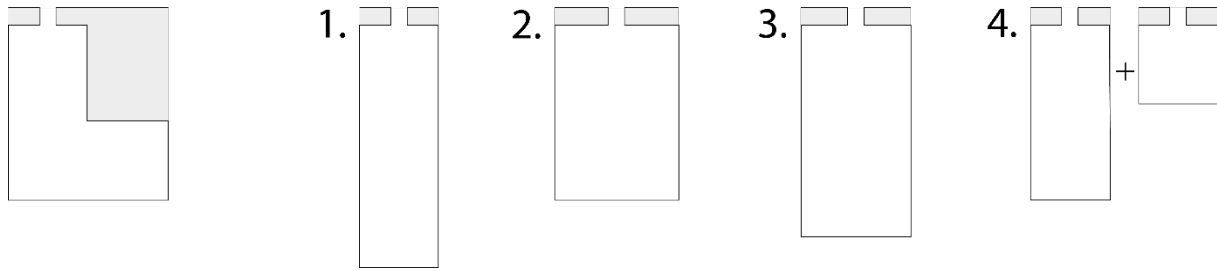


Figure 49: possible approximations for an L shaped cavity

To best approximate the impedance of the cavity while keeping the volume of the cavity constant four possible solutions are considered:

- The horizontal part of the L is added to the vertical part by increasing the depth of the resonator. Resulting in a deeper resonator compared to its actual dimensions.
- The horizontal part of the L is added to the vertical part by increasing the height and width of the cavity volume. Resulting in a wider resonator compared to its actual dimensions
- The horizontal part of the cavity is equally distributed over the height, width, and length of the cavity. Resulting in a wider, higher, and deeper resonator compared to its actual dimensions.
- The horizontal part of the cavity is considered as a separate impedance from the other part of the cavity. Resulting in two separate impedances for the cavity volume. The formula for the impedance of the cavity then becomes:

$$36. Z_v = \frac{-jz_{s1}\rho c \cot(k_2 d_2) + (\rho c)^2 \frac{S_a}{S_b}}{z_{s1} - j\rho c \cot(k_2 d_2)}$$

Formula for the combined impedance of two cavity's. With  $z_{s1}$  being the impedance of the first cavity,  $k_2$  being the wavenumber of the second cavity,  $d_2$  being the cavity depth of the second cavity.

$$37. z_{s1} = -j\rho c \cot(k_1 d_1)$$

Formula for the impedance of the first cavity. With  $k_1$  being the wavenumber of the first cavity,  $d_1$  being the cavity depth of the first cavity.

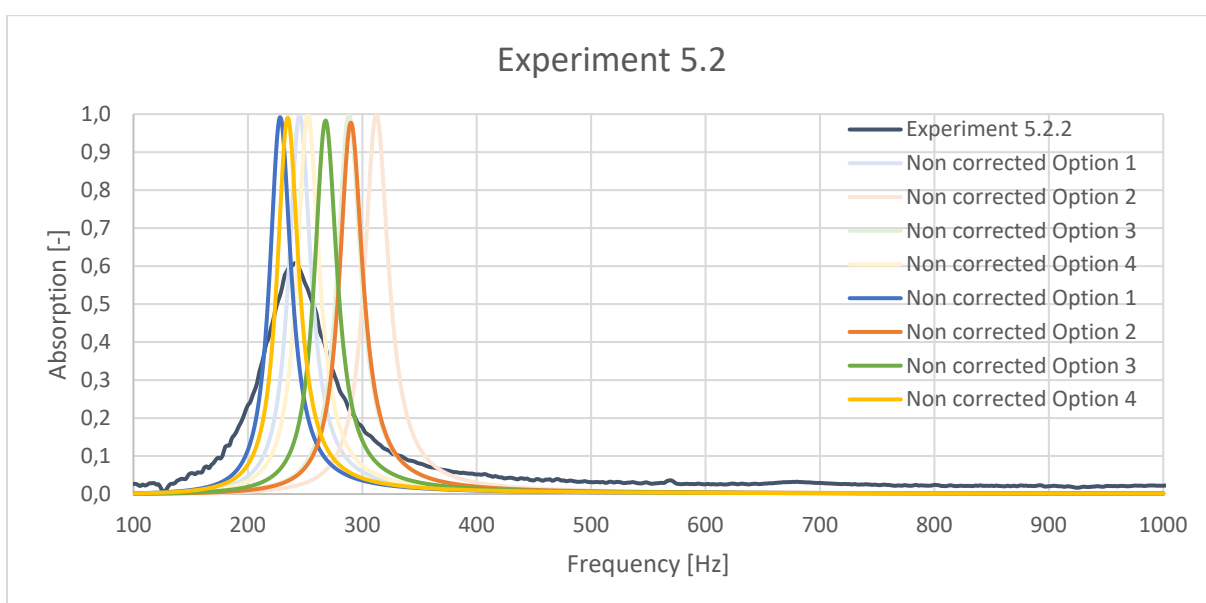
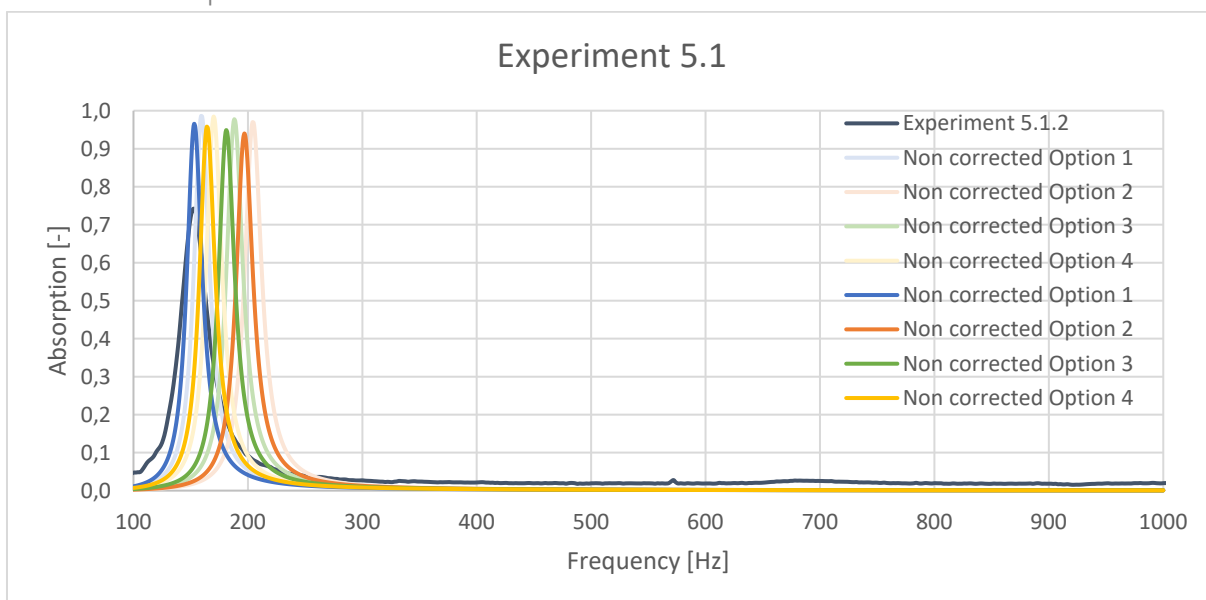
The difference between the different options of approximating the impedance differ more when the frequency becomes higher. Therefore 5 samples with increasing target frequencies have been designed.

	Cavity width bottom	Cavity height bottom	Cavity depth bottom	Cavity width top	Cavity height top	Cavity depth top	Orifice radius	Neck length	Sample radius	Infill percentage
Non corrected 5.1	69 mm	32 mm	40 mm	32 mm	32 mm	35 mm	3 mm	20 mm	100 mm	2 %
Non corrected 5.2	65 mm	30 mm	30 mm	30 mm	30 mm	30 mm	3 mm	10 mm	100 mm	2 %
Non corrected 5.3	45 mm	20 mm	30 mm	20 mm	20 mm	25 mm	3 mm	5 mm	100 mm	2 %

Non corrected 5.4	45 mm	20 mm	25 mm	20 mm	20 mm	25 mm	3 mm	3 mm	100 mm	2 %
Non corrected 5.5	45 mm	20 mm	20 mm	20 mm	20 mm	25 mm	4 mm	2 mm	100 mm	2 %
Corrected 5.1.2	68.80 mm	31.60 mm	40.00 mm	-	31.60 mm	35.00 mm	2.75 mm	20.00 mm	100 mm	5%
Corrected 5.2.2	65.00 mm	30.00 mm	30.00 mm	-	30.00 mm	30.00 mm	2.65 mm	10.00 mm	100 mm	5%
Corrected 5.3.2	45.00 mm	20.00 mm	30.00 mm	-	20.00 mm	25.00 mm	2.80 mm	5.10 mm	100 mm	5%
Corrected 5.4.2	45.00 mm	19.80 mm	24.90 mm	-	19.80 mm	25.10 mm	2.90 mm	3.00 mm	100 mm	5%
Corrected 5.5.2	44.80 mm	19.80 mm	20.00 mm	-	19.80 mm	25.00 mm	3.90 mm	2.00 mm	100 mm	5%

Table 9: Dimensions of the resonators from the fourth experiment

### 2.6.1 Results experiment 5



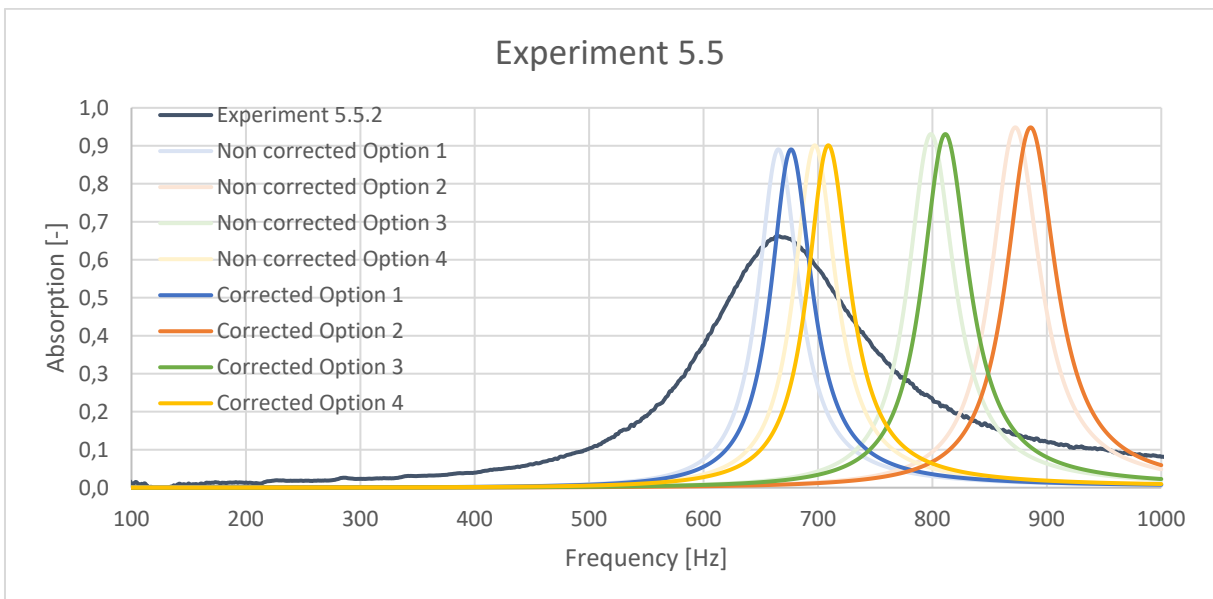
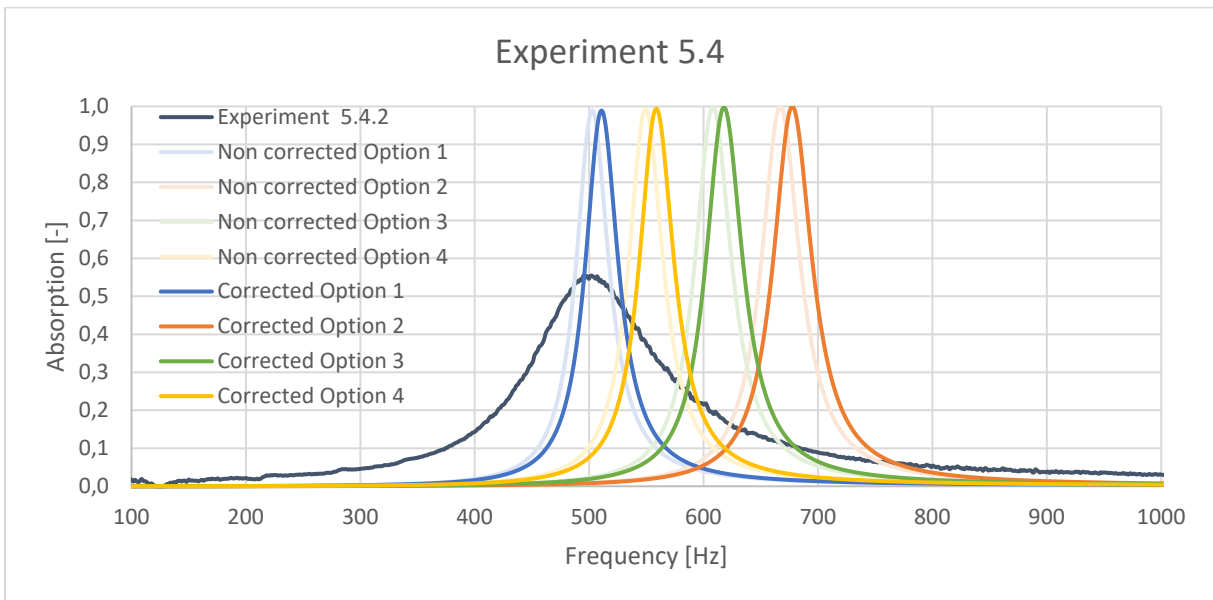
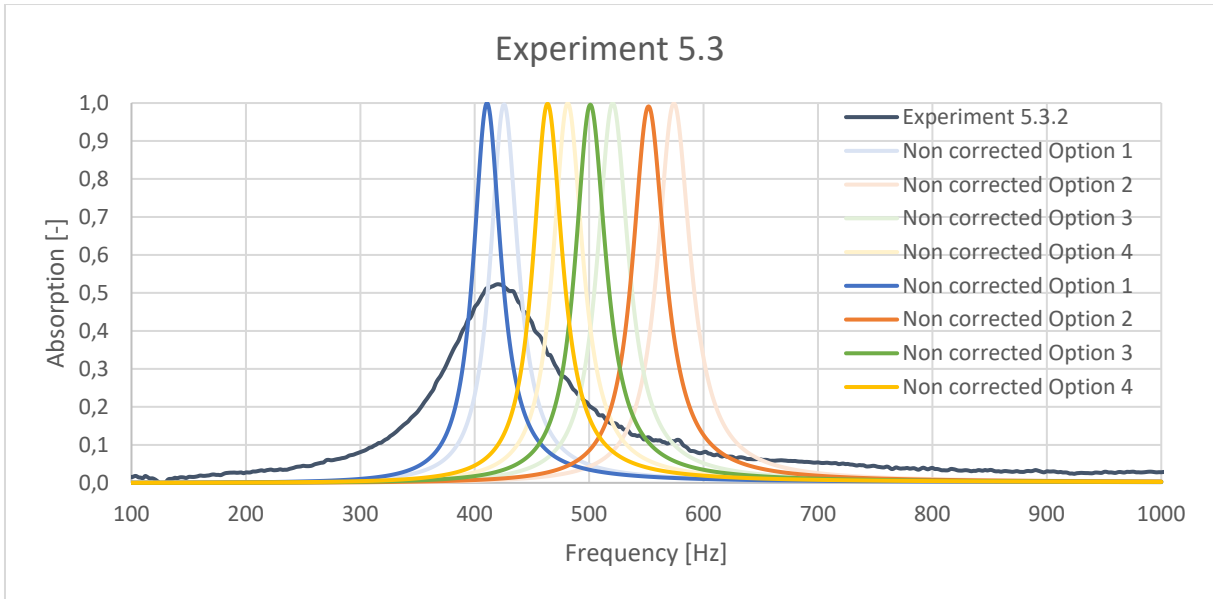


Figure 50: Graph containing the measured data form the samples in set 5 compared to the theoretical values

In contradiction to the other experiments the tested sample serves as a benchmark to compare to the theory. This introduces the problem that there is no certainty in knowing how fitting the samples are. Although the samples are measured with calipers and visually inspected after printing, there is a level of uncertainty.

The results resulting from samples 5.1 till 5.5 are far from the expected results. The suspicion arose that the unexpected results where not due to the geometry of the samples but due to an external factor. After further investigation the inaccuracies of the results are likely due to the infill pattern of the printed samples. Due to the belief that the change in infill pattern would make the samples overall more sturdy the decision was made to change it.

After the results from experiment 5 were investigated the decision was made to reprint the samples to test if the change in infill was the reason for the unexpected results. The infill pattern changed and the infill percentage was increased from 2% to 5%.

The results from experiment 5.1.2 till 5.5.2 confirmed the suspicion that the infill was the cause for the unexpected results. This part of the report therefor only presents the results of the second set of samples within experiment 5 because the other results where deemed invalid. Results from the original samples can be found in annex 2.

	Sample 5.1.2	Option 1	Option 2	Option 3	Option 4
Peak frequency	152	153	197	181	164
Absorption	0.741	0.965	0.940	0.949	0.957

	Sample 5.2.2	Option 1	Option 2	Option 3	Option 4
Peak frequency	242	228	290	268	235
Absorption	0.608	0.991	0.977	0.983	0.990

	Sample 5.3.2	Option 1	Option 2	Option 3	Option 4
Peak frequency	420	411	527	501	464
Absorption	0.523	0.999	0.973	0.995	0.997

	Sample 5.4.2	Option 1	Option 2	Option 3	Option 4
Peak frequency	502	511	678	618	559
Absorption	0.554	0.988	0.999	0.997	0.993

	Sample 5.5.2	Option 1	Option 2	Option 3	Option 4
Peak frequency	665	676	886	811	709
Absorption	0.662	0.889	0.948	0.930	0.901

Table 10: absorption and peak frequency from the samples of experiment five

### 2.6.2 Conclusion experiment 5

The results from experiment 5 mostly comply with option one. This option approximates the L shaped cavity as a longer rectangular cavity, keeping the width and height equal to the width and height of the vertical part of the cavity. Sample 5.2.2 deviates from this conclusion. This sample complies most with option 4. Due to the compliance of all of the other samples with options one, this will be the selected theory for the approximation of the L shaped cavity.

The results from this experiment allow for the use of Helmholtz resonators with L shaped cavities within the design of the resonant panel. L shaped cavities have the advantage that a larger volume for a resonator does not immediately result in a deeper panel or a larger spacing between the orifices. The larger resonators can use the space behind the smaller resonators to increase their volume if necessary.

### 2.7 Limitations regarding the experiments

All of the experiments presented in this chapter have very small sample sizes. All of the conclusions drawn from this chapter could be given with more certainty when the sample size is larger. The lack of sample size is mainly due to a lack of time. With more time more samples could have been tested and the conclusion drawn from the experiments could be presented with more certainty.

The samples used for the experiments had some defects. Some of the samples had a bump in the neck of the resonator at the orifice entrance due to a printing error. These needed to be removed by hand using a file. Besides the bump in the neck, some samples suffered from an uneven top surface. The assumption is that this does not influence the performance of the resonators because the defections are rather small. The inaccuracy and the defects of the prints could explain the small shifts in peak frequency.

Even though the sample sizes are small the results of the experiments still provide valuable insights for generating the resonant panel presented in the next chapter.

### 2.8 Overall conclusions

Experiment 1 was concerned with the location of the neck compared to the cavity. The result from this experiment is that the location of the neck only has a very slight effect on the performance of the resonator.

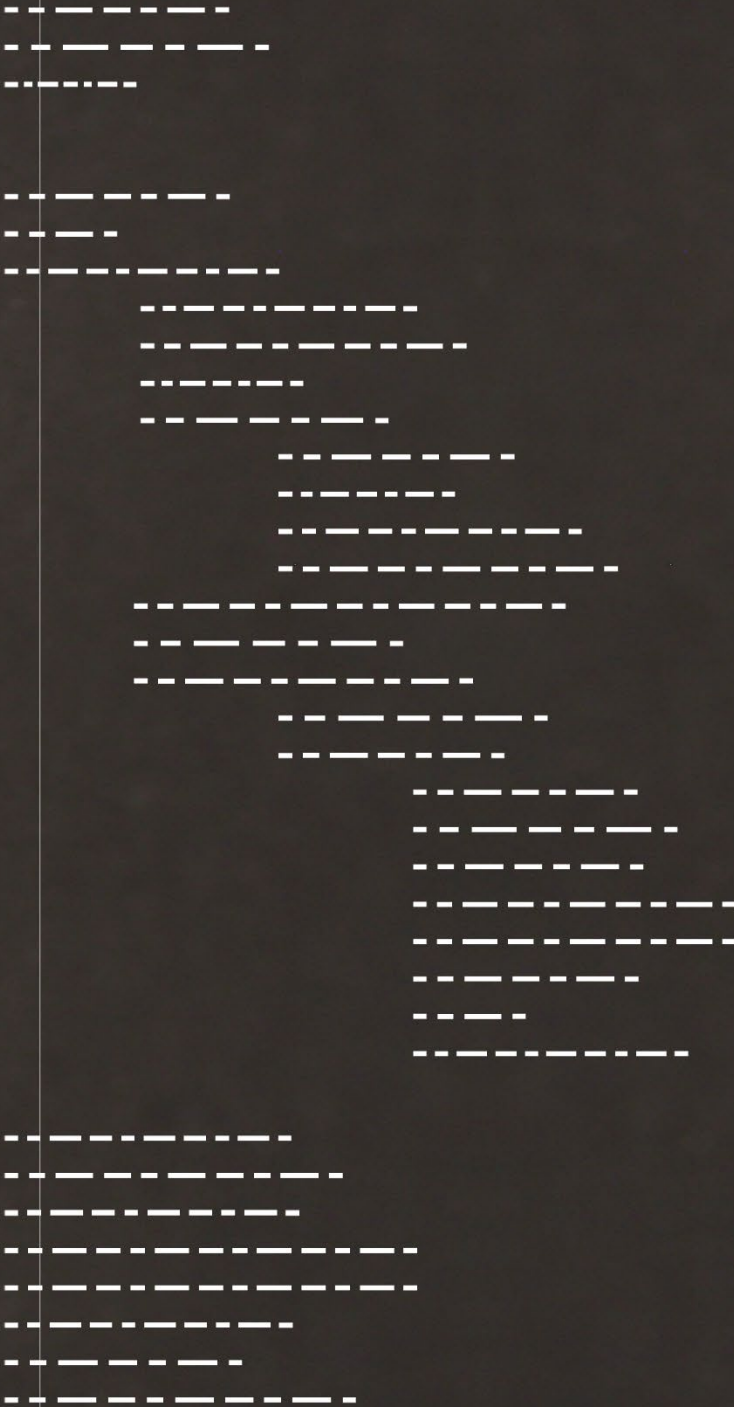
Experiment 2 was concerned with the cross talk effect. The result from this experiment is that the closer the orifices of two resonators are together the larger the cross talk effect is. However the effect is rather small.

Experiment 3 was concerned with the effect of the cavity separation between two resonators. The result from this experiment is that the cavity separation can be removed without a large effect on the absorption of the resonators. The location of the orifices can even be placed non symmetrical in the cavity.

Experiment 4 was concerned with the effect of the neck length on the width of the absorption curve. The result from this experiment is that the longer the neck of the resonator is the thinner the absorption curve is. Therefore when making a panel for broadband absorption the necks of the resonators should be kept as short as possible.

Experiment 5 was concerned with the theoretical approximation of L shaped cavity's. The result from this experiment is that the impedance of a L shaped cavity can be approximated by substituting the

cavity with a cavity that has the same horizontal section as the original resonator had right below the orifice, but with a greater depth to compensate for the volume of the resonator.



# 3

## Digital workflow

### 3 Digital workflow

The goal of this project is to design a broadband sound absorbing panel for low frequencies with reduced geometrical complexity. Designing this panel follows a couple of steps described in this chapter. These steps are:

- The acoustic optimizer: The tool takes a frequency range as an input. From this frequency range a number of resonators is designed based on the formulas for Helmholtz resonators found in Beranek and Ver (1992). These resonators are designed in a way that they can be easily combined in a panel without leaving large parts of the panel unused.

The dimensions of the resonators need to comply with a certain range. This is because the resonators need to fit within the panel, and the panel needs to be below a certain thickness otherwise the advantage over a porous layer is lost. These common dimensions will result in a lower absorption coefficient compared to when all of the resonators have their optimal dimensions. But when the step is made from individual resonators to resonators in a panel, the shared dimensions help greatly with packing the resonators and reducing the needed material.

- The resonator placement: When the dimensions are determined the resonators are placed into a panel. The panel is divided in a grid so the resonators can be placed easily in the panel. The placement starts in the bottom layer and works up to the top layer.

- Preparation for production: The third part is concerned with the conversion of the geometry so it can be handled by another software to prepare it for production. This part will take the resonant panel and generate all the boundaries between the resonator cavities.

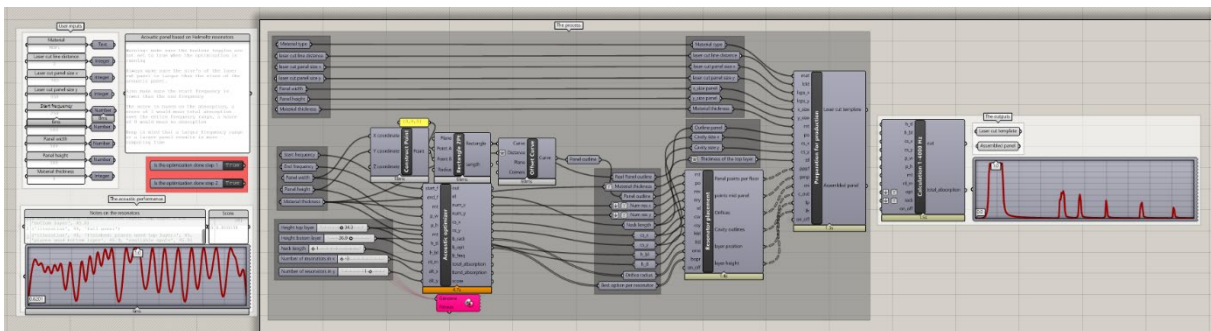


Figure 51: Digital tool within Grasshopper

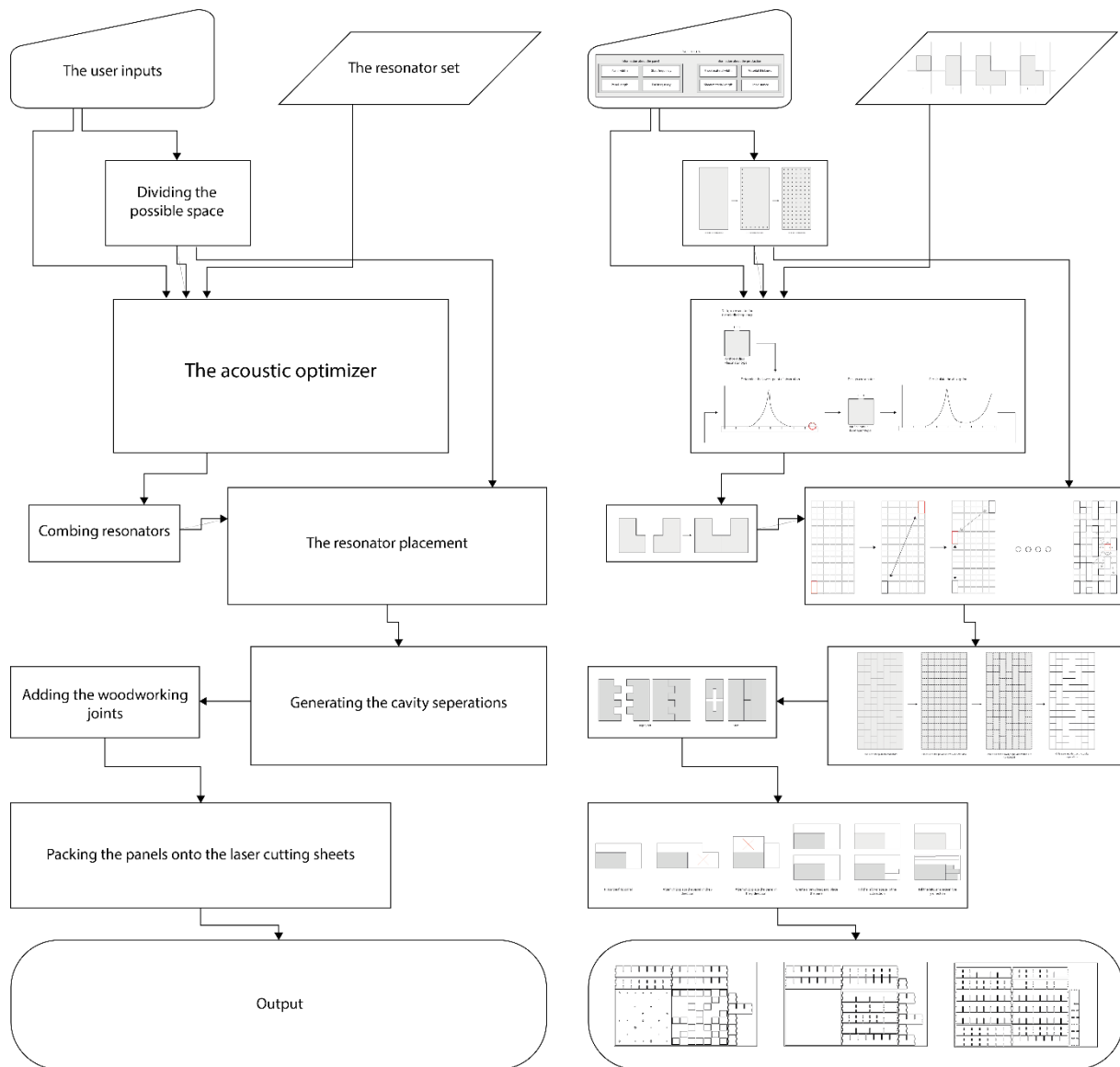


Figure 52: Flowchart of the digital tool in text and pictures

In the end, the parts will combine into a single tool to automatically generate the laser cutting plans for the resonant panel. This chapter will go over all of the individual parts of the tool and in the end give an overview over the entire tool. Figure 51 shows the actual digital workflow as it can be found within the Grasshopper file. Figure 52 shows a more comprehensible overview of all of the individual processes in names and in images.

### 3.1 The user inputs

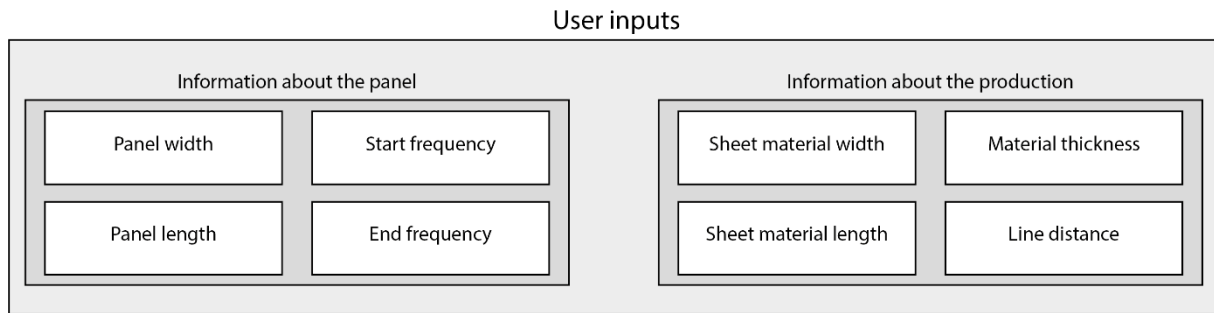


Figure 53: The user inputs

Before the tool can run, the user is asked to fill in some information about the panel and the limitations of the laser cutting device available. To generate the plans for the laser cutting machine the script needs to know the size of the sheet material that will be used to make the panels for the resonant panel. Besides the size, the thickness also needs to be provided in order to make sure the size of the cavities and the panel itself is correct. The laser cut line distance is used as a spacing between the different panels to make sure the lines do not overlap when laser cutting.

The information regarding the panel concerns the size that the panel can be, in both the x and y direction, and the frequency range that the panel needs to absorb. The script iterates through the frequencies and the number of positions available in the panel therefore the script will take a longer time to run. The inputs regarding the production have a smaller effect on the runtime of the script because these are introduced later in the process and do not have to be iterated multiple times.

### 3.2 The acoustic optimizer

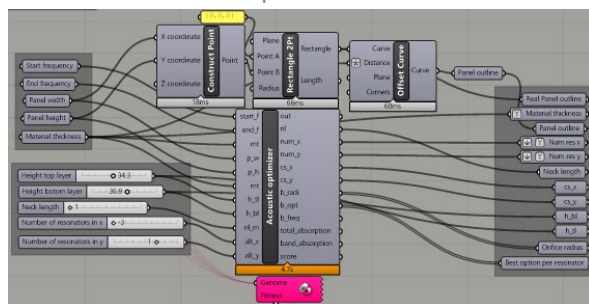


Figure 54: Acoustic optimizer part of the grasshopper script

The goal of the acoustic optimizer is to generate the dimensions of the resonators, calculate the number of resonators required and calculate the total sound absorption of the panel. The inputs required are the target frequency range, the size of the resonant panel and the material thickness.

Besides the user inputs, the optimizer also takes 5 inputs controlled by a Galapagos evolutionary solver. These 5 inputs are

- Height top layer: this controls the height of the top layer. It can range between 10.0 and 60.0 corresponding to 10.0 mm and 60.0 mm respectively. The precision is 0.1 mm.
- Height bottom layer: this controls the height of the bottom layer. As with the top layer this slider ranges between 10.0 and 60.0. Also with a precision of 0.1 mm.
- Neck length: this controls the height of the top panel covering the cavities. Because this covers the entire panel this can be considered to be the neck length. The slider ranges from 1 to 5 with a precision of 1. The result of this slider is not directly translated to a dimension. It serves

a multiplication factor for the material thickness since the material thickness is considered to be the minimal thickness.

- Number of resonators in x: this controls the additional resonators in the x direction. The slider ranges from -3 to 3 with a precision of 1. The number resulting from this slider serves as a modification to the panel division in the x direction.
- Number of resonators in y: this controls the additional resonators in the y direction. The slider ranges from -3 to 3 with a precision of 1. The number resulting from this slider serves as a modification to the panel division in the y direction.

The first thing that is determined within the acoustic optimizer is the amount of resonators that will be placed within the panel and with that the cavity sizes in both directions. The amount of cavities is determined by dividing the width of the frequency range by a number representing the approximate frequency interval between resonators, by default this is set to 5 (assuming a resonator approximately every 5 Hz is needed for broadband absorption). The panel is then divided into equal sizes so the resonators can be placed within a regular rectangular grid in a later stage. Because the panel consists of two layers there are twice as many places as needed. Assuming every resonator is used an equal amount the average size of a resonator is 2.25 positions. This then results in a bit under a resonator every 5 Hz.

### 3.2.1 Resonator types

Within the acoustic optimizer the resonator types are defined. When calculating the absorption the script can choose between four types of resonators.

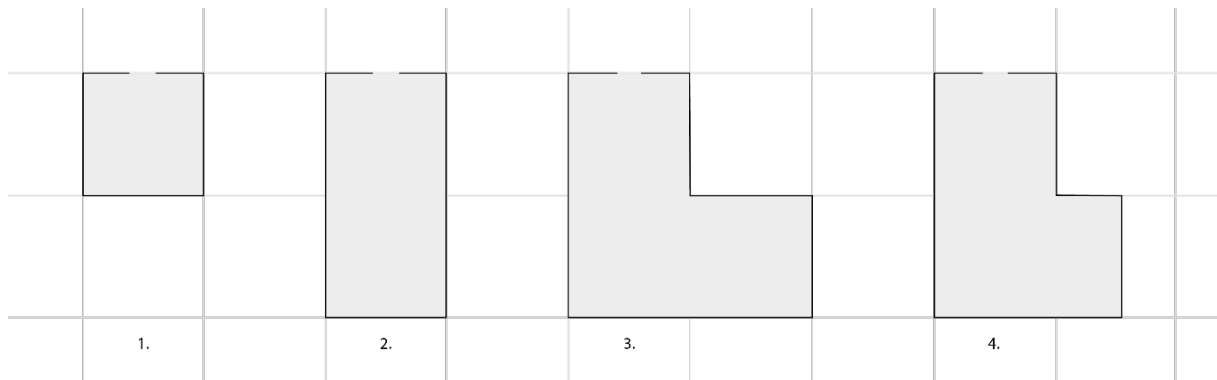


Figure 55: Resonator types

-Type 1: this resonator only resides in the top layer of the panel and takes up one space.

-Type 2: Is the elongated version of type 1. This resonator takes up one space in the top layer and one space in the bottom layer.

-Type 3: Is the L shaped resonator. This resonator takes up one space in the top layer and two spaces in the bottom layer. This reduces the need for additional thickness while allowing for extra volume.

-Type 4: is the smaller version of type 3. This resonator takes up one space in the top layer and 1.5 in the bottom layer. In a later stage two of these resonators will be combined to form two resonators with a shared cavity similar to the resonators in experiment 4.

In order to place these resonators efficiently into the panel, the panel must be divided into smaller elements that each represent a possible location for a resonator. The size of these smaller elements is determined based on the size of the frequency range that needs to be absorbed and the available size of the panel. This division thus also results in the maximum amount of resonators that can be placed

within the panel. The calculated amount of positions can be altered by the Galapagos solver using the number of resonators in x and y. This either increases or decreases the number of resonators but also alters the dimensions of the resonator cavity's.

The division of the panel is tied to the cavity size of the resonators, which is tied to the resonant frequency of the resonators. Therefore the division of the panel is placed within the iterative Galapagos loop and recalculated every iteration.

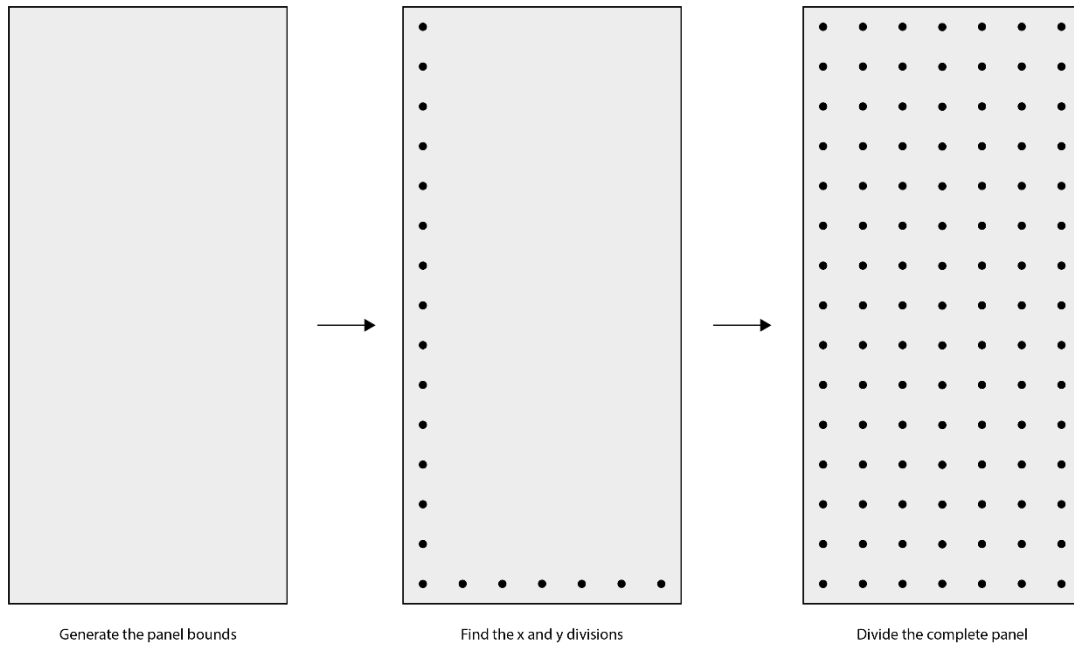


Figure 56: Division of the panel

### 3.2.2 The calculations

The calculations form the main part of the acoustic optimizer. The calculations are based on the formulas found within *Noise and vibration control engineering principles and applications* by Beranek and Ver (1992) and within the literature review part of this report. The contents of the script is presented below.

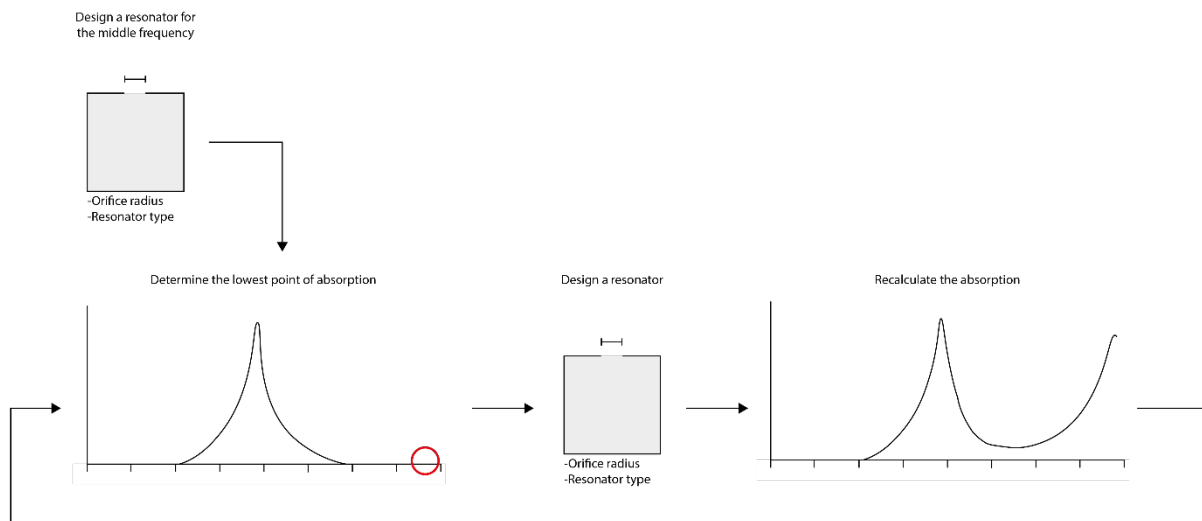


Figure 57: Visual representation of the workings of the acoustic optimizer

- In the first iteration the script takes the center frequency from the frequency range as the target frequency.
- The script starts with iterating through the resonator options that were defined before and can be seen in chapter 3.2.1. Within this loop another loop is created that iterates through all of the possible orifice dimensions. For each resonator type combined with each orifice dimension the absorption is calculated. After all of the options have been calculated the list is sorted and the best option is selected. If resonator type four is selected the index is remembered. This is done because the panel always needs to be fully filled, and an uneven number of resonator four does not allow the panel to be fully filled.
- After the first resonator has been designed, the total absorption over the entire frequency range is calculated. The frequency with the lowest absorption is selected, this becomes the new target frequency for the next iteration.

The loop continues this way until one of a couple of conditions is met.

- If in the bottom layer there is only enough room for half a resonator. The last placed resonator of type four is deleted and the option to choose resonator four is also deleted. This ensures that the panel will always be fully filled.
- If the bottom layer is full the resonators using the bottom layer are deleted as options so the top layer can be filled afterwards.
- If the panel is full the loop is broken. The absorption and the other relevant data is saved.

### 3.2.3 Verification of the resonators

The absorption is converted into a score for the Galapagos evolutionary solver to evaluate. The score is calculated by calculating the area under the absorption curve within the given frequency range and multiplying it with a bonus factor.

$$38. \text{bonus factor} = (1 - (a_{max} - a_{min})) + 1$$

Formula for the bonus factor with  $a_{max}$  being the maximum absorption found within the frequency range and  $a_{min}$  being the minimal absorption found within the frequency range

$$39. \text{score} = (\text{bonus factor} * \sum a) / (f_{range} * 2)$$

Formula for the score of a set of resonators with  $a$  being the absorption per frequency and  $f_{range}$  being the width of the frequency range.

The bonus factor is determined by the range of the absorption curve. If the lowest absorption in the range would be 0.2 and the highest absorption would be 0.8. The bonus factor would be 1.4. The bonus rewards a small range between the largest and the smallest absorption. This is because the panel attempts to provide broadband absorption. If the reverberation time would be equal over the entire frequency range an amount of panels needs to be placed based on the frequency with the lowest absorption following from formula 3 and 4. If the area under the curve would be very high but the absorption for a specific frequency very low the amount of panels would still have to be based on the low absorption of that frequency instead of on the high absorption of the other frequencies to receive the desired result. When the score is calculated the Galapagos solver changes the input values provided to attempt to increase the score.

The acoustic optimizer outputs the number of resonators that can be placed in the x and y direction, the cavity size in the x and y direction, the radius of the orifice per resonator, the resonator type per resonator and the neck length.

### 3.3 The resonator placement

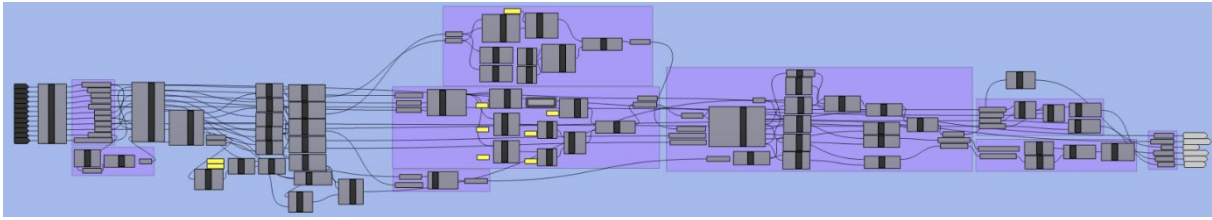


Figure 58: Resonator placement part of the grasshopper script

The goal of the resonator placement is to place the resonators calculated by the acoustic optimizer inside the panel. The inputs it takes to do this is the geometrical information from the acoustic optimizer and the size that the panel can be.

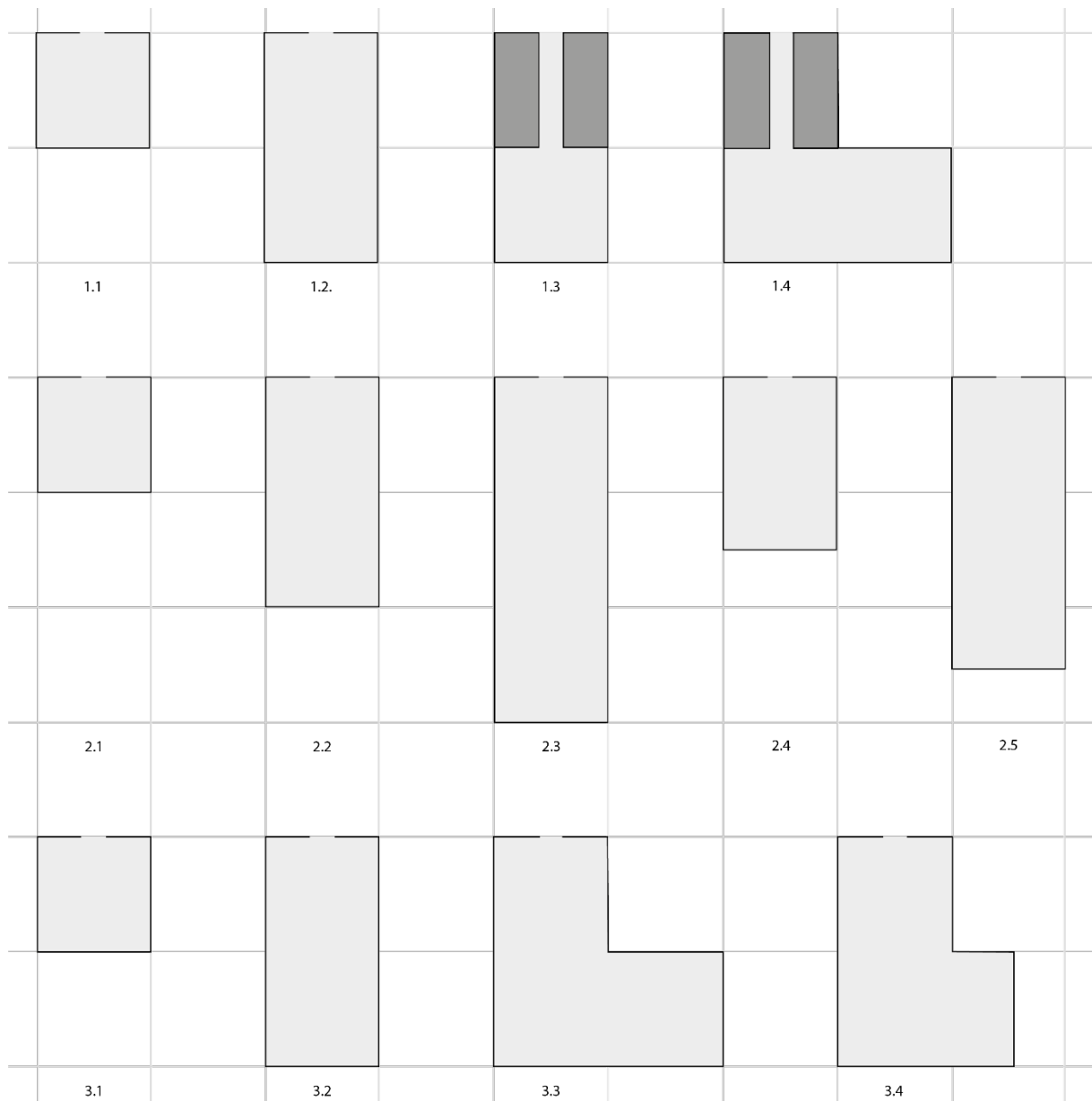


Figure 59: Resonator sets tested within the project

The initial idea for the resonant panel was to have all the resonators in one layer. But due to the large difference in optimal size for resonators in larger frequency ranges proved to be difficult. Placing the resonators in one layer could result in a panel where resonators of similar frequencies would be too far apart and would simply reflect the sound back into the room. The decision was taken to have multiple layers of resonators so the bigger resonators could be in the back layer and the smaller resonators in the top layer. This led to the design of experiment four. Which showed that the length of the neck should be kept short to make the absorption curve of the resonator wider which is beneficial when striving for broadband absorption. This in turn led to the design of experiment 5. To keep the necks of the resonators short but the depth of the panel low only rectangular cavities would not suffice. Therefore the L shaped resonator was designed.

The way the resonators are placed into the panel is very dependent on the design of the resonators. Therefore this step had a lot of iterations and different ways of packing the resonators into the panel. Other resonator designs and the way of placing those can be found within annex 3.

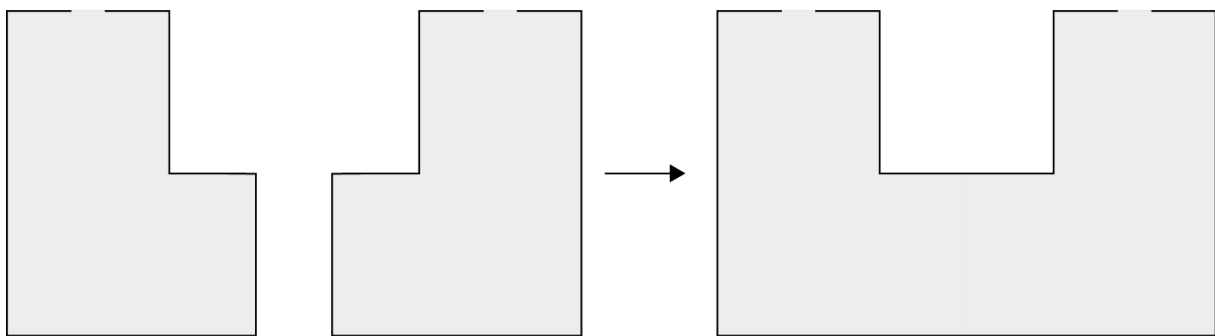


Figure 60: Combing resonators

The resonator placement starts with the separation of resonators that use only full cavities and resonators that use half cavities. The resonators using half cavities are then combined to form dual resonators that use only full cavities as seen in experiment 3. When all of the resonators are transformed into resonators that use only full cavity positions the actual placement of the resonators can begin.

Placing the resonators starts in the bottom layer of the resonant absorber. This is done because the bottom layer has an effect on the top layer but the top layer has no effect on the bottom layer. The cavities of the resonators in the bottom layer extend into the top layer, reducing the placement options the resonators in the top layer have.

Because no resonators have yet been placed, the first resonator is placed on the first available place, and since the grid is empty this is the bottom left corner, closest to the origin in rhino, because this is the first location in the list. When the resonator is placed, the locations it uses in the bottom layer and the top layer are deleted and added to the list of used positions. Because only the cavity outline is actually placed the resonator number is linked to the location to place the actual resonator later.

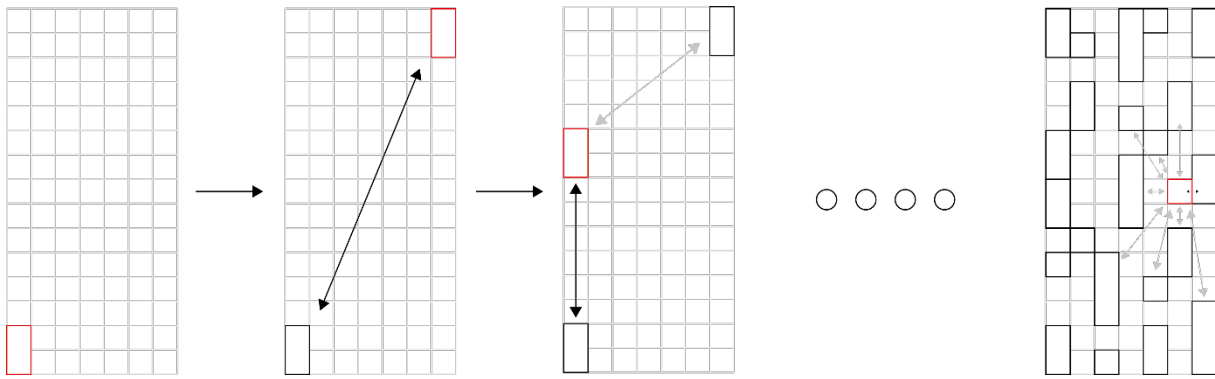


Figure 61: Resonator placement

In the second or higher iteration, resonators have already been placed and therefore these need to be taken into account. Even though experiment two showed the limited reduction in performance of the resonators when looking at the cross talk effect. An attempt has been made to place resonators with frequencies that lay close together as far apart as possible.

To find the optimal location for a resonator, the distance from each point to each unused point is calculated. For each of the unused positions, the shortest distance to another resonator is saved. All of these distances are then sorted to find the location that has the largest distance to the nearest resonator. To make sure this location is suitable for the resonator at hand, the cavity outline is placed on the location. The script then checks if the cavity outline contains as many locations as the amount of full cavity positions the resonator uses. If the resonator collides with another resonator, the cavity is rotated to see if this solves the problem. When this again leads to no results, the script selects the next point in the list from points with the largest distance to the nearest resonator.

The script continues until all of the resonators in the bottom layer have been placed. Because the acoustic optimizer took the amount of cavity positions into account the panel will be fully filled.

The placement of the resonators in the top layer follows the same procedure as the placement in the bottom layer. Because most of the locations for the top layer have been used by the resonators in the bottom layer the options for the top layer are a bit more slim.

The resonator placement outputs the cavity outlines for all of the resonators and the resonator orifices in their correct position.

### 3.4 Preparation for production

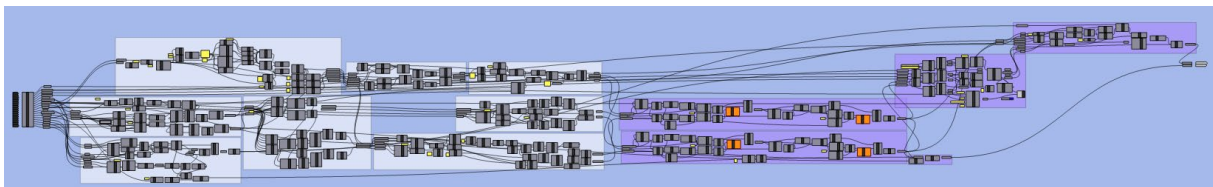


Figure 62: Preparation for production part of the grasshopper script

The goal for the preparation of production is taking the assembled panel from the resonator placement part of the script and turning it into 2D drawings that can be used by a laser cutting machine. The input it takes to do this is the geometrical information of the resonators, the locations of the resonators and the size of the panels that the laser cutter can handle.

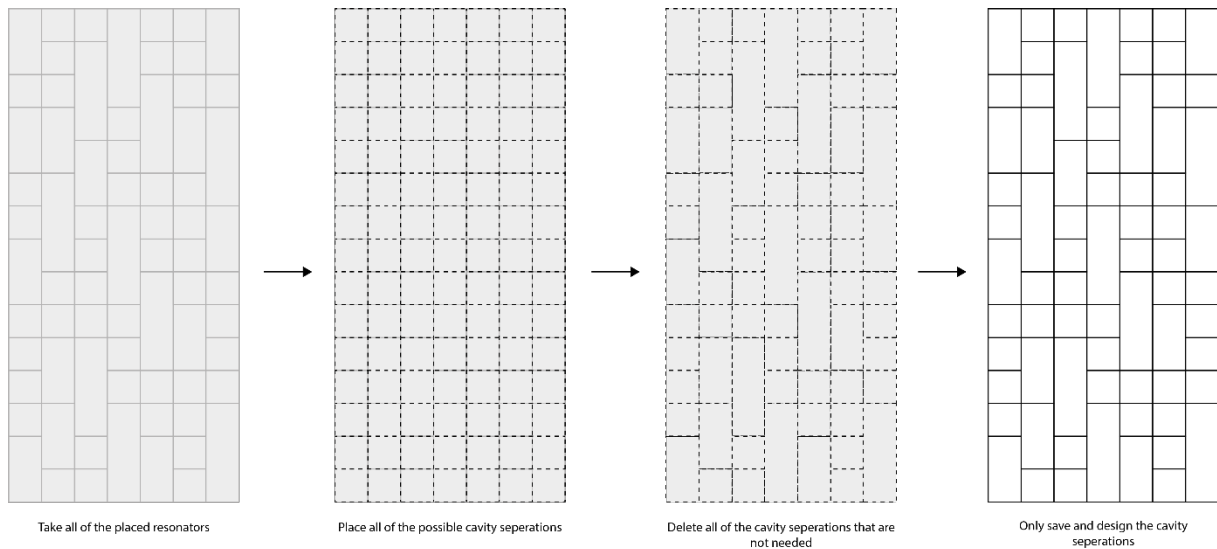


Figure 63: Cavity separations

The panels that will eventually be printed consist of the cavity separations and not of the resonators themselves. Thus the script generates the inverse of the resonators. Lines are placed in the positions where all of the cavity separations could be. When the cavity outlines are introduced within the grid they collide with the lines. All of the line segments inside of the cavity outlines are then deleted to generate the correct plans for both the top and the bottom layer of the resonant panel.

### 3.4.1 Intersections

To go from the 2D plans to the 3D panel the intersections between the panels play an important role in the ease of assembly and the strength of the eventual panel. Because the volume of the resonators influences the absorption and the peak frequency, it is important that the panel is assembled as precisely as possible. Connecting all the panels with Butt joints would increase the potential of incorrect placement of the cavity separations. To aid the assembly of the panel and to use the advantages of a laser cutter, the choice was made to have joints that use their geometry to force the correct placement.

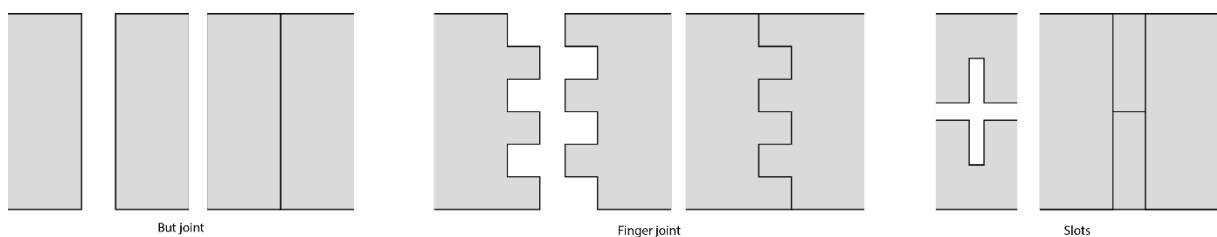


Figure 64: Woodworking joints

For the intersections happening at the end of a panel the finger joint was selected. This is done because a laser cutter can only engrave or cut completely through a panel. The depth of the engraving is hard to control. Therefore a joint was selected that uses the entire thickness of the material. A second reason to choose for this type of joint is its ability to connect the ends of two panels but also the end of one panel to the middle of another panel. The designed finger joints allow for only one possible connections. Panels in the x direction always have the bottom finger, ensuring the panels are connected correctly.

For intersections in the middle of two panels, finger joints were not an option. Therefore the choice was made to go with slots. As with the finger joints, the x direction always has the top part cut out while the y direction always has the bottom part cut out.

### 3.4.2 Packing the panels onto the sheet material

After the panels have been generated the conversion has to be made from a 3d panel to 2d sheet material. For the generation of the plans the laser cutting template from the faculty of Architecture at the Delft university of technology was used as a reference.

To make the packing of the panels onto the sheet material easier, the panels are converted into rectangles. Using a rectangular bounding box instead of the shape of the panel itself makes it so that only the four corners of the rectangular box have to be considered instead of the more complex geometry of the panels.

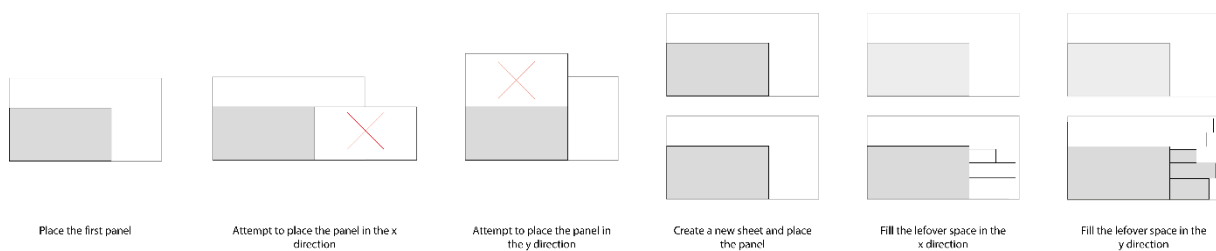


Figure 65: Placing the panels onto the sheet material

The first panels to be placed are the top middle and bottom panels. These are the largest panels and are thus least likely to fit in the leftover spaces of the panel.

The first step in the placement of the panels is to check if the largest dimension of the panels are in the same direction as the largest dimension of the sheet material. This is done to ensure that the panels fit onto the sheet material. The dimensions of the panel are compared to the dimensions left on the sheet. First the x direction is checked. If the x dimension of the panel is smaller than the x dimension that is left on the sheet, the panel is placed. If the left over space in the x direction is not enough, the script attempts to place the panel in a row above the panel that was just placed.

If in both the x and y direction there is not enough space for the current panel the script creates a new sheet to place the panel onto. The space that was left on the initial panel is used to place smaller panels before the second panel is filled further.

The script continues this process until all of the panels have been placed onto the sheet material. When all of the panels have been placed, the bounding boxes are replaced with the original panels. The sheets with the panels serve as the output of the entire tool. Besides the sheets, there is also a wireframe representation of the assembled panel to give an impression of what the panel will look like.

### 3.5 Overview of the tool

Operating the script requires nearly no additional inputs then the inputs discussed in part 3.1 of this report. The only thing the user has to do manually is to activate the Galapagos solver in order to optimize the acoustic absorption of the panel. The solver will stop automatically or can be stopped manually if so desired.

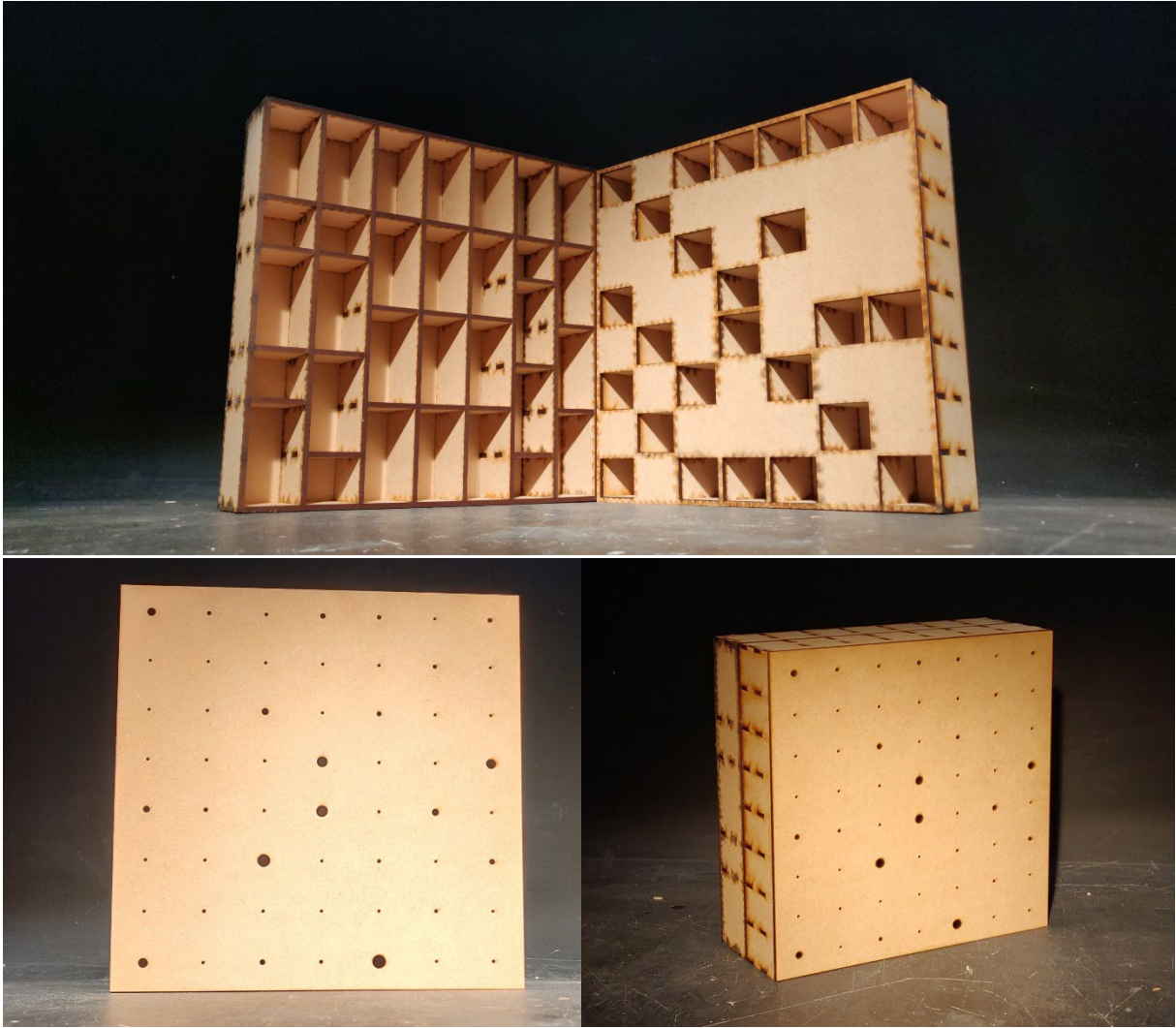
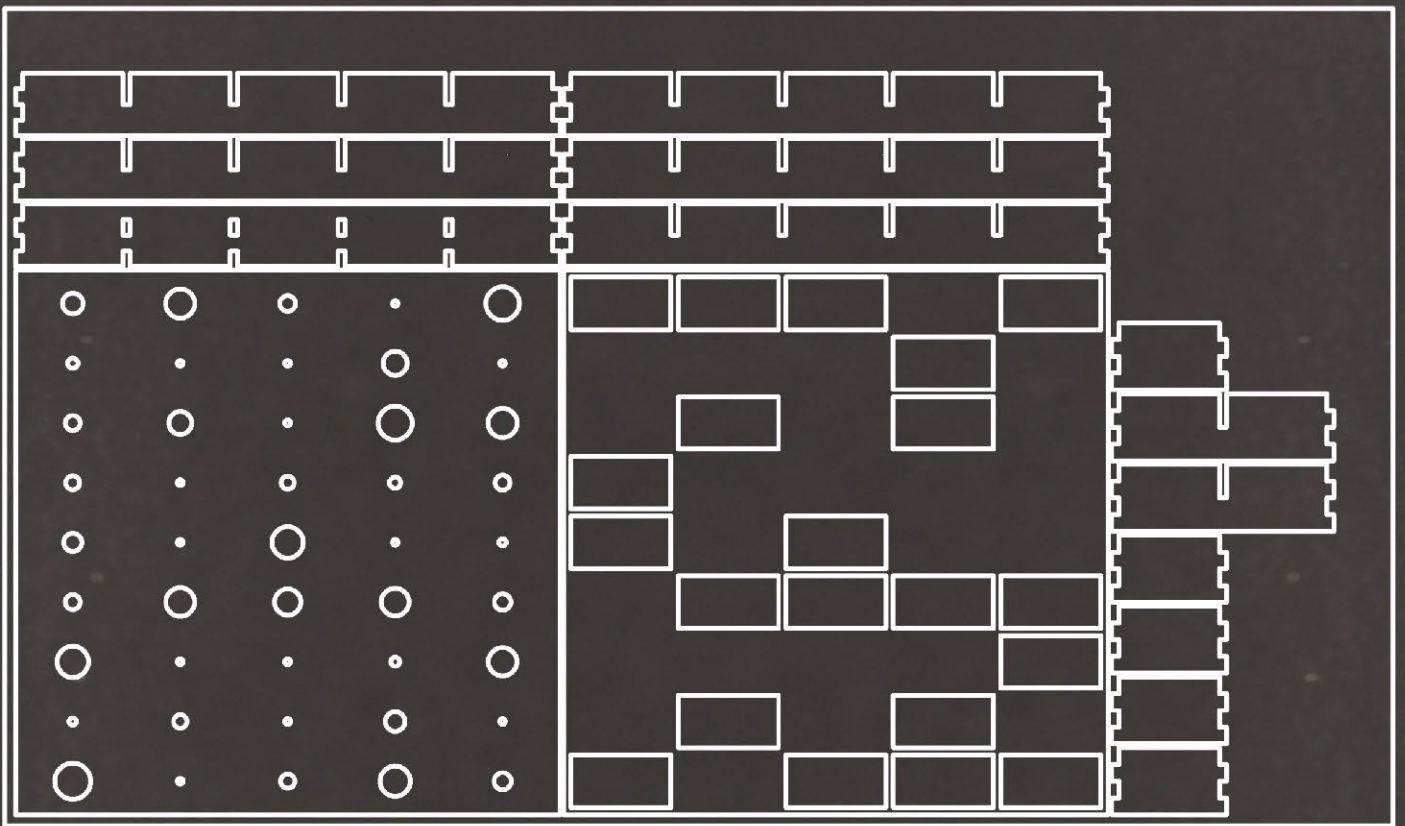


Figure 66: Assembled panel

Assembling the panel does require wood glue. Although the joints are chosen so the layers can be assembled without an adhesive. Glue is still required to ensure the panels stay in place and to attach the layer together.



4

Case study

## 4. Case study

The tool as presented in chapter three produces laser cutting plans to make panels that can be attached to a wall to improve the acoustic quality of a room. Besides this use case there are numerous other examples in which panels based on Helmholtz resonators can be used. This chapter will firstly attempt to theoretically validate the tool as presented in chapter three. Afterwards some other options for the use of the tool will be discussed.



Figure 67: 1.060 West

To validate the results presented in chapter three of this report a case study has been set up. The goal of this case study will be to improve the room acoustics of a small meeting room in the faculty of architecture in Delft. The chosen room is 1.060 West. The reverberation time of this room has already been measured by B. Gommer (2016). These measurements serve as the start of this case study.

## 4.1 Problem statement and method

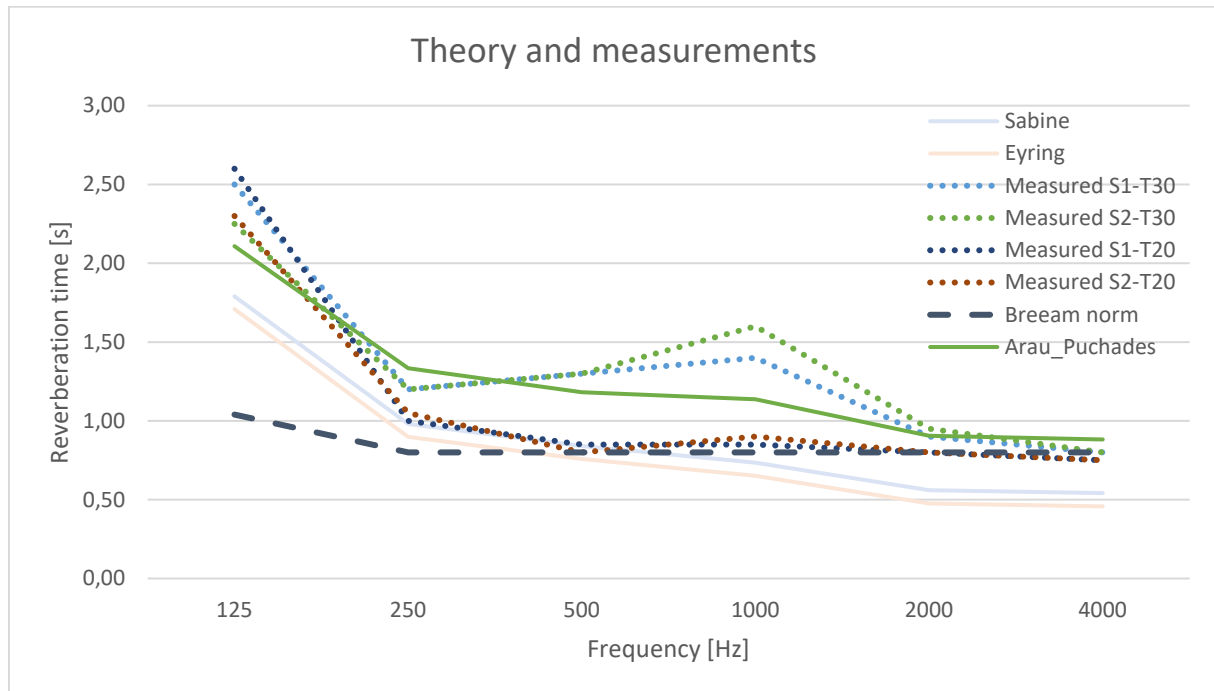


Figure 68: Measurement data from B. Gommer (2016) including theoretical approximations

Besides the measurement data figure 68 also shows the calculated reverberation time based on the formulas by Sabine and Eyring as presented in chapter one of this report. Because the theories by Sabine and Eyring do not comply well with the measurement data from Gommer (2016) an alternative way of calculating the reverberation time was used. The formulation by Arau-Puchades (1988) takes the absorption per direction into account. 1.060 West has unequally distributed absorption across the room, therefore it is important to keep the direction of the absorption into account. As can be seen in figure 68 this theory complies better with the measurements and will thus serve as the theoretical approximation.

$$40. T = \left( \frac{0.161V}{-S \ln(1-\bar{a}_x)} \right) \frac{S_x}{S} * \left( \frac{0.161V}{-S \ln(1-\bar{a}_y)} \right) \frac{S_y}{S} * \left( \frac{0.161V}{-S \ln(1-\bar{a}_z)} \right) \frac{S_z}{S}$$

Formula for the reverberation time by Arau-Puchades (1988). With  $S$  being the total surface area of all of the absorbing surfaces,  $\bar{a}_x$  [-] being the average absorption in the x direction with  $\bar{a}_y$  [-] and  $\bar{a}_z$  [-] representing the absorption in the y and z directions respectively,  $S_x$  [m<sup>2</sup>] being the surface area of all of the absorbing surfaces perpendicular to the x axis with  $S_y$  [m<sup>2</sup>] and  $S_z$  [m<sup>2</sup>] representing the perpendicular surfaces to the y and z axis respectively.

The goal is to comply with the Breeam regulations for acoustic comfort. Breeam regulation HEA 05 states that the reverberation time within a meeting room needs to be equal to or lower than 0.8 seconds. Section 3.a. states that the reverberation time of the octave band in 125 Hz can deviate a maximum of 30% from the average. Therefore the reverberation time in this frequency band can be 1.04 seconds.

To decrease the reverberation time in 1.060 West two panels will be designed. One panel absorbing frequencies between 100 and 250 Hz and another panel absorbing frequencies between 250 and 500 Hz. The higher part of the frequency range could also be absorbed with a resonant panel, but in these

higher frequency ranges porous absorbers are more efficient and are thus the chosen method of absorption.

#### 4.2 The panels

The two panels were designed with the laser cutters at the faculty of architecture in mind. The user inputs regarding the laser cutter are therefore based on those specifications and equal for both panels.

Material	Material thickness	Distance between lines	Panel size x direction	Panel size y direction
MDF	4 mm	2 mm	765 mm	450 mm

Table 11: inputs regarding the laser cutter

To keep the calculation time short the dimensions of the panel were chosen to be quite small. 300 mm in both the x and y directions. As mentioned before the first panel is set to absorb a frequency range of 100 to 250 Hertz and the second panel targets a frequency range of 250 to 500 Hz. The range is split into two parts because of the unequal absorption in the x and y direction. The x direction requires additional absorption in the 125 and 250 Hz octave bands, while the y direction requires more absorption in the 250 and 500 Hz octave bands. The additional absorption in the higher frequencies is mainly required in the y direction.

Inputting these values into the computational tool and running the optimization resulted in the following:

	Panel 1 100-250 Hz	Panel 2 250-500 Hz
Height of the top layer	59.5 mm	34.3 mm
Height of the bottom layer	53.5 mm	36.9 mm
Neck length	4 mm	4 mm
Resonators in the x direction	7	5
Resonators in the y direction	8	9

Table 12: dimensions of the resonant panels

For the additional absorption in the higher part of the frequency spectrum a similar absorbing panel to the one already in the room was chosen. This is because the panels have a high absorption at the required frequency bands.

	125 Hz	250 Hz	500 Hz	1000 Hz	2000 Hz	4000 Hz
Panel 1	0.71	0.39	0.02	0.03	0.01	0.01
Panel 2	0.01	0.63	0.46	0.02	0.06	0.03
Absorbing panel	0.16	0.35	0.50	0.80	0.95	0.95

Table 13: absorption of the chosen measures

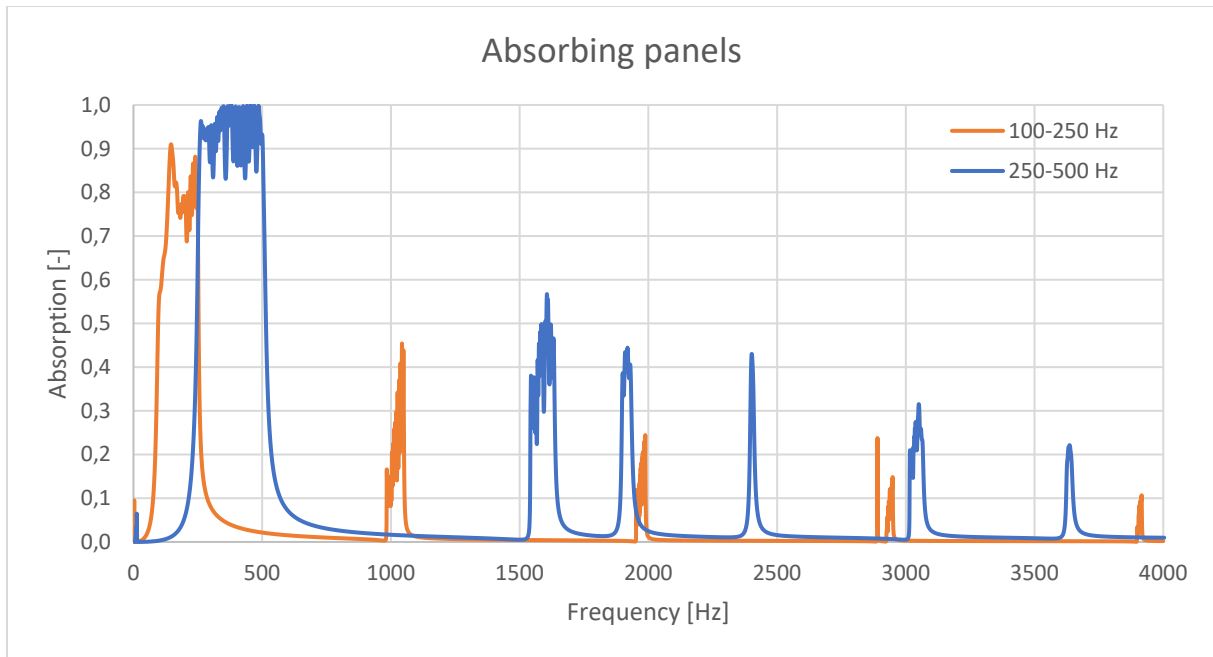


Figure 69: Absorption of the resonant panels

#### 4.3 Improvement of the room acoustics

After the panels have been designed the area that the panel needs to cover needs to be determined.

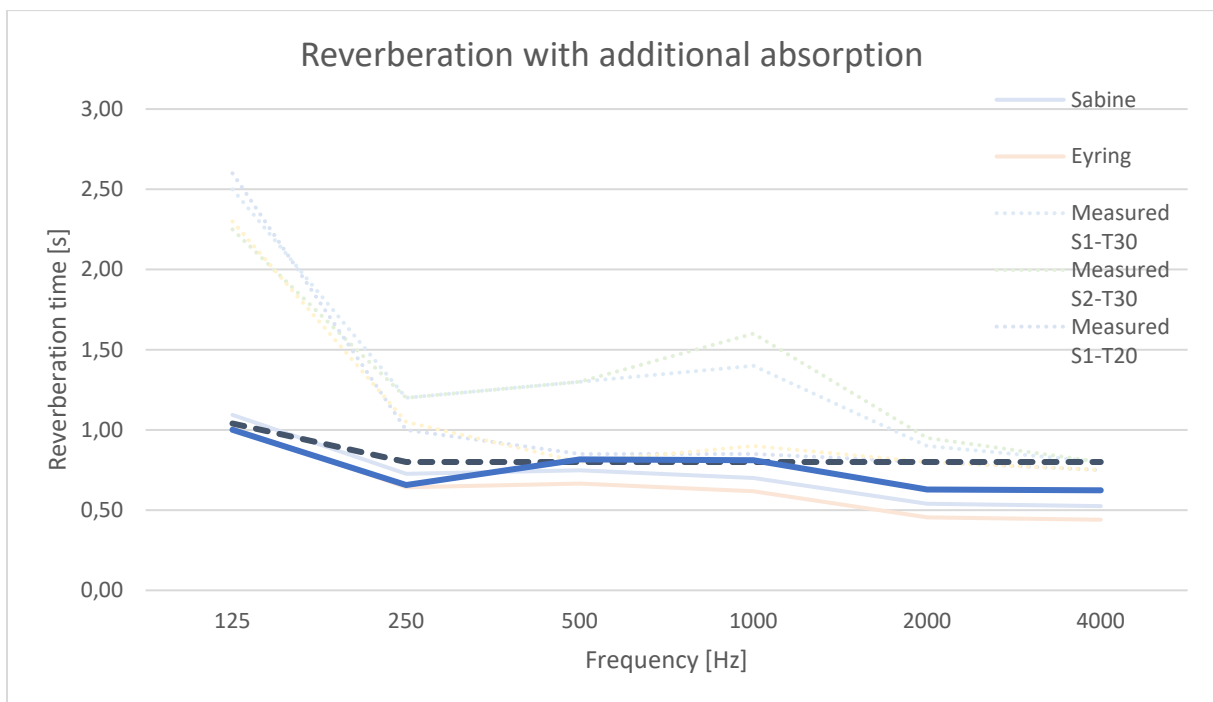


Figure 70: Reverberation time with the additional measures

	Area	Placement direction
Panel 1	21 m <sup>2</sup>	X
Panel 2	10 m <sup>2</sup>	Y
Absorbing panel	3 m <sup>2</sup>	y

Table 14: Areas and direction of the chosen measures

After the additional absorbing materials have been placed the room complies with the Bream norm for reverberation times in meeting rooms. Although the main focus in this chapter was on the Arau-Puchades formula for reverberation time, it can be seen that Eyring and Sabines reverberation times are also close to the norm. This case-study shows the theoretical potential of the tool presented in chapter three. The effectiveness at low frequencies is good and shows the potential of the tool. With more time a better solution could be generated, looking through panel sizes and allowing the optimizer to run for more iterations.



Figure 71: Renders of 1.060 West with additional acoustic measures

#### 4.4 Alternative applications:

Because the panel absorbs sound using its geometry the product is not tied to a single material. Any material with a sufficient degree of dimensional stability could be used to produce the panels.



Figure 72: Render displaying the resonant panels in glass

As can be seen in figure 72, the panel could be used inside a wall. Providing acoustic comfort without taking up any space inside the room. Here the panels are made from glass to allow for a transparent separation between rooms. Glass could be an alternative material to produce the panels. Other options might include: plastics, steel or ceramics.



Figure 73: Alternative options for the application of the resonant panel

Besides using the panel as a wall or to place onto a wall there is also the option to use it in a standalone item. Figure 73 shows the panels integrated into a call cell to improve the acoustics within the box. Because the panels are able to support themselves the panels can be stacked to create a room divider that could for instance be used within a large office. Besides the room divider and the call cell the panels could also be integrated into a closet or the back of a couch.



Figure 74: The call cell and the room divider in a office building

#### 4.5 Conclusion

As can be seen in this chapter the tool can be applied in multiple situations. The panel could be made from different materials and could even be used as something more than just an acoustic panel. The use of different materials could allow for a plethora of applications. Some examples might include a sporting facility for its rigidity or a sterile environment for the lack of need for a fibrous material to absorb sound.



## 5 Conclusions and recommendations

Acoustics combined with digital fabrication has been investigated for multiple years. Most research in this area has been focused on the combination of acoustics with additive manufacturing. This is mainly due to the ability of this technique to create any geometry, which allows for very high absorption. However, it has the downside that additive manufacturing is quite expensive and the production process is time-consuming. Therefore, this study has chosen to put the geometry first and the performance of the resonators second.

### 5.1 Conclusions

The literature review provided the starting points for this report, but also showed the gaps in knowledge needed to complete the project. These gaps in knowledge provided the opportunity to perform physical experiments in order to fill in these gaps. The experiments provided useful insights in the workings of the Helmholtz resonators.

- Experiment one was concerned with the position of the neck compared to the cavity. According to the results of the experiments the position of the neck has a minimal to no effect on the performance of the resonator.
- Experiment two was concerned with the cross-talk effect. According to the results of the experiments the effect of the cross-talk effect is minimal within the scope of this project. A small change in absorption was noticeable but so small as to be irrelevant.
- Experiment three was concerned with the removal of the cavity separations. According to the results of the experiments the cavity separation can be removed without a large effect on the absorption of the resonators.
- Experiment four was concerned with the influence of the neck length on the width of the absorption curve. According to the results of the experiments a longer neck causes the width of the absorption curve to decrease.
- Experiment five was concerned with the predictability of the impedance caused by resonators with a L shaped cavity. According to the results of the experiments a L shaped cavity can be approximated by replacing the L shaped cavity by a cavity with a identical horizontal section right below the orifice, but altering the height so the cavity has the same volume as the original L shaped cavity.

The experimental results provided the knowledge needed to be able to produce the digital workflow able to design a resonant panel based on Helmholtz resonators. The tool consists of three parts. The acoustic optimizer, which determines the resonator dimensions and the absorption of the total panel. The resonator placement, able to place the resonators designed by the acoustic optimizer inside the panel. The preparation for production, generates the two dimensional plans from the three dimensional geometry generated by the resonator placement.

The digital workflow was tested on a case study based on the measurements of 1.060 West at the faculty of architecture in Delft. The measurements were done by B. Gommer (2016). The case study proved the theoretical effectiveness of the tool. The reverberation time in the room was decreased to comply with the Breeam regulations for meeting rooms.

As for the answer to the main question: Can an acoustic panel based on Helmholtz resonators be designed with reduced geometrical complexity while retaining a broadband high absorption coefficient for low frequencies?

A resonant panel based on Helmholtz resonators can be designed with reduced geometrical complexity as presented in this report. However the high absorption for low frequencies is somewhat more

debatable. The design works well enough to provide sufficient absorption for the case study, but is not near perfect absorption over the entire frequency range. The reduction in geometrical complexity has been sufficient to be able to produce the panel with production techniques other than additive manufacturing.

## 5.2 Limitations

Due to time and financial concerns not everything could be optimally developed. Presented below are some of the limitations encountered during this study.

The experiments done within this project presented some interesting results. Due to time concerns no further research was done. Increasing the sample size for the experiments that were already done could increase the understanding and the predictability of Helmholtz resonators.

The performance of the digital workflow is only assessed theoretically. Physical measurements complying with ISO 354:2003 Measurement of sound absorption in a reverberation room or ISO 3382:2008 Measurement of room acoustic parameters could verify the results gained from the digital workflow. This physical verification is essential before the panel can be applied within a room.

## 5.3 Recommendations

During the project alternative routes and options were discovered that could lead to other solutions. Presented here are possibilities for further research and development of the project.

Currently the digital workflow is made within grasshopper. This is done because the author had previous experience with this program. In later stages of the project the idea came up to develop the entire project in python because large parts are already coded within python running inside grasshopper. Creating the workflow within python would make it more accessible because it eliminates the need for grasshopper and with that Rhino. Developing the project in python could also allow for more customizability in for example a user interface.

The goal of the project was to create a resonant panel, focused mainly on low frequencies, having a reduced geometrical complexity compared to other examples while being a thin panel. Because the geometry was the main focus, this was the starting point in most steps and the acoustic performance came second. An interesting avenue to investigate would be to take the absorption first and the geometry second. Starting with the geometry limited the options for the absorption to be optimized. Focusing on the absorption first could lead to better absorption if the geometry can be placed within the panels.

Within the current workflow there are multiple smaller things that could be developed to increase the useability of the tool. For example, at this moment the size of the panel is taken as just that the size of the actual panel. An improvement could be that the available space could be provided to the script. The script then divides the space into individual panels that together provide the desired absorption. Another example is the implementation of multiple frequency ranges. At this moment if two frequency ranges need to be absorbed two panels need to be designed. It might be more efficient to combine the two frequency ranges.

## References

1. Aish, R., & Woodbury, R. (2005). Multi-level Interaction in Parametric Design. *Smart Graphics 5th International Symposium*, 5, 151–162.
2. Akoestische prestaties - BREEAM-NL richtlijn. (n.d.). <https://richtlijn.breeam.nl/credit/akoestische-prestaties-1090>
3. Arau-Puchades, H. (1988). An improved reverberation formula. *International Journal of Acoustics*, 65 (1988), 163–180. [https://www.arauacustica.com/files/publicaciones/pdf\\_esp\\_7.pdf](https://www.arauacustica.com/files/publicaciones/pdf_esp_7.pdf)
4. Audet, C., & Hare, W. (2017). *Derivative-Free and Blackbox Optimization*. Springer Cham. <https://doi.org/10.1007/978-3-319-68913-5>
5. Bhatia, A., & Sehgal, A. K. (2021). Additive manufacturing materials, methods and applications: A review. *Materials Today: Proceedings*. <https://doi.org/10.1016/j.matpr.2021.04.379>
6. Bhavikatti, S. S. (2004). *Finite Element Analysis*. New Age International Ltd. <https://ebookcentral-proquest-com.tudelft.idm.oclc.org/lib/delft/detail.action?docID=358028>.
7. Birtu, C., & Avramescu, V. (2012). ABRASIVE WATER JET CUTTING - TECHNIQUE, EQUIPMENT, PERFORMANCES. *Revista de Tehnologii Neconventionale*, 16(1), 40–46.
8. Burczyński, T. (2010). Evolutionary and immune computations in optimal design and inverse problems. In *ADVANCES OF SOFT COMPUTING IN ENGINEERING* (pp. 57–132). SpringerWienNewYork.
9. Cai, X., Guo, Q., Hu, G., & Yang, J. (2014). Ultrathin low-frequency sound absorbing panels based on coplanar spiral tubes or coplanar Helmholtz resonators. *Applied Physics Letters*, 105(12), 121901. <https://doi.org/10.1063/1.4895617>
10. Chanaud, R. C. (1993). Effect of geometry on the resonance frequency of helmholtz resonators. *Journal of Sound and Vibration*, 178(3), 337–348.
11. Coons, S. A., & Mann, R. W. (1960, October). COMPUTER-AIDED DESIGN RELATED TO THE ENGINEERING DESIGN PROCESS. *Electronic Systems Laboratory Department of Electrical Engineering Massachusetts Institute of Technology*.
12. Cooper, K. (2001). *Rapid Prototyping Technology*. Marcel Dekker Inc.
13. Cox, T. J., & D'Antonio, P. (2009). *Acoustic Absorbers and Diffusers* (2nd ed.). Taylor & Francis.
14. Crivello, J. V., & Reichmanis, E. (2013). Photopolymer Materials and Processes for Advanced Technologies. *Chemistry of Materials*, 26(1), 533–548. <https://doi.org/10.1021/cm402262g>
15. Davoudinejad, A. (2021). Vat photopolymerization methods in additive manufacturing. In *Handbook in Advanced manufacturing: Additive manufacturing* (pp. 159–181). Elsevier. <https://doi.org/10.1016/B978-0-12-818411-0.00007-0>
16. Delany, M. E., & Bazley, E. N. (1970). Acoustical properties of fibrous absorbent materials. *Applied acoustics*, 3(2), 105–116. [https://doi.org/10.1016/0003-682X\(70\)90031-9](https://doi.org/10.1016/0003-682X(70)90031-9)
17. Dessing, J. B. (2005). *Praktijkgids bouwbesluit Geluid*. Nederlands Normalisatie-instituut.
18. Ekici, B., Cubukcuoglu, C., Turrin, M., & Sariyildiz, I. S. (2019). Performative computational architecture using swarm and evolutionary optimisation: A review. *Building and Environment*, 147, 356–371. <https://doi.org/10.1016/j.buildenv.2018.10.023>
19. Ermann, M. (2015). *Architectural Acoustics Illustrated*. Wiley.
20. Gibson, I., Rosen, D., Stucker, B., & Khorasani, M. (2021). *Additive Manufacturing Technologies* (3rd ed.). Springer Publishing.
21. Godbold, O. (2008, April). *Investigating broadband acoustic adsorption using rapid manufacturing* (Thesis). Loughborough University.

- [https://repository.lboro.ac.uk/articles/thesis/Investigating\\_broadband\\_acoustic\\_adsorption\\_using\\_rapid\\_manufacturing/9517877](https://repository.lboro.ac.uk/articles/thesis/Investigating_broadband_acoustic_adsorption_using_rapid_manufacturing/9517877)
22. Gommer, B. (2016). Resistance in Helmholtz resonators Exploring the potential of sound absorption created by additive manufacturing [MA Thesis]. Delft University of technology.
  23. Griffin, S., Lane, S. A., & Huybrechts, S. (2000). Coupled Helmholtz Resonators for Acoustic Attenuation. *Journal of Vibration and Acoustics*, 123(1), 11–17. <https://doi.org/10.1115/1.1320812>
  24. Groover, M. P. (2010). *Fundamentals of Modern Manufacturing: Materials, Processes and Systems* (4th ed.). Wiley.
  25. Hilton, P. A. (2007, August). The early days of laser cutting. 11th Nordic Conference in Laser Processing of Materials, Lappeenranta, Finland.
  26. Holland, J. H. (1992). Genetic Algorithms. *Scientific American*, 267(1), 66–72. <https://www.jstor.org/stable/10.2307/24939139>
  27. Hooke, R., & Jeeves, T. A. (1960). 'Direct Search' Solution of Numerical and Statistical Problems. *Journal of the ACM*, 8(2), 212–229. <https://doi.org/10.1145/321062.321069>
  28. HUBS. (2020, January). 3D printing trends 2020 Industry highlights and market trends. [https://downloads.hubs.com/3D\\_printing\\_trends\\_report\\_2020.pdf](https://downloads.hubs.com/3D_printing_trends_report_2020.pdf)
  29. Hudson, R. (2010). Strategies for parametric design in architecture. An application of practice led research (Thesis). University of Bath.
  30. Ingard, U. (1953). On the Theory and Design of Acoustic Resonators. *The Journal of the Acoustical Society of America*, 25(6), 1037–1061. <https://doi.org/10.1121/1.1907235>
  31. James, M. (2005, December). Fundamental studies of the Herschel-Quincke tube concept with mode measurements. Virginia Polytechnic institute and state university. <https://vtechworks.lib.vt.edu/handle/10919/35862?show=full>
  32. Kalpakjian, S., & Schmid, S. (2007). *Manufacturing Processes for Engineering Materials* (5th Edition) (5th ed.). Pearson.
  33. Kals, H. J. J., Buiting-Csikós, C., van Luttervelt, C. A., Moulijn, K. A., Ponsen, J. M., & Streppel, A. H. (2007). *Industriële productie* (4th ed.). Academic Service.
  34. Kief, H. B., & Roschiwal, H. A. (2013). *CNC Handbook*. McGraw-Hill Education.
  35. Kinsler, L. E., Frey, A. R., Coppens, A. B., & Sanders, J. V. (2000). *Fundamentals of Acoustics*. Wiley.
  36. Li, J., Wang, W., Xie, Y., Popa, B. I., & Cummer, S. A. (2016). A sound absorbing metasurface with coupled resonators. *Applied Physics Letters*, 109(9), 091908. <https://doi.org/10.1063/1.4961671>
  37. Liu, Z. (2018). *Multiphysics in Porous Materials*. Springer Publishing. <https://doi.org/10.1007/978-3-319-93028-2>
  38. Miles, J. (2010). Genetic algorithms for design. In *Advances of soft computing in engineering* (Vol. 512, pp. 1–56). SpringerWienNewYork.
  39. Nijs, L. (2007). Schoonheid en hinder De positieve en negatieve aspecten van geluid. Ruimteakoestiek En/of Zaalakoestiek. Retrieved 30 May 2022, from <https://bk.nijsnet.nl/default.aspx>
  40. Olsson, D. M., & Nelson, L. S. (1975). The Nelder-Mead Simplex Procedure for Function Minimization. *Technometrics*, 17(1), 45–51. <https://doi.org/10.1080/00401706.1975.10489269>
  41. Ren, Z., Cheng, Y., Chen, M., Yuan, X., & Fang, D. (2022). A compact multifunctional metastructure for Low-frequency broadband sound absorption and crash energy dissipation. *Materials & Design*, 215, 110462. <https://doi.org/10.1016/j.matdes.2022.110462>

42. Rossing, T. (2007). *Springer Handbook of Acoustics*. Springer Publishing. <https://link.springer.com/referencework/10.1007/978-0-387-30425-0>
43. Sacerdote, G. G., & Gigli, A. (1951). Absorption of Sound by Resonant Panels. *The Journal of the Acoustical Society of America*, 23(3), 349–352. <https://doi.org/10.1121/1.1906771>
44. Setaki, F., Tenpierik, M., Turrin, M., & van Timmeren, A. (2014). Acoustic absorbers by additive manufacturing. *Building and environment*, 2014(72), 188–200. <https://doi.org/10.1016/j.buildenv.2013.10.010>
45. Siemiński, P. (2021). Introduction to fused deposition modeling. In *Handbooks in advanced manufacturing: Additive manufacturing* (pp. 217–275). Elsevier. <https://doi.org/10.1016/B978-0-12-818411-0.00008-2>
46. Tijdeman, H. (1975). On the propagation of sound waves in cylindrical tubes. *Journal of Sound and Vibration*, 39(1), 1–33. [https://doi.org/10.1016/s0022-460x\(75\)80206-9](https://doi.org/10.1016/s0022-460x(75)80206-9)
47. van der Eerden, F. (2000, November). Noise reduction with coupled prismatic tubes (Thesis). University of Twente. <https://research.utwente.nl/en/publications/noise-reduction-with-coupled-prismatic-tubes>
48. van der Linden, A. C., Erdsieck, P., Gaalen, I. M. K., & Zeegers, A. (2011). *Bouwfysica*. ThiemeMeulenhoff.
49. Vér, I. L., & Beranek, L. L. (2005). *Noise and Vibration Control Engineering: Principles and Applications* (2nd ed.). Wiley.
50. Wortmann, T. (2018, July). Efficient, Visual, and Interactive Architectural Design Optimization with Model-based Methods (Thesis). Singapore University of Technology and Design. <https://doi.org/10.13140/RG.2.2.15380.55685>
51. Yang, D., Sun, Y., di Stefano, D., Turrin, M., & Sariyildiz, S. (2016). Impacts of problem scale and sampling strategy on surrogate model accuracy: An application of surrogate-based optimization in building design. 2016 IEEE Congress on Evolutionary Computation (CEC), 4199–4207. <https://doi.org/10.1109/cec.2016.7744323>
52. Yasa, E. (2021). Selective laser melting: principles and surface quality. In *Handbooks in advanced manufacturing: additive manufacturing* (pp. 77–120). Elsevier. <https://doi.org/10.1016/B978-0-12-818411-0.00017-3>
53. Zhang, X., & Liou, F. (2021). Introduction to additive manufacturing. In *Handbooks in Advanced Manufacturing: Additive manufacturing* (pp. 1–31). Elsevier. <https://doi.org/10.1016/B978-0-12-818411-0.00009-4>
54. Zwicker, C., & Kosten, C. W. (1949). *Sound absorbing materials*. Elsevier.

## List of figures

Figure 1: The lick, from: <https://blogs.horacemann.org/mix/the-lick/>

Figure 2: Workflow through the project, own work

Figure 3: Resonant panel, own work

Figure 4: Absorption, reflection, transmission, adapted from: Cox, D'Antonio (2009)

Figure 5: Viscous boundary layer, adapted from: Godbold (2008)

Figure 6: Reverberation room, from: <https://www.soundonsound.com/reviews/choosing-using-porous-absorbers>

Figure 7: Impedance tube, adapted from: Cox, D'Antonio (2009)

Figure 8: Two microphone free field method, adapted from: Cox, D'Antonio (2009)

Figure 9: Porous material, from: <https://www.hornbach.nl/shop/MACLEAN-Geluidsisolatieplaat-Antraciet-1000-x-500-x-20-mm-pak-2-platen-1-m2/4111083/artikel.html>

Figure 10: Particle velocity, adapted from: van der linden (2016)

Figure 11: Helmholtz resonator, own work

Figure 12: Quarter wavelength tube, own work

Figure 13: Panel absorber, own work

Figure 14: Micro perforated panel, from: <https://decoceiling.en.made-in-china.com/product/dZpnOEFvAAVx/China-Micro-Perforated-Soundproof-Panels-Acoustical-Sound-Absorbing-Wall-Panels-with-MDF.html>

Figure 15: Conclusion table regarding resonators, own work

Figure 16: Godbold (2008), from: Godbold (2008)

Figure 17: Cai et al. (2014), from: Cai et al. (2014)

Figure 18: Li et al. (2016), from: Li et al. (2016)

Figure 19: Ren et al. (2022), from: Ren et al. (2022)

Figure 20: Setaki (2012), from: Setaki (2012)

Figure 21: Gommer (2016), from: Gommer (2016)

Figure 22: Costa (2016), from: Costa (2016)

Figure 23: Christia (2017), from: Christia (2017)

Figure 24: Scholten (2018), from: Scholten (2018)

Figure 25: Primary groups of production techniques, own work

Figure 26: 3 Axes CNC machine, from: <https://www.directindustry.com/prod/mecanumeric/product-16536-111311.html>

Figure 27: 6 Axes CNC machine, from: <https://materialdistrict.com/article/3d-printing-fibreglass-composites-6-axis-robot-arm/3d-printing-fibreglass-composites-with-a-6-axis-robot-arm-1/>

Figure 28: CNC milling machine, from: <https://industrytoday.com/cnc-milling-machines/>

Figure 29: Laser cutter, from: <https://www.gettingsmart.com/2016/10/13/introduction-design-laser-cutter/>

Figure 30: Water jet cutter, from: <https://www.machinemfg.com/waterjet-cutting-guide/>

Figure 31: Stereolithography, adapted from: [https://en.wikipedia.org/wiki/Stereolithography#/media/File:Schematic\\_representation\\_of\\_Stereolithography.png](https://en.wikipedia.org/wiki/Stereolithography#/media/File:Schematic_representation_of_Stereolithography.png)

Figure 32: Selective laser sintering, adapted from: [https://en.wikipedia.org/wiki/Selective\\_laser\\_sintering#/media/File:SLS\\_schematic.svg](https://en.wikipedia.org/wiki/Selective_laser_sintering#/media/File:SLS_schematic.svg)

Figure 33: Fused filament printing, adapted from: [https://en.wikipedia.org/wiki/Fused\\_filament\\_fabrication#/media/File:Schematic\\_representation\\_of\\_Fused\\_Filament\\_Fabrication\\_01.png](https://en.wikipedia.org/wiki/Fused_filament_fabrication#/media/File:Schematic_representation_of_Fused_Filament_Fabrication_01.png)

Figure 34: Concluding table regarding production techniques, own work

Figure 35: Performative computational architecture, from: <https://www.youtube.com/watch?v=BNv4jYQiQiw&t=15s>

Figure 36: Finite element modeling, from: [https://www.researchgate.net/figure/Stress-field-obtained-from-the-finite-element-method-FEM-analysis-for-LR2G15\\_fig3\\_339376763](https://www.researchgate.net/figure/Stress-field-obtained-from-the-finite-element-method-FEM-analysis-for-LR2G15_fig3_339376763)

Figure 37: Direct search optimization algorithm, adapted from D. M. Olsson and L. S. Nelson 1975

Figure 38: B&K 4206, own work

Figure 39: Creality Ender 3 S1 3d printer, own work

Figure 40, printed resonator with altering neck positions, sample 1.1 to 1.3, picture by Sanne Maring

Figure 41: Graph containing the measured data form the samples in set 1, compared to the theoretical values, own work

Figure 42: samples with altering neck positions, sample 2.1 to 2.4, picture by Sanne Maring

Figure 43: Graph containing the measured data form the samples in set 2 compared to the theoretical values, own work

Figure 44: Samples with and without cavity separations, sample 3.1 to 3.5, picture by Sanne Maring

Figure 45: Graph containing the measured data form the samples in set 3 compared to the theoretical values, own work

Figure 46: Samples with altering neck lengths, Sample 4.1 to 4.3, picture by Sanne Maring

Figure 47: Graphs containing the measured data form the samples in set 4 compared to the theoretical values, own work

Figure 48: Samples with L shaped cavities, Sample 5.4.2 and 5.5.2, picture by Sanne Maring

Figure 49: possible approximations for an L shaped cavity, own work

Figure 50: Graph containing the measured data form the samples in set 5 compared to the theoretical values, own work

Figure 51: Digital tool within Grasshopper, own work

Figure 52: Flowchart of the digital tool in text and pictures, own work

Figure 53: The user inputs, own work

Figure 54: Acoustic optimizer part of the grasshopper script, own work

Figure 55: Resonator types, own work

Figure 56: Division of the panel, own work

Figure 57: Visual representation of the workings of the acoustic optimizer, own work

Figure 58: Resonator placement part of the grasshopper script, own work

Figure 59: Resonator sets tested within the project, own work

Figure 60: Combing resonators, own work

Figure 61: Resonator placement, own work

Figure 62: Preparation for production part of the grasshopper script, own work

Figure 63: Cavity separations, own work

Figure 64: Woodworking joints, own work

Figure 65: Placing the panels onto the sheet material, own work

Figure 66: Assembled panel, own work

Figure 67: 1.060 West, own work

Figure 68: Measurement data from B. Gommer (2016) including theoretical approximations, own work

Figure 69: Absorption of the resonant panels, own work

Figure 70: Reverberation time with the additional measures, own work

Figure 71: Renders of 1.060 West with additional acoustic measures, own work

Figure 72: Render displaying the resonant panels in glass, own work

Figure 73: Alternative options for the application of the resonant panel, own work

Figure 74: The call cell and the room divider in a office building, own work

## List of tables

Table 1: Dimensions of the samples from the first experiment

Table 2: absorption and peak frequency from the samples of experiment one

Table 3: Dimensions of the individual resonators from the second experiment

Table 4: absorption and peak frequency from the samples of experiment two

Table 5: Dimensions of the individual resonators from the third experiment

Table 6: absorption and peak frequency from the samples of experiment three

Table 7: Dimensions of the samples from the fourth experiment

Table 8: absorption, peak frequency, and the frequency range at  $\frac{1}{2}$  of the absorption from the samples of experiment four

Table 9: Dimensions of the resonators from the fourth experiment

Table 10: absorption and peak frequency from the samples of experiment five

Table 11: inputs regarding the laser cutter

Table 12: dimensions of the resonant panels

Table 13: absorption of the chosen measures

Table 14: Areas and direction of the chosen measures

**X**

**Annexes**

# Annex 1: Measurement setup and sample measurements

## Measurements of the samples after printing

	Neck length		Orifice diameter		Cavity width		Cavity height		Cavity depth		Sample Height		Sample diameter	Remarks
1.1														
Measured	8		4,75		39,8		39,8		31,8		39,75		100	10% filling
Suposed	8		5,2		40		40		32		40		100	
1.2														
Measured	8		4,8		39,8		39,8		32		39,8		100	10% filling rough top surface round sample edge
Suposed	8		5,2		40		40		32		40		100	
1.3														
Measured	8		4,8		39,8		39,8		32		39,8		100	10% infill
Suposed	8		5,2		40		40		32		40		100	
2.1														
Measured	6	6	5	5	29,9	29,9	29,9	29,9	29,9	39,5	40	45,5	100	5% filling round sample edge
Suposed	6	6	5,4	5,6	30	30	30	30	30	40	40	46	100	
2.2														
Measured	6	6	5	5	29,75	29,75	29,75	29,75	29,75	39,5	40	45,5	100	5% filling
Suposed	6	6	5,4	5,6	30	30	30	30	30	40	40	46	100	
2.3														
Measured	6	6	5	5	29,75	29,75	29,75	29,75	29,75	40	40	45,5	100	5% filling
Suposed	6	6	5,4	5,6	30	30	30	30	30	40	40	46	100	
2.4														
Measured	6	6	4,9	5	29,75	29,75	29,75	29,75	29,75	40	40	45,5	100	5% filling rough top surface
Suposed	6	6	5,4	5,6	30	30	30	30	30	40	40	46	100	
3.1														
Measured	12,5	12,5	6,5	7,2	25,8	25,8	25,8	25,8	25,8	41	41	53,2	100	2% filling
Suposed	12,6	12,6	7,2	7,8	26	26	26	26	26	41	41	53,6	100	
3.2														
Measured	12,5	12,5	6,5	7,1	25,8					51,8	41	53,2	100	2% filling
Suposed	12,6	12,6	7,2	7,8	26					52	41	53,6	100	
3.3														
Measured	12,5	12,5	6,5	7,1	25,8					51,8	40,8	53,2	100	2% filling
Suposed	12,6	12,6	7,2	7,8	26					52	41	53,6	100	
3.4														
Measured	12,5	12,5	6,5	7,1	25,6					51,8	41	53,2	100	2% filling
Suposed	12,6	12,6	7,2	7,8	26					52	41	53,6	100	
3.5														
Measured	12,5	12,5	6,5	7,1	25,6					51,8	40,8	53,1	100	2% filling very rough top surface edge imperfections
Suposed	12,6	12,6	7,2	7,8	26					52	41	53,6	100	
4.1														
Measured	7		7,1		37,5		37,5			46		51,8	100	5% filling slightly rough surface
Suposed	6		7,8		38		38			46		52	100	
4.2														
Measured	16		8,9		31,8		31,8			48,8		65	100	5% filling edge imperfections slightly rough surface
Suposed	16,2		9,4		32		32			49		65,2	100	
4.3														
Measured	53		12,4		31,8		31,8			37		90	100	5% filling slightly rough surface
Suposed	53,4		13,2		32		32			37		90,4	100	
5.1														
Measured	20		5,2		68,8 ?		31,5	31,5	40	74,5		94,3	100	2% filling
Suposed	20		6		69	32	32	32	40	75		95	100	
5.2														
Measured	10		6		65 ?		29,8	29,8	30	60		70	99,8	2% filling other printer
Suposed	10		6		65	30	30	30	30	60		70	100	
5.3														
Measured	5		5,2		44,9 ?		20	20	30	55		59,5	100	2% filling
Suposed	5		6		45	20	20	20	30	55		60	100	
5.4														
Measured	3		5,5		44,9		20	20	25	50		52,5	100	2% filling
Suposed	3		6		45		20	20	25	50		53	100	
5.5														
Measured	2		7,5		44,8		20	20	20	44,8		46,2	100	2% filling
Suposed	2		8		45		20	20	20	45		47	100	
5.4.2														
Measured	3		5,8		45		19,8	19,8	24,9	50		52,7	100	5% filling
Suposed	3		6		45		20	20	25	50		53	100	
5.5.2														
Measured	2		7,8		44,8		19,8		20	45		46,5	100	5% filling
Suposed	2		8		45		20		20	45		47	100	
5.1.2														
Measured	20		5,5		68,8		31,6		40	75		94,5	100	5% filling
Suposed	20		6		69		32		40	75		95	100	
5.2.2														
Measured	10		5,3		65		30		30	60		69,5	100	5% filling
Suposed	10		6		65		30		30	60		70	100	
5.3.2														
Measured	5,1		5,6		45		20		30	55		59,9	100	5% filling
Suposed	5		6		45		20		30	55		60	100	

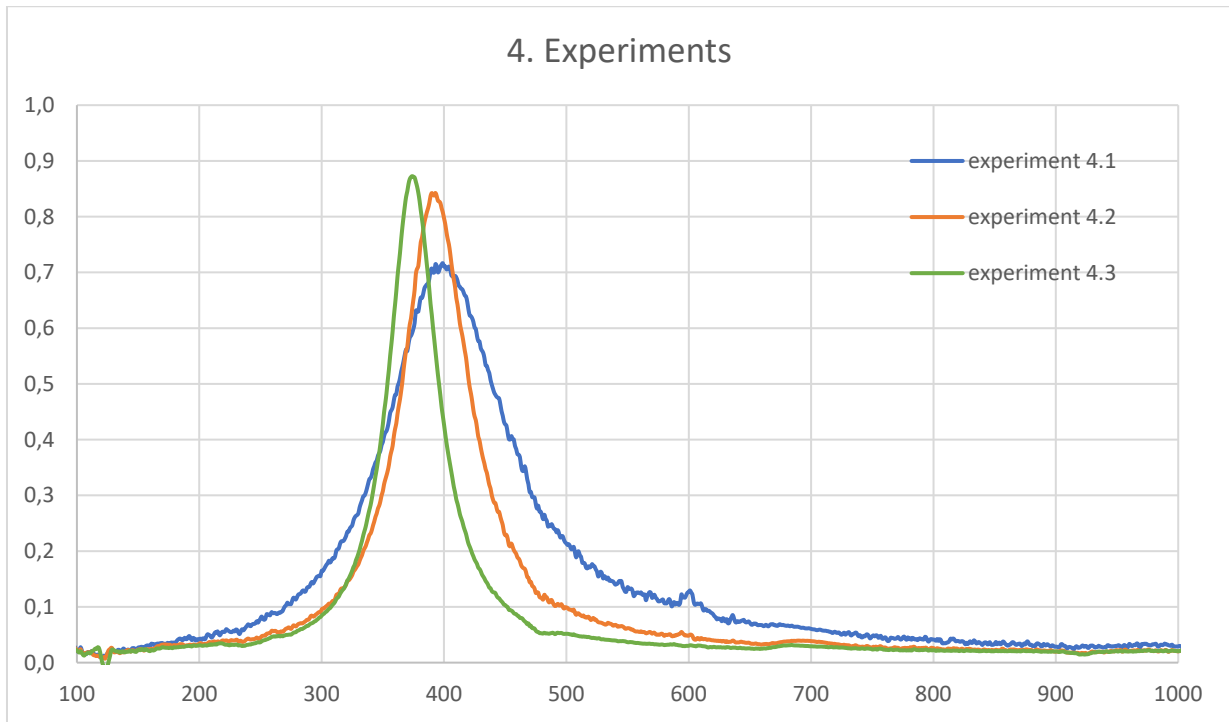
## Impedance tube measurement setup

<b>Tube</b>		
Type	Large	
Microphone Spacing:	0,05 m	
Distance to Sample from Mic. B, Pos. 3:	0,1 m	
Distance to Source from Mic. A, Pos. 2:	0,15 m	
Diameter:	0,100 m	
Lower Frequency Limit:	50 Hz	
<b>Measurement</b>		
Lines	1600	
Span	1.6 kHz	
Averages	150	
Zoom	ONWAAR	
Centre Frequency (Hz):	800,0	
<b>Generator</b>		
Generator Active	WAAR	
Waveform:	Random	
Signal Level:	1,400 Vrms	
Pink Filter:	Off	
<b>Environment</b>		
Atmospheric Pressure:	1013,25 hPa	
Temperature:	21,00 °C	
Relative Humidity:	50,0 %	
Velocity of Sound: 343,82 m/s		
Density of Air: 1,198 kg/m <sup>3</sup>		
Characteristic Impedance of Air: 411,9 Pa/(m/s)		
<b>Options</b>		
Signal-to-Noise Ratio below:	10,0 dB	
Autospectrum (Max-Min) above:	60,0 dB	
Calibration Factor exceeds:	2,0 dB	
Calibration Factor exceeds:	2,0 degrees	
Transfer Function Estimate:	H1	

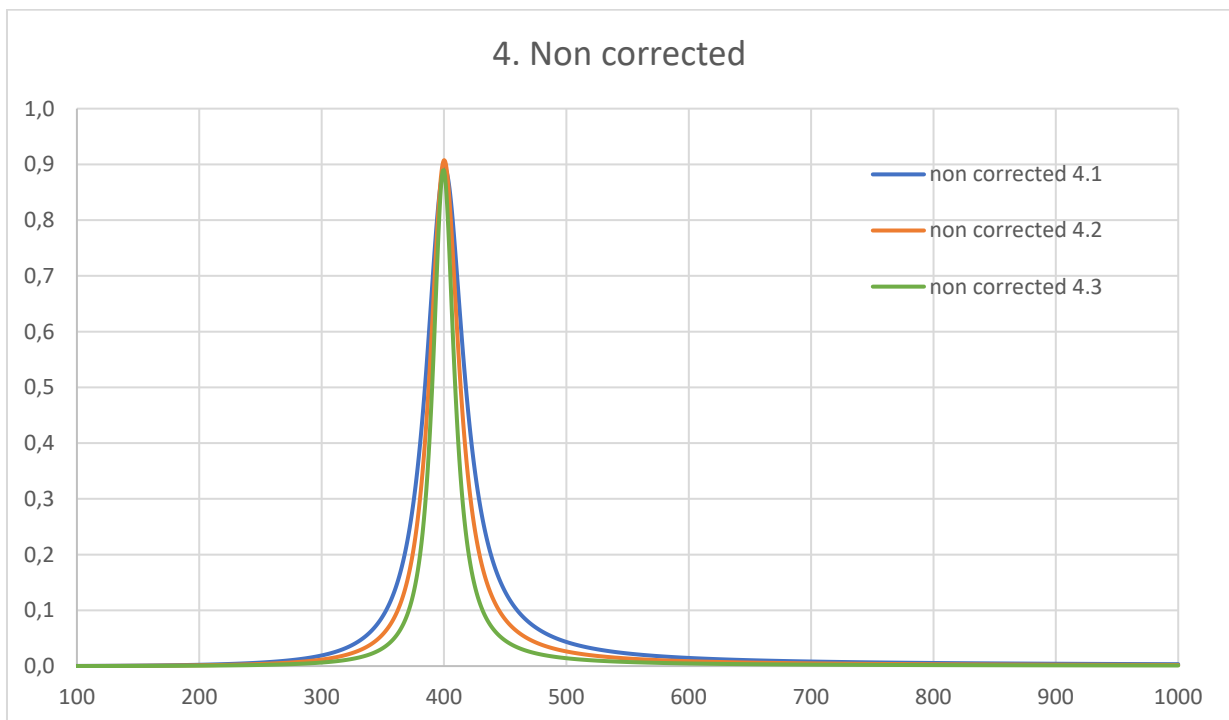
## Annex 2: Results from the experiments

Due to the large amount of graphs available from the test data it was not feasible to place all of them in the main report therefore this annex presents all of the graphs not presented in the main part of the report.

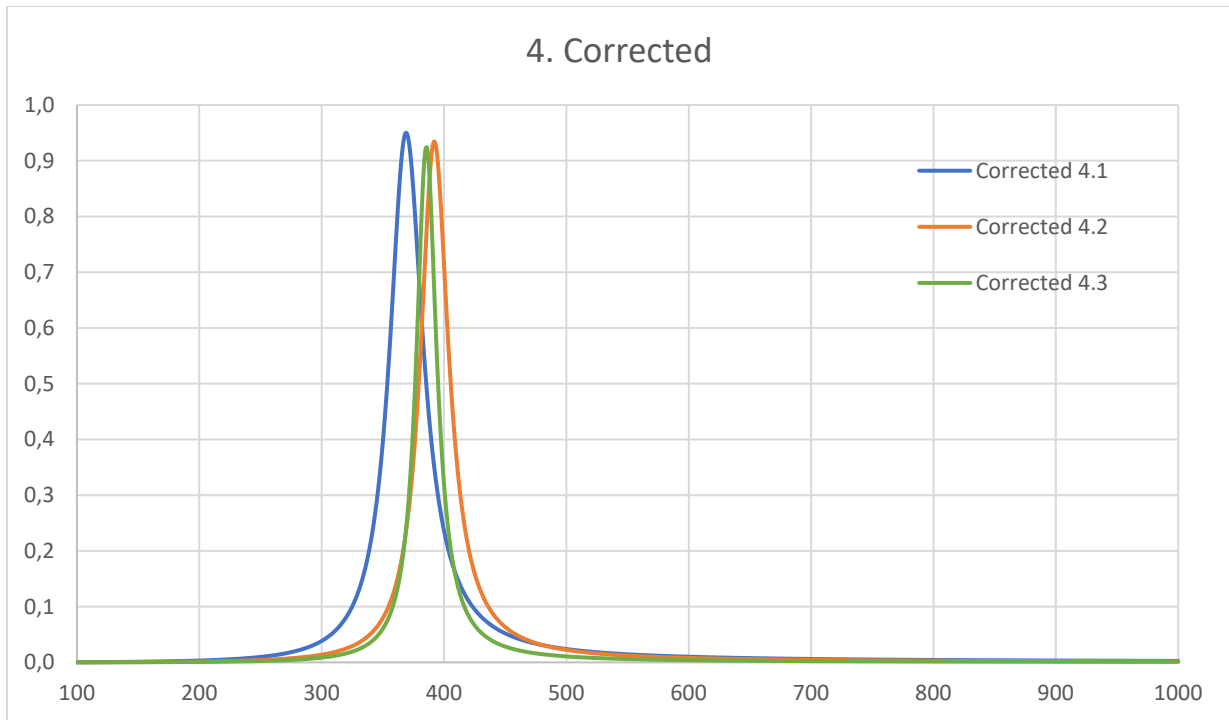
### Additional graphs experiment 4



### Experimental results from experiment 4

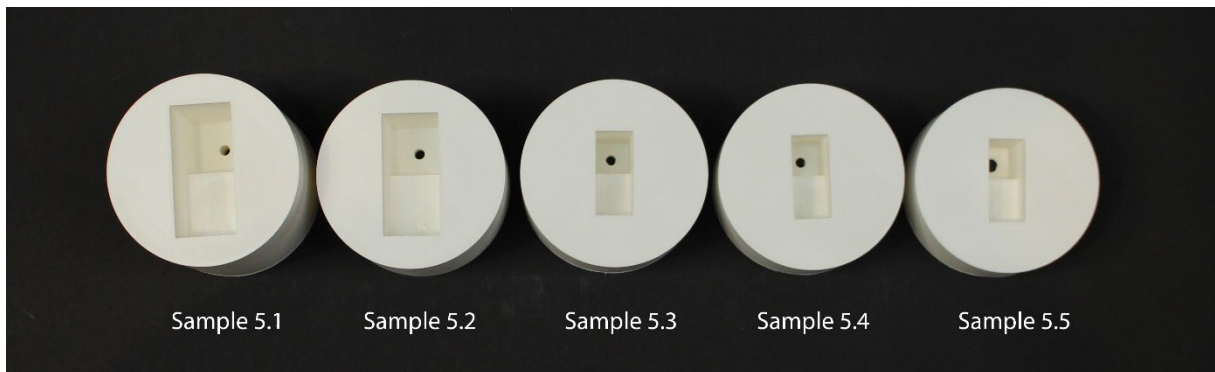


### Non corrected results from experiment 4



Corrected results from experiment 4

Original results experiment 5



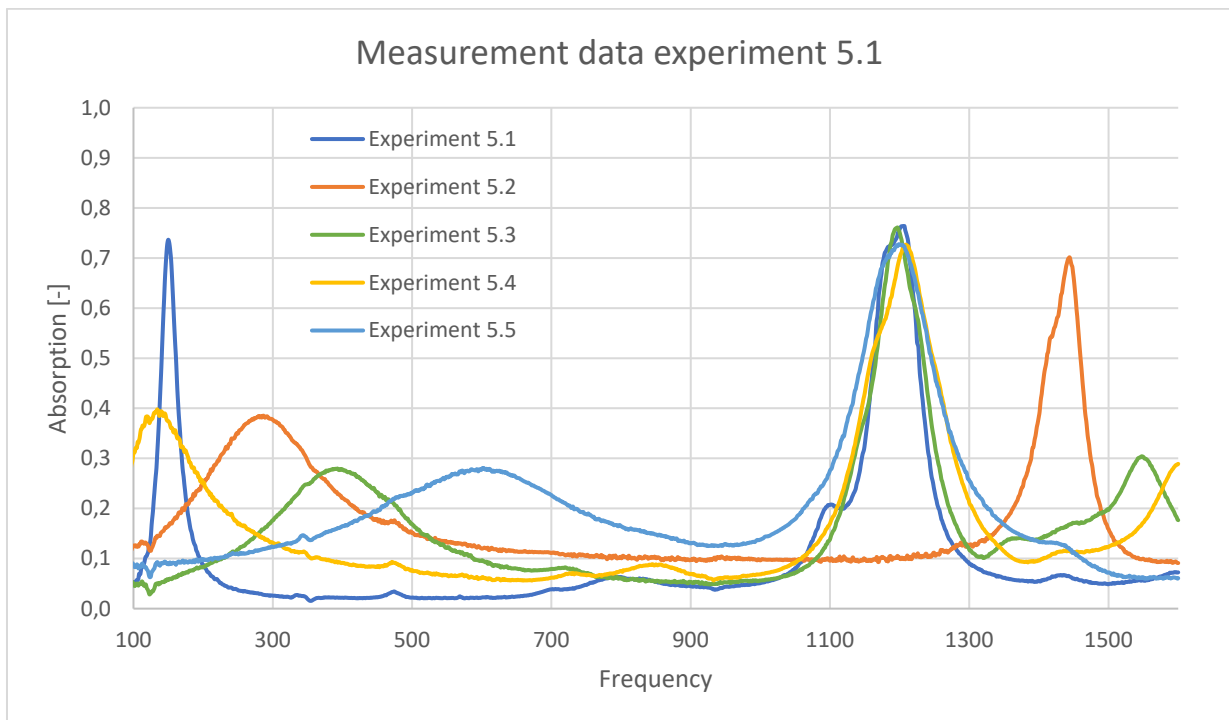
Samples from experiment 5

As explained in chapter 2.6.1 of the main report the first set of samples from experiment 5 did not give the expected results. This is likely due to the low amount of infill material and choosing the “wrong” infill pattern. This resulted in the vibration of the top plate of the sample, this resulted in an absorption peak at 1200 Hz across all samples except 5.2. Sample 5.2 was printed using another printer with a slightly different infill pattern. The graph show this sample to have the same problem but about 200 Hz higher.

	Cavity width bottom	Cavity height bottom	Cavity depth bottom	Cavity width top	Cavity height top	Cavity depth top	Orifice radius	Neck length	Sample radius	Infill percentage
Non corrected 5.1	32 mm	69 mm	40 mm	32 mm	32 mm	35 mm	3 mm	20 mm	100 mm	2 %
Non corrected 5.2	30 mm	65 mm	30 mm	30 mm	30 mm	30 mm	3 mm	10 mm	100 mm	2 %

Non corrected 5.3	20 mm	25 mm	30 mm	20 mm	20 mm	25 mm	3 mm	5 mm	100 mm	2 %
Non corrected 5.4	20 mm	25 mm	25 mm	20 mm	20 mm	25 mm	3 mm	3 mm	100 mm	2 %
Non corrected 5.5	20 mm	25 mm	20 mm	20 mm	20 mm	25 mm	4 mm	2 mm	100 mm	2 %
Corrected 5.1	31.50 mm	68.80 mm	40.00 mm	31.50 mm	-	34.50 mm	5.20 mm	20.00 mm	100 mm	2%
Corrected 5.2 (1)	29.80 mm	65.00 mm	30.00 mm	29.80 mm	-	30.00 mm	6.00 mm	10.00 mm	100 mm	2%
Corrected 5.3	20.00 mm	44.90 mm	30.00 mm	20.00 mm	-	25.00 mm	5.20 mm	5.00 mm	100 mm	2%
Corrected 5.4	20.00 mm	44.90 mm	25.00 mm	20.00 mm	-	25.00 mm	5.50 mm	3.00 mm	100 mm	2%
Corrected 5.5	20.00 mm	44.80 mm	20.00 mm	20.00 mm	-	24.80 mm	7.50 mm	2.00 mm	100 mm	2%

(1) Sample 5.2 was printed using a Prusa MK3S+, settings where the same as the other printer



#### Original measurement data from experiment 5

Due to the peak occurring at the same frequency across all samples the suspicion arose that the design of the resonators was not the cause for the unexpected results. The fact that the sample printed with another printer had the same issue but at another frequency made the main suspicion the printer settings.

Aside from the additional peaks in absorption the expected regular peaks were also unexpected. Samples 5.1, 5.2, 5.3 and 5.5 resonated around the frequency that was expected. Sample 5.4 has a peak at around 150 Hz which at the moment of writing this report an explanation has not yet been found. The expected peak at 650 Hz is non-existent.

### Annex 3: Alternative resonator placement method

Throughout the project multiple resonator sets were designed according to the experiments that were done. For each resonator set an alternative placement method was needed. These methods are not part of the final workflow and are thus presented in the main report.

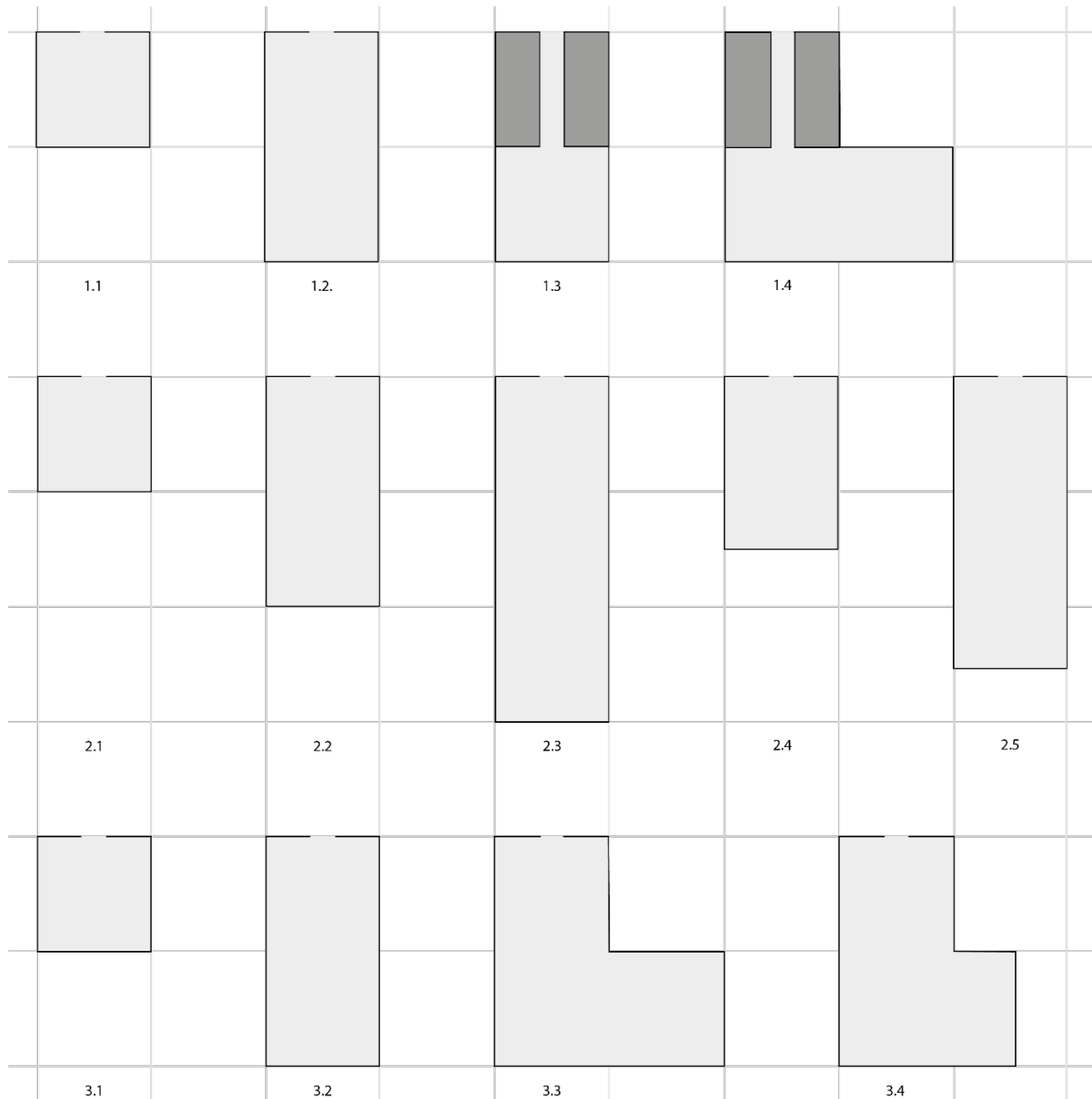


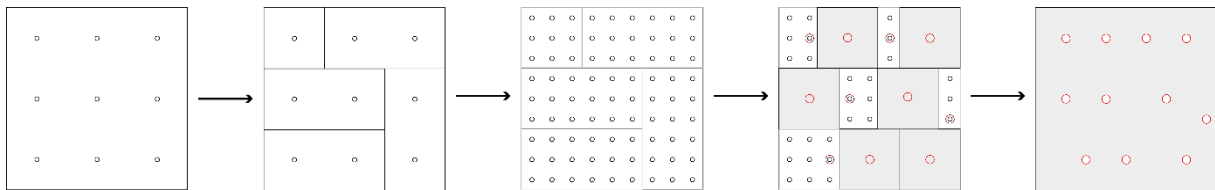
Figure x: resonator sets throughout the project

The first iteration of the panel had the necks of the resonators that were in the bottom take up the space of a full resonator in the top panel (figure x). According to the rules about proximity of the resonators the orifices can be a lot closer together without causing cross-talk. Packing the necks and the resonators in the top layer more efficiently leads to more resonators in the panel, which in turn can lead to more absorption. To make this tighter packing possible a finer grid needs to be used for the top layer compared to the bottom layer. The bottom layer only consists of cavities who always occupy the entire space of a point. In the top layer the dimensions are less constant therefore a finer grid with more possibilities can be very beneficial.



Resonator placement method 1.1

To optimally pack the top layer with resonators it is beneficial to place the neck of the resonator in the bottom layer separate to the cavities when filling in the top layer. The flexibility this provides allows for the placement of more resonators in the same panel area. Figure x shows this. In the old placement method four resonators could be paced within the top layer while the new method allows for six resonators to be placed.



Resonator placement method 1.2

The resonators in the bottom row are placed in order of the peak frequency. The resonator with the lowest frequency is placed first in one of the panel corners. Then the next resonator is placed as far away as possible from the first resonator, this can be a resonator with the same peak frequency if two of the same kind are required or a resonator with a higher peak frequency if only one of the first resonator is required. This is done to prevent interference from resonators with similar frequency ranges. This process continues placing the following resonator as far as possible from each other resonator. When all the resonators are placed. The script sees if there is still room for more. If there is it starts at the top of the list again, placing resonators until the panel is full. Because the cross-talk is only influenced by the position of the orifice and not of the cavity ,because this is not where the resonance takes place, the orifices are generally kept in the middle of the cavity. In theory this should be sufficient to prevent a large cross-talk effect. Small occurrences of the effect will probably take place but because effects are very small the effect on the absorption is acceptable.

While the resonators are assigned to their positions in the bottom layer, their possible orifice positions in the top layer are being recorded. The placement of the resonators in the top layer functions similarly to the placement in the bottom layer with the exception that out of the possible orifice positions of the resonators in the bottom layer one possible position should always stay available. Figure x shows the process of placing the resonators in the panel.

Explained below is the text variant of the python code found within the grasshopper script.

Resonator placement for the bottom layer:

- Find a resonator that needs to be placed in the bottom layer
- Find the distance between all of the unused points and all of the used points.
- Sort the unused points in order of there smallest distance to another point. Order them from largest to smallest distance
- Start at the top of the list and attempt to place the resonator. If the initial attempt fails, rotate the resonator. Continue through the list until a suitable location is found.
- Check the location

- Remove the used points from the unused list and place them into the used list.
- Continue cycling through the resonators until the panel is full or the placement has failed an X number of times.

Resonator placement for the top layer:

- Find a resonator that needs to be placed in the top layer
- Find the distance between all of the unused points and all of the used points.
- Sort the unused points in order of their smallest distance to another point. Order them from largest to smallest distance
- Start at the top of the list and attempt to place the resonator. If the initial attempt fails, rotate the resonator. Continue through the list until a suitable location is found.
- Check if the chosen location does not block all of the possible locations for the neck of the resonators in the bottom layer.
- Check the location
- Remove the used points from the unused list and place them into the used list.
- Continue cycling through the resonators until the panel is full or the placement has failed an X number of times.

The second resonator set is placed with placement method 1.1. This is due to the fact that all of the resonators in this set have to reach the top panel in order to keep the neck as short as possible. Resonator set two does not contain any resonators that go underneath another resonator therefore the script runs with only one layer.

## Annex 4: Python code

### Acoustic optimizer

```
__author__ = "jordy"
__version__ = "2022.12.2"

import rhinoscriptsyntax as rs
import math

#initialize the division of the panel
interval = 5 #aproxiamte frequency interval between resonators
f_ran = int(end_f-start_f)
in_num = f_ran/interval

#calculate the number of positions and the cavity size in both directions
if p_w > p_h:
    ver = p_w/p_h
    num_s = math.sqrt(in_num/ver)
    num_l = num_s*ver
    num_x = math.ceil(num_l)+alt_x
    num_y = math.ceil(num_s)+alt_y
    tot_num = num_x*num_y
    cs_x = ((p_w-mt)/num_x)-mt
    cs_y = ((p_h-mt)/num_y)-mt
else:
    ver = p_h/p_w
    num_s = math.sqrt(in_num/ver)
    num_l = num_s*ver
    num_y = math.ceil(num_l)+alt_y
    num_x = math.ceil(num_s)+alt_x
    tot_num = num_x*num_y
    cs_x = ((p_w-mt)/num_x)-mt
    cs_y = ((p_h-mt)/num_y)-mt

##### resonator options #####
cw = []
ch = []
cd = []
cav_t = []
cav_b = []
c_opt = []

#option 1
c_opt.append(0)
cw.append(cs_x)
ch.append(cs_y)
cd.append(h_tl)
cav_t.append(1)
cav_b.append(0)
#option 2
c_opt.append(1)
cw.append(cs_x)
ch.append(cs_y)
cd.append(h_tl+mt+h_bl)
cav_t.append(1)
cav_b.append(1)
#option 3
c_opt.append(2)
cw.append(cs_x)
ch.append(cs_y)
cd.append((((cs_x*2+mt)*cs_y*h_bl)+((h_tl+mt)*cs_x*cs_y))/cs_x/cs_y) #total volume divide
by the width and height of the top part
cav_t.append(1)
cav_b.append(2)
#option 4
```

```

c_opt.append(3)
cw.append(cs_x)
ch.append(cs_y)
cd.append(((cs_x*1.5+mt)*cs_y*h_bl)+((h_tl+mt)*cs_x*cs_y))/cs_x/cs_y) #total volume
divide by the width and height of the top part
cav_t.append(1)
cav_b.append(1.5)
#amount of options
opt = len(cw)

#Initialize the range for the orifice
o_min = 1
o_max = 10
o_step = 0.1
o_range = int((o_max-o_min)/o_step)

# initialize the other values
ps = p_w*p_h/1000000
nl = (mt*n1_m)/1000
mt = mt/1000
sos = 343
doa = 1.198
sai = sos*doa
vis = 15.1*10**-6

#initialize the lists
b_ab = []
b_opt = []
b_radi = []
b_cav_t = []
b_cav_b = []
b_cav_d = []
b_cav_w = []
b_cav_h = []
b_freq = []
total_absorption = []
bonus = 0
halve_t = -1
halve_b = -1
min_a_bot = min([n for n in cav_b if n>0])
min_a_top = min(cav_t)
fullbot = 0
nearfull = 0

#as a resonator is placed every iteration the amount of positions in the top layer is the
maximum amount of iterations
for a in range(int(tot_num)):
    #The first iteration: the centre frequency of the range is selected as the initial
    frequency
    if len(b_opt) == 0:
        a_ab = []
        a_opt = []
        a_radi = []
        a_cav_t = []
        a_cav_b = []
        a_cav_d = []
        a_cav_w = []
        a_cav_h = []
        in_freq = start_f+(f_ran/2)
        #iterate through the options
        for b in range(opt):
            cav_w = cw[b]/1000
            cav_h = ch[b]/1000
            cav_d = cd[b]/1000
            #iterate through the possible orifice radii
            for d in range(o_range):

```

```

rad = (o_min+o_step*d)/1000
ec = (8/3/math.pi)*rad
fo = (math.pi*rad**2)/(ps)
wn = (2*math.pi*in_freq)/340
af = 2*math.pi*in_freq
z1 = -sos*doa*(1/math.tan(wn*cav_d))*((math.pi*rad**2)/(cav_w*cav_h))
z2 = doa*(math.sqrt(8*(vis)*af)*(1+n1/(2*rad)))+(2*af*rad)**2/16/sos)
z3 = ((2*ec+n1)*af*doa)
z4 = (complex(z2,(z1+z3)))/fo
R = (z4-(doa*sos))/(z4+(doa*sos))
absorption = 1-abs(R)**2
#save the relevant data
a_ab.append(absorption)
a_opt.append(c_opt[b])
a_radi.append(rad)
a_cav_t.append(cav_t[b])
a_cav_b.append(cav_b[b])
a_cav_d.append(cav_d)
a_cav_w.append(cav_w)
a_cav_h.append(cav_h)
#sort the possible options based on their absorption at the chosen frequency
t_opt = ([a_opt for _,a_opt in sorted(zip(a_ab,a_opt))])
t_rad = ([a_radi for _,a_radi in sorted(zip(a_ab,a_radi))])
t_cav_t = ([a_cav_t for _,a_cav_t in sorted(zip(a_ab,a_cav_t))])
t_cav_b = ([a_cav_b for _,a_cav_b in sorted(zip(a_ab,a_cav_b))])
t_cav_d = ([a_cav_d for _,a_cav_d in sorted(zip(a_ab,a_cav_d))])
t_cav_w = ([a_cav_w for _,a_cav_w in sorted(zip(a_ab,a_cav_w))])
t_cav_h = ([a_cav_h for _,a_cav_h in sorted(zip(a_ab,a_cav_h))])
#take the best option and add it to the resonant panel
b_opt.append(t_opt[-1])
b_radi.append(t_rad[-1])
b_cav_t.append(t_cav_t[-1])
b_cav_b.append(t_cav_b[-1])
b_cav_d.append(t_cav_d[-1])
b_cav_w.append(t_cav_w[-1])
b_cav_h.append(t_cav_h[-1])
b_freq.append(in_freq)
#if the resonator takes up half a space remember it
if type(t_cav_t[-1]) == float:
    halve_t = len(b_opt)-1
if type(t_cav_b[-1]) == float:
    halve_b = len(b_opt)-1
#The other iterations: the process is the same as the initial iteration
#the target frequency is the frequency with the lowest absorption from the last
iteration
else:
    a_ab = []
    a_opt = []
    a_radi = []
    a_cav_t = []
    a_cav_b = []
    a_cav_d = []
    a_cav_w = []
    a_cav_h = []
    for b in range(opt):
        cav_w = cw[b]/1000
        cav_h = ch[b]/1000
        cav_d = cd[b]/1000
        for d in range(o_range):
            rad = (o_min+o_step*d)/1000
            ec = (8/3/math.pi)*rad
            fo = (math.pi*rad**2)/(ps)
            wn = (2*math.pi*new_target)/sos
            af = 2*math.pi*new_target
            z1 = -sos*doa*(1/math.tan(wn*cav_d))*((math.pi*rad**2)/(cav_w*cav_h))
            z2 = doa*(math.sqrt(8*(vis)*af)*(1+n1/(2*rad)))+(2*af*rad)**2/16/sos)

```

```

        z3 = ((2*ec+n1)*af*doa)
        z4 = (complex(z2,(z1+z3)))/fo
        R = (z4-(doa*sos))/(z4+(doa*sos))
        absorption = 1-abs(R)**2
        a_ab.append(absorption)
        a_opt.append(c_opt[b])
        a_radi.append(rad)
        a_cav_t.append(cav_t[b])
        a_cav_b.append(cav_b[b])
        a_cav_d.append(cav_d)
        a_cav_w.append(cav_w)
        a_cav_h.append(cav_h)
    t_opt = ([a_opt for _,a_opt in sorted(zip(a_ab,a_opt))])
    t_rad = ([a_radi for _,a_radi in sorted(zip(a_ab,a_radi))])
    t_cav_t = ([a_cav_t for _,a_cav_t in sorted(zip(a_ab,a_cav_t))])
    t_cav_b = ([a_cav_b for _,a_cav_b in sorted(zip(a_ab,a_cav_b))])
    t_cav_d = ([a_cav_d for _,a_cav_d in sorted(zip(a_ab,a_cav_d))])
    t_cav_w = ([a_cav_w for _,a_cav_w in sorted(zip(a_ab,a_cav_w))])
    t_cav_h = ([a_cav_h for _,a_cav_h in sorted(zip(a_ab,a_cav_h))])
    #check if the resonator still fits in the panel
    if u_t1+t_cav_t[-1] <= tot_num and u_b1+t_cav_b[-1] <= tot_num:
        b_opt.append(t_opt[-1])
        b_radi.append(t_rad[-1])
        b_cav_t.append(t_cav_t[-1])
        b_cav_b.append(t_cav_b[-1])
        b_cav_d.append(t_cav_d[-1])
        b_cav_w.append(t_cav_w[-1])
        b_cav_h.append(t_cav_h[-1])
        b_freq.append(new_target)
        #remember the resonator if it uses half a cavity
        if type(t_cav_t[-1]) == float:
            halve_t = len(b_opt)-1
        if type(t_cav_b[-1]) == float:
            halve_b = len(b_opt)-1
    #calculate the total absorption
    u_t1 = sum(b_cav_t)
    u_b1 = sum(b_cav_b)
    if len(total_absorption) > 1:
        total_absorption = []
    #iterate through the frequency range
    for e in range(f_ran+1):
        z = []
        freq = e+start_f
        wn = 2*math.pi*freq/sos
        af = 2*math.pi*freq
        #iterate through all the resonators currently in the panel
        for b in range(len(b_opt)):
            oa = (b_radi[b]**2)*math.pi
            fo = oa/ps
            ec = (8/3/math.pi)*b_radi[b]
            #calculate the absorption per resonator and per frequency
            z1 = -
            sos*doa*(1/math.tan(wn*b_cav_d[b]))*((math.pi*b_radi[b]**2)/(b_cav_w[b]*b_cav_h[b]))
            z2 = doa*(math.sqrt(8*vis*af)*(1+n1/(2*b_radi[b]))+(2*af*b_radi[b])**2/16/sos)
            z3 = ((2*ec+n1)*af*doa)
            z4 = (complex(z2,(z1+z3)))/fo
            z.append(1/z4)
        #calculate the total absorption per frequency
        z_tot = 1/sum(z)
        R = (z_tot-(doa*sos))/(z_tot+(doa*sos))
        ab = 1-abs(R)**2
        total_absorption.append(ab)
    #Break the loop if the panel is full
    if u_t1 == tot_num:
        print('iteration',a,'full panel')
        break

```

```

#Delete resonators when that cavity type does not fit the panel anymore
if u_bl+2 > tot_num and nearfull != 1:
    print('iteration',a,'delete large bottom resonator, top layer',u_tl,'bottom
layer',u_bl)
    del_num = cav_b.index(2)
    del ch[del_num]
    del cw[del_num]
    del cd[del_num]
    del cav_t[del_num]
    del cav_b[del_num]
    del c_opt[del_num]
    opt = opt-1
    nearfull = 1
if u_bl == tot_num and fullbot != 1:
    print('iteration',a,'delete bottom layer, top layer',u_tl,'bottom layer',u_bl)
    del_num = cav_b.index(1)
    del ch[del_num]
    del cw[del_num]
    del cd[del_num]
    del cav_t[del_num]
    del cav_b[del_num]
    del c_opt[del_num]
    opt = opt-1
    if 1.5 in cav_b:
        del_num = cav_b.index(1.5)
        del ch[del_num]
        del cw[del_num]
        del cd[del_num]
        del cav_t[del_num]
        del cav_b[del_num]
        del c_opt[del_num]
        opt = opt-1
    fullbot = 1
    #if half a cavity is left delete the last resonator that uses half a cavity to make
sure the panel can be filled fully
    if tot_num-u_bl-min_a_bot < 0 and tot_num != u_bl:
        if halve_b != -1:
            print('iteration',a,'bottom layer to full, top and bottom
number:',sum(b_cav_t),sum(b_cav_b))
            del b_opt[halve_b]
            del b_radi[halve_b]
            del b_cav_t[halve_b]
            del b_cav_b[halve_b]
            del b_cav_d[halve_b]
            del b_cav_w[halve_b]
            del b_cav_h[halve_b]
            del b_freq[halve_b]
            print('new top and bottom number',sum(b_cav_t),sum(b_cav_b))
            del_num = cav_b.index(1.5)
            del ch[del_num]
            del cw[del_num]
            del cd[del_num]
            del cav_t[del_num]
            del cav_b[del_num]
            del c_opt[del_num]
            opt = opt-1
        #find the lowest absorption and make that the new target for the next resonator
        freq_list = range(int(start_f),int(end_f)+1)
        freq_l = list(freq_list)
        i_sort = ([freq_l for _,freq_l in sorted(zip(total_absorption,freq_l))])
        new_target = i_sort[0]
    #give a bonus based on how small the range is, smaller range means hihger bonus
    u_tl = sum(b_cav_t)
    u_bl = sum(b_cav_b)
    diff = max(total_absorption)-min(total_absorption)
    bonus = 1+(1-diff)

```

```

score = sum(total_absorption)*bonus/(f_ran*2)
print('iteration',a,'finished: places used top layer:',u_tl,'places used bottom
layer',u_bl,'available spots',tot_num)

```

## Resonator placement

```

__author__ = "jordy"
__version__ = "2022.09.19"

```

```

import rhinoscriptsyntax as rs
import ghpythonlib.treehelpers as th

```

```

#initialize the lists for the bottom layer

```

```

used = []
res = []
q = []
q_id = []
fail = 0
att_1 = 0
rot = []

```

```

#safety measure for when the toggle is set to false

```

```

if cavity_outline.BranchCount > 1:

```

```

    #continue placing resonators until the panel is full or as a safety measure stop after
    200 iterations

```

```

    #while grid.BranchCount > 0 and att_1 < 200:

```

```

        #iterate through the resonators

```

```

    for a in range(cavity_outline.BranchCount):

```

```

        #check if the resonator needs to be placed in the bottom layer

```

```

        if cavity_number_b.Branch(a)[0] > 0:

```

```

            place = 0

```

```

            #check if some resonators have already been placed

```

```

            if len(used) > 0 :

```

```

                dist = []

```

```

                dist_id = []

```

```

                #iterate through the possible locations

```

```

                for s in range(grid.BranchCount):

```

```

                    tot_dist = []

```

```

                    #look at all of the resonators that already have been placed and find

```

```

the location that is furthest away from all of them

```

```

                    for h in range(len(used)):

```

```

                        temp_dist = rs.Distance(grid.Branch(s)[0],used[h])

```

```

                        tot_dist.append(temp_dist)

```

```

                        tot_dist.sort()

```

```

                    dist.append(tot_dist[0])

```

```

                    dist_id.append(s)

```

```

                #sort the new locations from best to worst

```

```

                new_loc = [dist_id for _,dist_id in sorted(zip(dist,dist_id))]

```

```

                new_loc.reverse()

```

```

                #iterate through the locations

```

```

                for e in range(len(new_loc)):

```

```

                    #check if the resonator has not yet been placed

```

```

                    if place == 0:

```

```

                        loc = grid.Branch(new_loc[e])[0]

```

```

                        temp_obj = rs.CopyObject(cavity_outline.Branch(a)[0],loc)

```

```

                        #rotate the resonator if this allows it to fit

```

```

                        for d in range(2):

```

```

                            if place == 0:

```

```

                                rs.RotateObject(temp_obj,loc,180*d)

```

```

                                hit = []

```

```

                                #check if the resonator takes up the amount of space it is

```

```

supposed to

```

```

                                for b in range(grid.BranchCount):

```

```

                                    inside =

```

```

rs.PointInPlanarClosedCurve(grid.Branch(b)[0],temp_obj)

```

```

                                    if inside == 1:

```

```

        hit.append(b)
    #if a suitable location is found place the resonator
    if len(hit) == cavity_number_b.Branch(a)[0]:
        if place == 0:
            place = 1
            res.append(rs.CopyObject(temp_obj))
            q.append(loc)
            q_id.append(a)
            rot.append(d)
            #remove the locations used by the resonator in both
the top and the bottom layer
            if cavity_number_t.Branch(a)[0] == 1:
                grid_2.RemovePath(grid.Path(new_loc[e]))
            for c in range(len(hit)):
                temp_hit = hit[c]-c
                used.append(grid.Branch(temp_hit)[0])
                if cavity_number_t.Branch(a)[0] == 2:
                    if c == 0 or c == len(hit)-1:
                        grid_2.RemovePath(grid.Path(temp_hit))
                grid.RemovePath(grid.Path(temp_hit))
    #if no resonators have been placed, take the location in the bottom left corner
    else:
        loc = grid.Branch(0)[0]
        rs.MoveObject(cavity_outline.Branch(a)[0],loc)
        #rotate the resonator if this llows it to fit
        for d in range(2):
            if place == 0:
                rs.RotateObject(cavity_outline.Branch(a)[0],loc,180*d)
                hit = []
                #check if the resonator takes up the amount of space it is supposed
to
                for b in range(grid.BranchCount):
                    inside =
rs.PointInPlanarClosedCurve(grid.Branch(b)[0],cavity_outline.Branch(a)[0])
                    if inside == 1:
                        hit.append(b)
            #if a suitable location is found place the resonator
            if len(hit) == cavity_number_b.Branch(a)[0]:
                res.append(rs.CopyObject(cavity_outline.Branch(a)[0]))
                q.append(loc)
                q_id.append(a)
                rot.append(d)
                #remove the locations used by the resonator in both the top and
the bottom layer
                if cavity_number_t.Branch(a)[0] == 1:
                    grid_2.RemovePath(grid.Path(0))
                place = 1
                for c in range(len(hit)):
                    temp_hit = hit[c]-c
                    used.append(grid.Branch(temp_hit)[0])
                    if cavity_number_t.Branch(a)[0] == 2:
                        if c == 0 or c == len(hit)-1:
                            grid_2.RemovePath(grid.Path(temp_hit))
                    grid.RemovePath(grid.Path(temp_hit))
            #if the bottom layer is full, give a sign and break the loop
            if grid.BranchCount == 0:
                print("vol")
                break
            #if no resonators could be placed, consider it a failed attempt
            if place == 0:
                fail = fail+1
        #if the script failed to place a resonator 10 times, break the loop
        #if fail > 10:
            #print("niet vol")
            #break
        #att_1+1

```

```

#initialize the lists for the top layer
used_2 = []
res_t = []
q_t = []
q_id_t = []
att = 0
#continue placing resonators until the panel is full or as a saftey measure stop after
50 itterations
while grid_2.BranchCount > 0 and att <50:
    #iterate through the resonators
    for j in range(cavity_outline.BranchCount):
        #check if the resoantor needs to be placed in the bottom layer
        if cavity_number_b.Branch(j)[0] < 1:
            ob = cavity_outline.Branch(j)
            #check if some resonators have already been placed
            if len(used_2) > 0:
                dist = []
                dist_id = []
                #iterate through the possible locations
                for s in range(grid_2.BranchCount):
                    tot_dist = []
                    #look at all of the resonators that already have been placed and
                    find the location that is furthest away from all of them
                    for h in range(len(used_2)):
                        temp_dist = rs.Distance(grid_2.Branch(s)[0],used_2[h])
                        tot_dist.append(temp_dist)
                        tot_dist.sort()
                    dist.append(tot_dist[0])
                    dist_id.append(s)
                #sort the new locations from best to worst
                new_loc = [dist_id for _,dist_id in sorted(zip(dist,dist_id))]
                new_loc_id = new_loc[-1]
                #place the resonator on the best location
                mo = grid_2.Branch(new_loc_id)[0]
                #remove the locations used by the resonator in the top layer
                used_2.append(grid_2.Branch(new_loc_id)[0])
                grid_2.RemovePath(grid_2.Path(new_loc_id)[0])
                #if the panel is full place the last resonator and break the loop
                if grid_2.BranchCount == 0:
                    res_t.append(rs.CopyObject(ob[0],mo))
                    q_t.append(mo)
                    q_id_t.append(j)
                    break
            #if no resonators have been placed, place the resonator on the first
            position possible
        else:
            mo = grid_2.Branch(0)[0]
            used_2.append(grid_2.Branch(0)[0])
            grid_2.RemovePath(grid_2.Path(0))
            #place the resonator, save the location and the resonator number
            res_t.append(rs.CopyObject(ob[0],mo))
            q_t.append(mo)
            q_id_t.append(j)
    att = att+1

```

## Preparation for production

```

__author__ = "jordy"
__version__ = "2022.10.31"

import rhinoscriptsyntax as rs
import ghpythonlib.treehelpers as th
import math

#convert the data tree's into lists
x_list = th.tree_to_list(rec_x)

```

```

y_list = th.tree_to_list(rec_y)

#initialize the needed lists and values
text_point = []
pt_list = []
rq_list = []
id_list = []
p_num = []
r_bound = []
x_cor = 0
y_cor = 0
num_p = 1
plane = rs.WorldXYPlane()
r_bound.append(rq_bound)
text_point.append(rs.AddPoint(0,y_size+20,0))
o_y_size = y_size
y_row = []

#iterate through the list of panels that need to be placed
for a in range(len(x_list)):
    #check if the panel has not yet been placed
    if a not in id_list:
        #if the y dimation is larger than the x dimation rotate the panel
        if x_list[a] < y_list[a]:
            d = x_list[a]
            x_list[a] = y_list[a]
            y_list[a] = d
        #calculate the top right position
        x_temp = x_cor + x_list[a]
        y_temp = y_cor + y_list[a]
        #check if the position is within the y bound of the laser cut panel
        if y_temp < y_size:
            #check if the position is within the x bound of the laser cut panel
            if x_temp < x_size:
                #again check if the panel has not yet been placed
                if a not in id_list:
                    #add the point and the rectangle for a visual check
                    pt_list.append(rs.AddPoint(x_cor,y_cor,0))
                    rectangle = rs.AddRectangle(plane,x_list[a],y_list[a])
                    rq_list.append(rs.MoveObject(rectangle,(x_cor,y_cor,0)))
                    id_list.append(a)
                    p_num.append(num_p)
                    #correct the starting point
                    x_cor = x_cor + x_list[a]
                    #remember the y
                    y_row.append(y_list[a])
            #if the panel does not fit in the x direction of the panel
            else:
                #move up one row and note the space that is left
                s_left = x_size-x_cor
                y_left = 0
                x_cor_temp = x_cor
                y_cor_temp = y_cor
                y_row.sort()
                height = y_row[-1]
                #itterate through the panels that have not been placed
                for b in range(len(x_list)):
                    if b not in id_list:
                        #if the x of the panel is smaller than the x that was left in this
                        row
                            if x_list[b] < s_left:
                                y_left = y_left+y_list[b]
                                #check if the panel fits in the y direction
                                if y_list[b] <= y_row[-1] and y_list[b] <= height:
                                    #place the panel in the left over space
                                    pt_list.append(rs.AddPoint(x_cor_temp,y_cor_temp,0))

```

```

        rectangle = rs.AddRectangle(plane,x_list[b],y_list[b])

rq_list.append(rs.MoveObject(rectangle,(x_cor_temp,y_cor_temp,0)))
        y_cor_temp = y_cor_temp + y_list[b]
        id_list.append(b)
        p_num.append(num_p)
        height = height - y_list[b]
        #if nothing fits break the loop
        else:
            break
just placed #not the space that is left in the y direction above the panel that was
x_cor = 0
y_row.sort()
y_cor = y_cor + y_row[-1]
y_temp = y_cor + y_list[a]
y_row = []
#check if the panel fits above the other panel
if y_temp < y_size:
    #check if the panel has not yet been placed and if not place the panel
    if a not in id_list:
        pt_list.append(rs.AddPoint(x_cor,y_cor,0))
        rectangle = rs.AddRectangle(plane,x_list[a],y_list[a])
        rq_list.append(rs.MoveObject(rectangle,(x_cor,y_cor,0)))
        id_list.append(a)
        p_num.append(num_p)
        x_cor = x_cor + x_list[a]
        y_row.append(y_list[a])
    #if you go out of bounds create a new panel
    else:
        y_left = y_size-y_cor
        x_left = x_size
        y_row_2 = []
        #find panels that fit in the leftover space on the old panel
        for c in range(len(x_list)):
            #check if the panel fits in the left over y space
            if y_list[c] < y_left:
                #check if the panel fits in the left over x space
                if x_list[c] < x_left:
                    #check if the panel has not yet been placed
                    if c not in id_list:
                        #add the point and the rectangle for a visual check
                        pt_list.append(rs.AddPoint(x_size-x_left,y_size-
y_left,0))
                        rectangle = rs.AddRectangle(plane,x_list[c],y_list[c])
                        rq_list.append(rs.MoveObject(rectangle,(x_size-
x_left,y_size-y_left,0)))
                        id_list.append(c)
                        p_num.append(num_p)
                        #correct the starting point
                        x_left = x_left - x_list[c]
                        y_row_2.append(y_list[c])
                    #if the panel does not fit in the left over x space move up the
                    amount of the largest y placed in the previous loop
                    else:
                        x_left = x_size
                        y_row_2.sort()
                        y_left = y_left-y_row_2[-1]
        #create a new panel
        num_p = num_p + 1
        x_cor = 0
        y_cor = (o_y_size+40)*(num_p-1)
        y_size = (o_y_size+40)*(num_p-1)+o_y_size
        r_bound.append(rs.CopyObject(rq_bound,[0,y_cor,0]))
        text_point.append(rs.AddPoint(0,y_size+20,0))
        if a not in id_list:

```

```
#place the panel that we where initaly placing on the new pannel
pt_list.append(rs.AddPoint(x_cor,y_cor,0))
rectangle = rs.AddRectangle(plane,x_list[a],y_list[a])
rq_list.append(rs.MoveObject(rectangle,(x_cor,y_cor,0)))
id_list.append(a)
p_num.append(num_p)
#correct the starting point
x_cor = x_cor + x_list[a]
y_row.append(y_list[a])
```



